

Madeleine Eriksen

# Cross-Laminated Timber in Fires: A Study of Factors Affecting Ignition, Reignition, Self-Extinction, and Charring

Master's thesis in Civil and Environmental Engineering  
Supervisor: Kathinka Leikanger Friquin  
June 2023



Madeleine Eriksen

# **Cross-Laminated Timber in Fires: A Study of Factors Affecting Ignition, Reignition, Self-Extinction, and Charring**

Master's thesis in Civil and Environmental Engineering  
Supervisor: Kathinka Leikanger Friquin  
June 2023

Norwegian University of Science and Technology  
Faculty of Engineering  
Department of Civil and Environmental Engineering





# Summary

This master's thesis has addressed certain critical elements of the utilization of mass timber from the fire safety standpoint. A higher demand for timber materials requires more research on using exposed cross-laminated timber (CLT) in buildings. Its bearing properties make it possible to use it as a substitute for steel and concrete in structural systems. However, timber is combustible, and exposed mass timber in buildings will also lead to higher fire loads, giving more intense and longer-lasting fires. Therefore, it is necessary to investigate how CLT behaves during a fire. Three different methodologies are used in the thesis to examine how CLT responds to various fire exposures.

Initially, a literature review was conducted to form a foundation for the tests and the analysis. Information regarding mass timber reactions under various fire exposure is found through earlier research. Furthermore, in the fall of 2022, a large-scale compartment test with exposed CLT elements in the ceiling was conducted by Andreas S. Bøe as a part of the FRIC project. A few results from this test regarding charring and temperature development in the elements have been chosen and analyzed. Finally, the central part of the thesis is based on testing of small samples of CLT in a cone calorimeter and investigating the critical heat flux (HF) for unpiloted ignition and extinction on fresh and charred samples. Thermocouples were placed inside the elements during the tests making it possible to measure the continuous temperature rise during the tests. The results have been used to predict how the pyrolysis in the timber develops.

The cone calorimeter tests show that fresh timber has a lower critical heat flux than charred timber, which correlates with the theory in the literature review. However, the difference is not severe, indicating that a charred layer does not protect the inner layer enough to keep it from reigniting during a fire development with as high temperatures as were seen in the Compartment Test. It was also observed that samples with no external heat flux radiations led to extinction within 5 minutes. Nevertheless, the critical heat flux for self-extinction has yet to be found.

Analysis of charring rates has been conducted in both the small samples and the CLT elements used in the large-scale compartments tests, indicating that density affects the charring rate. Findings show that the average charring rate from the cone calorimeter is slightly lower than the one found in ISO standards but higher than the one found in the Compartment Test. Nevertheless, the charring rate from the Compartment Test has been affected by several factors, and the premises for calculating and comparing the charring rate may not be correct as the heat exposure varies during the Compartment Test, unlike the cone calorimeter tests with continuous heat flux.

# Sammendrag

Denne masteroppgaven har adressert noen kritiske faktorer ved bruk av massivtre sett fra et brannsikkerhetsperspektiv. En økende etterspørsel etter trematerialer krever mer forskning på bruk av eksponert krysslaminert tre (KLT) i bygninger. Dets lastbærende egenskaper gjør det mulig å bruke det som erstatning for stål og betong i konstruksjonssystemer. Imidlertid er tre brennbar, og eksponert massivtre i bygninger vil føre til høyere brannbelastning, som igjen fører til mer intense branner med lengre varighet. Tre forskjellige metoder brukes i oppgaven for å undersøke hvordan CLT reagerer på ulike brannpåkjenninger.

Først ble det gjennomført en litteraturstudie for å danne et grunnlag for testene og analysene. En gjennomgang av eksisterende kunnskap og tidligere forskning har gjort det mulig å finne informasjon om hvordan massivtre reagerer under ulike branneksposeringer og hvilke faktorer som påvirker forbrenningen av tre. Videre ble det høsten 2022 gjennomført en stor-skala romtest med eksponerte KLT-elementer i taket som en del av FRIC-prosjektet av Andreas S. Bøe. Forkulling i noen av disse elementene ble valgt ut og analysert. Til slutt ble den sentrale delen av oppgaven gjort ved å teste små prøver av massivtre i en konkalorimeter og undersøke den kritiske varmefluksen for antennelse og selvslukking på ferske og forkullede prøvestykker. Termoelementer ble plassert inne i elementene under testene, noe som gjorde det mulig å måle den kontinuerlige temperaturutviklingen under testene. Disse ble brukt til å beregne hvordan pyrolysen i treet utvikler seg.

Konkalorimeter-testene viser at ferskt tre har en lavere kritisk varmefluks enn forkullet tre, noe som stemmer overens med teorien i litteraturgjennomgangen. Imidlertid er forskjellen liten, noe som indikerer at et forkullet lag ikke beskytter det indre laget tilstrekkelig fra å reantenne under brannutvikling med like høye temperaturer som ble sett i branntesten. Det ble også observert at prøver uten ekstern varmestråling førte til sløkking innen 5 minutter. Den kritiske varmefluksen for selvslukking ikke funnet.

Analyse av forkullingshastigheter er gjort både på de små prøvene og CLT-elementene som ble brukt i branntestene i stor skala, og dette indikerer at tettheten påvirker forkullingshastigheten. Resultatene viser at gjennomsnittlig forkullingshastighet fra konkalorimeteret er litt lavere enn den som er funnet i ISO-standarder, men høyere enn den som er funnet i romtesten. Likevel har forkullingshastigheten fra branntesten i rommet blitt påvirket av flere faktorer, og forutsetningene for å beregne og sammenligne forkullingshastigheten kan være feil, ettersom varmeeksponeringen varierer under branntesten i rommet, i motsetning til konkalorimeter-testene med kontinuerlig varmefluks.

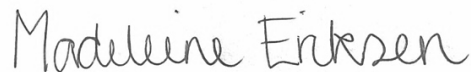
# Preface

The master's thesis marks the culmination of five years of studying at the Department of Civil and Environmental Engineering at the Norwegian University of Science and Technology (NTNU). The thesis was carried out in the period from January 2023 to June 2023 and amounts to 30 credits in the study profile building technology, with a specialization in fire safety.

First, I would like to thank my master advisor, Kathinka Leikanger Friquin. Your expertise, advice, and support throughout the period have been beneficial and motivating. Second, I would like to thank Andreas S. Bøe for allowing me to participate and use the results from your Ph.D. project. Your project has been an inspiration for my thesis and has also contributed with information and results to use in the report.

I would also like to thank the rest of the employees at RISE Fire Research for their help and advice during the preparation of the test materials and the test period. They have been available for support throughout the entire period I worked on the master's thesis, which has helped me greatly.

NTNU, Trondheim, June 8, 2023

A handwritten signature in black ink that reads "Madeleine Eriksen". The script is cursive and fluid.

Madeleine Eriksen





# Table of Contents

List of Figures .....	xii
List of Tables .....	xiv
1 Introduction.....	15
1.1 Background .....	15
1.2 Fire Research and Innovation Centre .....	16
1.2.1 Compartment Test by Andreas S. Bøe .....	16
1.3 Research Questions.....	17
1.4 Limitations.....	17
1.5 A Readers Guide.....	18
2 Materials and Methods .....	19
2.1 Literature Study to Map Existing Research.....	19
2.1.1 Reuse of Material from the Project Thesis .....	19
2.2 Setup and Method for Analysis of the Compartment Test.....	20
2.2.1 Compartment Setup .....	20
2.2.2 Temperature Measurements in the Compartment Test.....	22
2.2.3 Charring Depth Measurements .....	23
2.3 Fire Testing in Cone Calorimeter .....	23
2.3.1 Cone Calorimeter Setup .....	24
2.3.2 Temperature Measurements.....	25
2.3.3 Test Procedure.....	26
2.3.4 Heat Flux Levels Tested in the Cone Calorimeter.....	27
2.3.5 Samples.....	27
3 Literature Review .....	31
3.1 Fire Development .....	31
3.2 Steady-State and Transient State .....	32
3.3 Theoretical Fire Curves .....	33
3.3.1 Standard Fire Curves .....	33
3.3.2 Parametric Fire Curves .....	33
3.4 Informative Parameters in a Fire.....	33
3.4.1 Ignition.....	33
3.4.2 Extinction.....	35
3.4.3 Charring.....	36
3.4.4 Heat Release Rate .....	37
3.4.5 Thermally Thin and Thick Materials .....	37
3.4.6 Mass Loss.....	37

3.4.7	Mass Loss Rate .....	38
3.4.8	Orientation, Surface and Scale Effect .....	38
3.4.9	Density .....	39
3.4.10	Moisture Content.....	40
3.5	Temperature Measurements inside Timber Samples.....	40
4	Results from the Compartment Test .....	43
4.1	Results from Compartment Test by Andreas S. Bøe .....	43
5	Results from Cone Calorimeter Testing .....	48
5.1	Test Group 1: 40 kW/m <sup>2</sup> – 0 kW/m <sup>2</sup> – 30 kW/m <sup>2</sup> .....	48
5.2	Test Group 2: 35 kW/m <sup>2</sup> – 0 kW/m <sup>2</sup> – 50 kW/m <sup>2</sup> – 30 kW/m <sup>2</sup> .....	51
5.3	Test Group 3: 30 kW/m <sup>2</sup> – 0 kW/m <sup>2</sup> – 40 kW/m <sup>2</sup> – 40 kW/m <sup>2</sup> .....	54
5.4	Test Group 4: 33 kW/m <sup>2</sup> – 0 kW/m <sup>2</sup> – 35 kW/m <sup>2</sup> .....	56
5.5	Test Group 5: 32 kW/m <sup>2</sup> – 30 kW/m <sup>2</sup> – 38 kW/m <sup>2</sup> – 30 kW/m <sup>2</sup> .....	61
5.6	Test Group 6: 31 kW/m <sup>2</sup> – 25kW/m <sup>2</sup> – 37 kW/m <sup>2</sup> – 25 and 37 kW/m <sup>2</sup> .....	64
5.7	Test Group 7: a Combination of Different Heat Fluxes .....	66
5.8	Critical Heat Flux for Ignition .....	71
5.9	Critical Heat Flux for Extinction .....	72
5.10	Critical Heat Flux for Ignition According to Janssens Method.....	72
5.11	Calculation of Char Depth from Mass Loss .....	73
6	Discussion .....	75
6.1	Criticism of the Methods .....	75
6.1.1	Uncertainties with ISO 5660 Adjustments .....	75
6.1.2	The Impact of Lids and Thermocouples.....	76
6.2	Differences in the Material .....	78
6.2.1	Orientation .....	79
6.2.2	Premises for Calculating Charring Rate .....	80
6.3	Heat Release Rate and Temperature Development .....	80
6.4	Critical Heat Flux for Ignition.....	82
6.5	Critical Heat Flux for Extinction .....	83
6.6	Relationship between Ignition Time and Density for Fresh and Charred Timber 85	
6.7	Charring Rate Depending on Heat Flux and Density .....	86
6.8	Mass Loss and Mass Loss Rate.....	88
6.9	Calculation of Char Depth Based on Mass Loss.....	90
6.10	Char Development in the Cone Calorimeter Compared to Compartment Test..	92
7	Conclusion.....	94
7.1	Further Work.....	95

References..... 96

# List of Figures

Figure 1.1 Exposed CLT in ZEB laboratory in Trondheim (Lolli, 2020). .....	15
Figure 2.1 Sketch of compartment setup showing locations of PTs (black square) and TCs (white circle). .....	21
Figure 2.2 Wood crib inside the compartment representing a fuel load for an office or living room area. ....	22
Figure 2.3 Holes in the ceiling elements from the Compartment Test, in 50 cm x 50 cm grids used for charring depth measurements. ....	23
Figure 2.4 Caliper used to measure charring depth from ceiling elements used in the Compartment Test. ....	23
Figure 2.5 Cone calorimeter. 1: computer. 2: rack. 3: cone calorimeter.....	24
Figure 2.6 Retainer with a sample covered with a gypsum lid in the cone calorimeter. 1: built-in lid. 2: cone heater. 3: gypsum lid on top of sample. 4: sample inside container. 5: wire from thermocouple. ....	24
Figure 2.7 Temperatures with corresponding heat fluxes radiating from the cone towards the sample. The first number represents the heat flux and the last represents the temperatures. ....	25
Figure 2.8 Sample showing TC depths in the samples with four thermocouples. For samples with one thermocouple, only the placement of the TC at 25 mm is valid.....	26
Figure 2.9 The back of a ceiling element from the compartment test. The unexposed back is used to cut samples used in the cone calorimeter tests. ....	28
Figure 2.10 CLT sample inside the aluminum foil before testing seen from the side. ....	30
Figure 2.11 Fresh CLT sample inside the retainer before testing. ....	30
Figure 3.1 Fire development over time. A fire going to decay is shown in dark grey and a fire that reignites and gets second flashovers is shown in light grey. ....	32
Figure 3.2 Some of the correlations found by Janssens (1991) for piloted ignition on different oven-dried wood materials. ....	34
Figure 3.3 Figures by Terrei <i>et al.</i> (2021) showing temperatures in TCs at different depths for 16,5 kW/m <sup>2</sup> (a) and 38,5 kW/m <sup>2</sup> (b). ....	41
Figure 3.4 Figures by Terrei <i>et al.</i> (2021) showing temperatures in TCs at different depths for 60 kW/m <sup>2</sup> (a) and 93,5 kW/m <sup>2</sup> (b). ....	41
Figure 3.5 Figures by Reszka and Torero (2006) showing temperatures in TC at different depths at 25 kW/m <sup>2</sup> . ....	42
Figure 4.1 Showing the fire spread along the wood crib over time (Bøe et al., 2023). The stippled line shows end of crib. ....	43
Figure 4.2 Heat flux in PTs at three different locations in the compartment. ....	44
Figure 4.3 Results from char measurements, reused from (Bøe et al., 2023).....	44
Figure 4.4 Thermocouples placed in ceiling element at different depths, 4,7 m from the ignition source.....	45
Figure 4.5 Thermocouples placed in ceiling element at different depths, 9,5 m from the ignition source.....	46
Figure 4.6 Thermocouples placed in the ceiling elements at different depths, 14,3 m from the ignition source. ....	46
Figure 5.1 Test group 1: HRR and temperature. ....	49
Figure 5.2 Test 1-3: HRR and temperature. ....	49
Figure 5.3 Observations from Test 1-3, when the flames went around the lid in Phase 2. ....	50
Figure 5.4 Test group 1: mass loss rate. ....	50

Figure 5.5 Test 2-2 shows burning in one side in Phase 2. ....	52
Figure 5.6 Test 2-2 showing cracks of char on the same side as the burning continued. ....	52
Figure 5.7 Test group 2: HRR and temperature. ....	52
Figure 5.8 Test 2-3: HRR and temperature. ....	53
Figure 5.9 Test group 2: mass loss rate. ....	53
Figure 5.10 Test group 3: HRR and temperature. ....	55
Figure 5.11 Test 3-2: HRR and temperature. ....	56
Figure 5.12 Test group 3: mass loss rate.....	56
Figure 5.13 Sample 4-3 showing holes in the surface. ....	58
Figure 5.14 Sample 4-2 showing a spline in the middle. ....	58
Figure 5.15 Sample 4-2 during the test with no ignition in Phase 1 and 1.2.....	58
Figure 5.16 Flames right after ignition and Test 4-3.....	59
Figure 5.17 Test 4-3 10 minutes after ignition.....	59
Figure 5.18 Test group 4: HRR and temperature. ....	59
Figure 5.19 Test 4-3: HRR and temperature. ....	60
Figure 5.20 Test group 4: mass loss rate.....	60
Figure 5.21 Surface of sample 5-1 showing a spline at the left side.....	62
Figure 5.22 Surface of sample 5-2 showing no twigs or splines.....	62
Figure 5.23 Surface of sample 5-3 showing a twig in the middle of the sample. ....	62
Figure 5.24 Test group 5: HRR and temperature. ....	63
Figure 5.25 Test 5-3: HRR and temperature. ....	63
Figure 5.26 Test group 5: mass loss rate.....	64
Figure 5.27 Test group 6: HRR and temperature. ....	66
Figure 5.28 Test group 6: mass loss rate.....	66
Figure 5.29 Sample 7-3 showing a spline in the surface. ....	69
Figure 5.30 Sample 7-4 showing irregularities in the surface.....	69
Figure 5.31 Sample 7-5 showing a smooth surface, besides a few irregularities on the bottom edge. ....	69
Figure 5.32 Test 7-1: HRR and temperature. ....	69
Figure 5.33 Test 7-2: HRR and temperature. ....	70
Figure 5.34 Test 7-3: HRR and temperature. ....	70
Figure 5.35 Test 7-4: HRR and temperature. ....	70
Figure 5.36 Test 7-5: HRR and temperature. ....	71
Figure 5.37 Test group 7: mass loss rate.....	71
Figure 5.38 Janssens method for predicting critical heat flux the CLT samples. ....	72
Figure 5.39 Average mass loss and char depth in percentage.....	73
Figure 5.40 Average mass loss and char depth in grams and millimeters. ....	74
Figure 6.1 Mass loss rate with original data. ....	76
Figure 6.2 Showing cracks at the same place a TC in Test 1-2.....	78
Figure 6.3 Splines between two planks glued together. ....	78
Figure 6.4 Splines between two planks glued together. ....	78
Figure 6.5 Holes and twigs in the surface in sample 4-3. ....	79
Figure 6.6 Irregularities and a spline in the surface in Test 7-4.....	79
Figure 6.7 Peak heat release rate and density for samples that ignited within 15 minutes. .....	81
Figure 6.8 Peak heat release rate and time to ignition for samples that ignited within 15 minutes. ....	81
Figure 6.9 Relationship between ignition time and density for fresh wood. ....	85
Figure 6.10 Relationship between ignition time and density for charred wood. ....	86
Figure 6.11 Charring rate dependent on heat flux.....	87

Figure 6.12 Charring rates at various densities..... 88  
 Figure 6.13 Equation 1. Char depth and mass loss in percent of the total depth and mass.  
 ..... 91  
 Figure 6.14 Equation 2. Char depth and mass loss in percent of the total depth and mass.  
 ..... 92

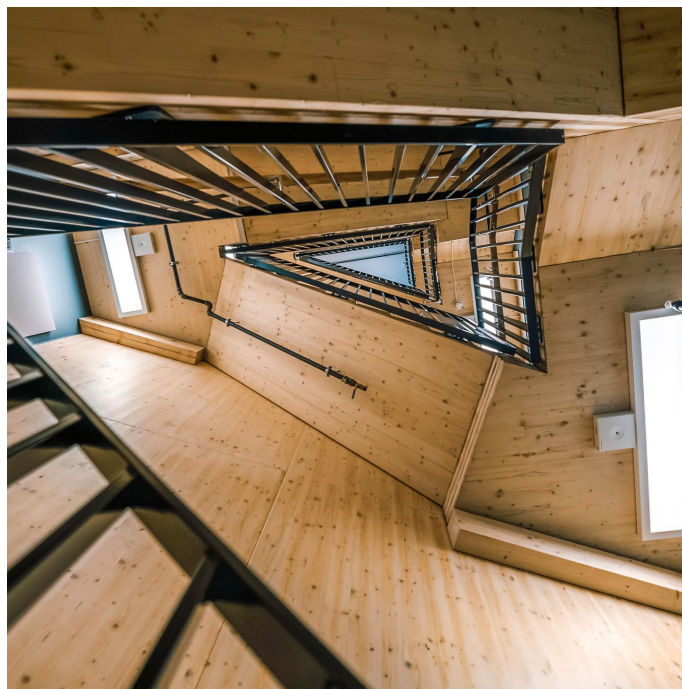
## List of Tables

Table 2.1 Heat flux levels tested in the cone calorimeter tests for each group..... 27  
 Table 2.2 Density and moisture content of the CLT samples..... 29  
 Table 4.1 Charring depth and corresponding charring rate based on temperatures in the  
 thermocouples inside the ceiling elements in the Compartment Test. .... 47  
 Table 5.1 Test group 1: set up..... 48  
 Table 5.2 Test group 1: results. .... 48  
 Table 5.3 Test group 2: setup..... 51  
 Table 5.4 Test group 2: results. .... 51  
 Table 5.5 Test group 3: setup..... 54  
 Table 5.6 Test group 3: results. .... 55  
 Table 5.7 Test group 4: setup..... 57  
 Table 5.8 Test group 4: results ..... 57  
 Table 5.9 Test group 5: setup..... 61  
 Table 5.10 Test group 5: results ..... 62  
 Table 5.11 Test group 6: setup..... 64  
 Table 5.12 Test group 6: results. .... 65  
 Table 5.13 Test group 7: setup ..... 67  
 Table 5.14 Test group 7: results. .... 68

# 1 Introduction

## 1.1 Background

European building regulations have generally assumed that the load-bearing parts of a building cannot consist of combustible materials (Kotsovinos et al., 2022). However, with higher demand from architects and users of fresh and exposed timber, this will no longer be a valid assumption. Cross-laminated timber (CLT) has emerged as a more climate-friendly alternative to steel and concrete and is used in innovative projects like the Zero Emission Building Laboratory (ZEB lab) in Trondheim. Figure 1.1 shows how CLT is used in the ZEB lab in the staircase with exposed timber in the walls and the ceiling. As more research is available, the demand for CLT in multi-story buildings increases, and using cross-laminated timber in buildings will expose large areas of combustible materials. Increasing the amount of combustible materials leads to higher intensity and duration of the fire, in addition to more rapid growth (Buchanan et al., 2022a). At the beginning of a fire, it is primarily the fire growth that is affected. In contrast, during a fully developed fire and in the decay phase, it will be critical how fast the charring moves through the timber, reducing the remaining cross-section and leading to lower load-bearing capacity.



**Figure 1.1 Exposed CLT in ZEB laboratory in Trondheim (Lolli, 2020).**

Cross-laminated timber elements consist of several cross-laminated lamellas. These are usually attached with glue. Standardized sizes in Europe vary between 20, 30, and 40 mm per layer, where a standard CLT element consists of five layers (Brandner et al., 2016). As a minimum, it must consist of three layers, and can, as a maximum, consist of eleven. As the layers lie across each other, the plates can be load-bearing in both directions, but usually, the outermost layers lie above the most loaded direction to maximize utilization

(Hasburgh et al., 2016). The most common types of wood used in CLT are pine and spruce (Reitan et al., 2019).

Studies summarized by Drysdale (2011) have shown that thermally thin materials will continue burning independent of external heat flux, while thermally thick materials will self-extinguish after a while without an external source. This indicates that building lasting load-bearing compartment parts should be possible in wood materials if they are thick enough to prevent collapse under a fire. While smaller test samples are only affected by one external heat flux source, fires in compartments will also be affected by several factors and heat from other combustible materials in the compartment. Whether timber will auto-extinguish is crucial in researching and deciding if timber materials can be used in tall buildings. Therefore, it is necessary to gain more knowledge of the use and properties of CLT during fire exposure. A vital element for CLT to extinguish is the charred layers' properties and ability to protect and insulate the unburned fresh wood and, after a while, self-extinguish when no new timber contributes to the fire. Another factor affecting the possibilities for self-extinction is the chances of char fall-off and delamination, which largely depends on the adhesive between the layers. Where char fall-off occurs, the chances of secondary flashovers increase, and wood that was going to extinction flashes up again, which again will contribute to a higher heat flux towards the rest of the materials in the compartment and can lead to a structural collapse eventually.

As to this issue with wood materials, it is helpful to investigate how charring behaves and to what degree it insulates the fresh wood under a fire. An interesting factor to look at is, therefore, already charred materials' ability to ignite for a second time and at what heat fluxes both ignition and self-extinction of fresh and charred material occur.

## 1.2 Fire Research and Innovation Centre

The master's thesis is written as a part of an ongoing research project for Fire Research and Innovation Centre (FRIC). FRIC commenced in the spring of 2019 (FRIC, 2019). The aim is to increase the knowledge of fire safety to make optimal decisions and develop better solutions to improve fire safety in buildings. FRIC is led by RISE Fire Research in Trondheim, with NTNU and SINTEF as research partners. FRIC has partners from public organizations, fire safety consultants, producers, and suppliers of building products and building installations, and property development and management. The research centre is funded by all partners, in addition to funding from the Research Council of Norway, program BRANNSIKKERHET, project number 294649.

### 1.2.1 Compartment Test by Andreas S. Bøe

As a part of FRIC, one of the experiments was conducted in the fall of 2022 by Andreas S. Bøe, where a 180 m<sup>2</sup> large compartment with exposed CLT in the ceiling was ignited from a fuel source (Bøe et al., 2023). It will henceforth be referred to as *Compartment Test*. The method and materials used in the Compartment Test will be explained in more detail in Chapter 2.2. However, the findings from the experiment used in this report are strongly limited to focus on charring, heat flux, and temperatures at given points in the compartment.



## 1.3 Research Questions

The main research question forming the basis for this study is as follows:

How does cross-laminated timber behave under various heat exposures, with particular emphasis on ignition, reignition, charring, and self-extinction?

To delimit the scope of the study, four secondary research questions have been chosen to focus on in this thesis:

1. What is the critical heat flux for unpiloted ignition of fresh and charred timber?
2. Does a flaming sample extinguish when the external heat flux is reduced, and when will it happen?
3. How do factors like density, heat flux exposure and irregularities in the surface impact the charring of CLT?
4. Is it possible to find a relationship between the mass loss and the charring rate during the fire?

Three methods have been used to answer the research questions: literature review, analysis of results from a large-scale Compartment Test by Andreas S. Bøe, and cone calorimeter testing of CLT. A literature review is conducted to map existing research on the topic, especially on the material properties of timber regarding ignition, extinction, and charring. The charring and temperature development from Compartment Test has been used to investigate how the heat moved through the material. Yet, the fundamental element to answer the research questions centers around the findings from the cone calorimeter testing of CLT under various heat fluxes.

## 1.4 Limitations

The thesis has focused on investigating the ignition, reignition, extinction, and charring properties of CLT in a cone calorimeter and comparing the results against a large-scale compartment test of the same material. The cone calorimeter testing is examined according to ISO 5660-1 (ISO, 2015) with some adjustments to get the possibility to test materials without using vast amounts of materials or costs.

Fire testing in large and small scales is delimited to yield CLT of untreated Norwegian Spruce with the density and humidity used during the tests. The cone calorimeter testing is targeted around the expected critical heat flux for ignition, reignition, and self-extinction of wood. The heat flux levels create the basis for further discussion regarding mass loss, charring, and other parameters impacting the fire. Especially results regarding charring and temperature development are used in comparisons against the Compartment Test, to investigate the differences between large- and small-scale tests. Some of the research questions will only be answered by literature and cone calorimeter testing.

Parts of the results come from Andreas S. Bøe and his publication (Bøe et al., 2023). This yields the results concerning the Compartment Test. Some of the received data is used directly, such as figures, while other data tracked during the test is used as a basis for further calculations or analysis. It is explained continuously in the thesis when this applies.

## 1.5 A Readers Guide

**Chapter 2** describes the methods and materials used in the study. The methods used are a literature study, results from the Compartment Test, and fire testing in a cone calorimeter.

**Chapter 3** reviews the theoretical basis for the assignment.

**Chapter 4** presents the chosen results from the large-scale Compartment Test conducted by S. Bøe.

**Chapter 5** presents the results from the fire testing in the cone calorimeter.

**Chapter 6** consists of a discussion of the results from the Compartment Test and the cone calorimeter test. Uncertainties and sources of errors through the testing are reviewed. Lastly, a comparison with the findings from the literature is performed.

**Chapter 7** tries to answer the research questions and conclude from these.

## 2 Materials and Methods

### 2.1 Literature Study to Map Existing Research

In order to create a basis for the upcoming experiments, acquire knowledge on the use, development, and research of mass timber, and see what knowledge gaps exist, a literature study is performed. The focus of the literature study is mass timber and its material properties regarding ignition, extinction, and charring, and gives a broader aspect on how mass timber behaves under fire exposures.

A literature review can be qualitative or quantitative, depending on the aim of the study. In this project, it has been necessary to conduct both types. Through qualitative research, it has been possible to establish a theoretical basis for the upcoming cone calorimeter test and the knowledge to analyze results from the large-scale Compartment Test by (Bøe et al., 2023). In the quantitative study, results from earlier research have been presented to investigate how other fire tests have ended and what parameters that has been crucial for the outcome.

Some principles for choosing sources are used to ensure that the sources used in a literature review are trustworthy and relevant. Source criticism is a process of evaluating the credibility of both the sender of the information and the information itself (NTNU, n.d.). This involves assessing the source's relevance, the type of documents, the aging of the publication, and where it is published. It should also be considered what methods are used in the document, how the document is structured, and their sources. Another essential step in evaluating sources is to check if the document has been peer-reviewed. The goal of source criticism is to assess credible and accurate information for the given purpose that is unbiased and trustworthy.

The literature used in the study is based on peer-reviewed articles and publications. A peer-reviewed article has gone through a quality assessment to ensure the validity (BioMed Central, 2023). It makes the publications more useful and easier to read, in addition to ensuring that the content fulfills the requirements for originality, validity, and significance. The peer-reviewed articles used are therefore considered a trustworthy and reliable source as a basis for the thesis.

#### 2.1.1 Reuse of Material from the Project Thesis

As a part of an earlier semester in the master's degree, a literature study was written in the same study field, mass timber. The focus of the thesis was mainly on charring and charring rates for CLT under a variety of heat exposures. Unlike the literature review conducted in the previous semester, the range of this master's thesis is more focused on the necessary heat flux for ignition and extinction of fresh and charred timber, and what parameters that will affect this. Hence the different focus, a new literature study has been conducted to find relevant literature, but the previous review is a basis for this thesis.

The project thesis is not published and cannot be referenced directly. Therefore, the theory seen as necessary is reused in this thesis, either as a direct transcript or rewritten and implemented together with new findings.

Sections that have been reused in the thesis can be found in:

- Chapter 1.1. Parts of the first section, and the second section.
- Chapter 3.1. The whole section.
- Chapter 3.3. The whole section.
- Chapter 3.4.3. The first two sections.

## 2.2 Setup and Method for Analysis of the Compartment Test

In August and September of 2022, Andreas S. Bøe conducted a large-scale fire test. The test was conducted at the RISE Fire Research facility in Trondheim, where a compartment was constructed using ceiling elements made from CLT. The experiment aims at investigating how large areas with exposed CLT affect the fire dynamics and spread. Information regarding the setup of the Compartment Test is received from Bøe et al. (2023). Figure 2.1 is based on this information, and Figure 2.2 is captured before test start in the Compartment Test.

### 2.2.1 Compartment Setup

Exposed timber was present in the ceiling of the test, while gypsum boards encapsulated the walls. All ceiling elements consisted of five-ply CLT where the two outer layers were 40 mm, and the three inner layers were 20 mm. The CLT consisted of Norwegian spruce with a humidity of approximately 12 %. The adhesive used between the plies was Henkel Loctite PUR, a non-heat-resistant adhesive.

The dimensions of the compartment are 18,8 m x 5,0 m x 2,45 m, where the front walls mainly consisted of four large openings split up by insulated columns, giving an opening factor of 0,16 m<sup>1/2</sup>. In the front wall where the openings are, there is also a beam encapsulated in fireproof insulation that goes 40 cm down from the compartment top. Temperatures have been measured continuously through thermocouples (TC) and plate thermocouples (PT) during the tests at several locations, but a few data points are chosen to analyze. Figure 2.1 illustrates the compartment setup, showing the façade of the back wall and the front wall with openings, in addition to a floor plan showing the location of the ignition point, relevant thermocouples and plate thermocouples. The black squares illustrate the placement of the plate thermocouples, and the white circles illustrates the placement of the thermocouples that have been used in the following analysis.

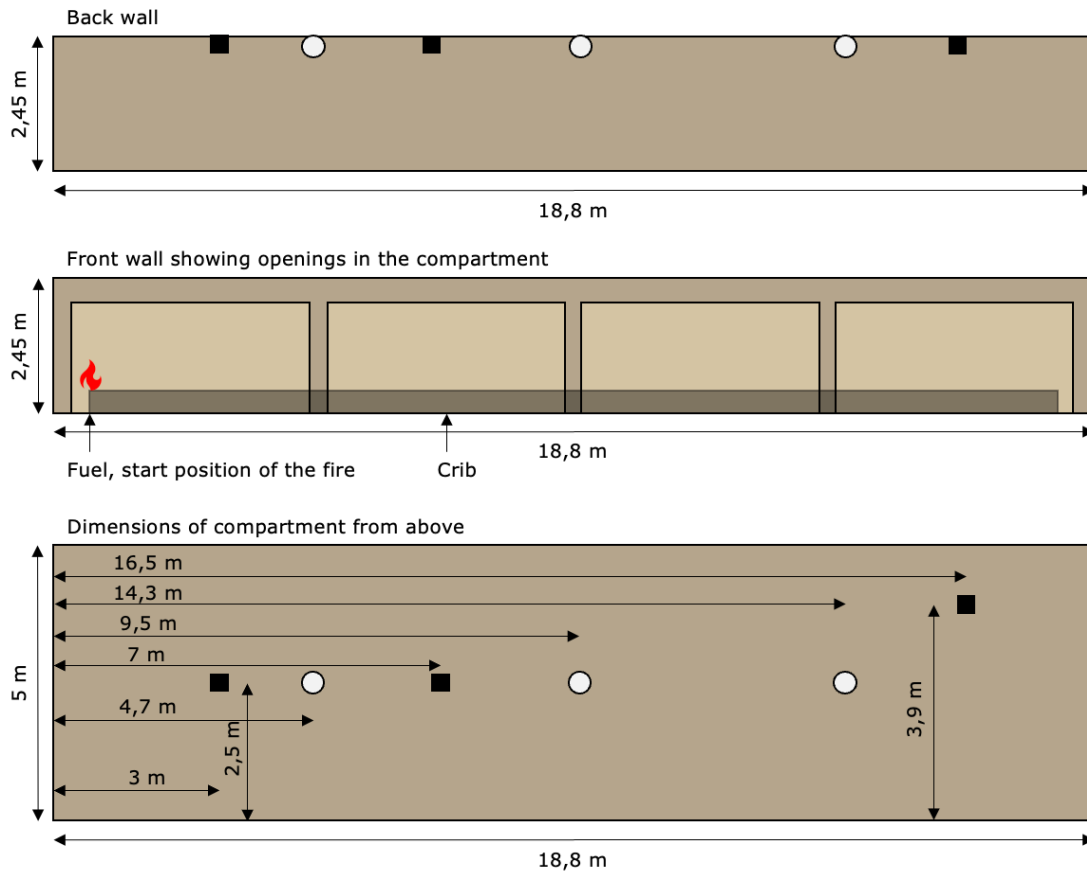


**Figure 2.1 Sketch of compartment setup showing locations of PTs (black square) and TCs (white circle).**

The fire load inside the compartment represents the fuel in offices, living rooms, and dining rooms and is approximately  $420 \text{ MJ/m}^2$ . It was represented by a large wood crib consisting of long wood sticks of Norwegian Spruce with dimensions  $50 \text{ mm} \times 50 \text{ mm}$  in the middle of the compartment, as shown in Figure 2.2. The dimensions are approximately  $2,8 \text{ m} \times 16,6 \text{ m} \times 0,4 \text{ m}$ , placed about  $1 \text{ m}$  from all the walls. The sticks were stacked in four cross layers with a  $50 \text{ mm}$  distance between each other. Five liters of heptane were used as fuel to ignite the compartment in the location shown in Figure 2.1.



**Figure 2.2 Wood crib inside the compartment representing a fuel load for an office or living room area.**

### 2.2.2 Temperature Measurements in the Compartment Test

Thermocouples of type K and plate thermocouples were used to measure the temperature inside the compartment and inside the CLT elements. The thermocouples have been placed at several locations spread evenly across the compartment, covering different heights and depths. So has the plate thermocouples but with fewer measurement points. The location of the relevant thermocouples and plate thermocouples from where the measurements were registered can be seen in Figure 2.1.

The thermocouples inside the ceiling elements are placed at 0 mm, 10 mm, 20 mm, 30 mm, and 40 mm from the exposed surface. This will make it possible to measure how temperature develops through the material, which can help predict the pyrolysis process in the wood. The different locations that were used is 4,7 m, 9,5 m, and 14,3 m, from the start position of the fire. All TCs was placed 2,5 meters from the window side, corresponding to the middle of the compartment.

Temperatures in the TCs and PTs are measured in °C. Data concerning temperatures is received from Andreas S. Bøe. A transformation from °C to heat flux in kW/m<sup>2</sup> is calculated in this thesis, following the procedure described in Wickström (2016), Chapter 9.3.2, equation 9.18, using the standardized constants he lists in the chapter, and can also be seen in Wickström-equation below, with belonging values. The temperature from the PTs and the ambient temperature from the TCs from Compartment Test is inserted in the equation, giving the results in kW/m<sup>2</sup>, and presented as graphs in Chapter 4.1.

$$q''_{inc} = \sigma T_{PT}^4 - \frac{1}{\varepsilon_{PT}} \left[ (h_{PT} + K_{PT})(T_g - T_{PT}) - C_{PT} \frac{dT_{PT}}{dt} \right] \quad (\text{Wickström, 2016})$$

Where  $q''_{inc}$  is the incident radiation,  $\frac{dT_{PT}}{dt} \cong \frac{\Delta T_{PT}}{\Delta t} = \frac{T_{PT}^{j+1} - T_{PT}^j}{t^{j+1} - t^j} = \frac{T_{PT}^{j+1} - T_{PT}^j}{\Delta t}$ ,  $T_{PT}$  is the temperature from the plate thermocouples [K],  $T_g$  is the temperature in the thermocouples [K],  $\Delta t$  is the time interval between the time measurements [s],  $\sigma$  is the Stefan Boltzmann constant and is equal to  $5,67 * 10^{-8} \frac{W}{m^2 K^4}$ ,  $\varepsilon$  is the emissivity and is assumed to be 0,9,  $h_{PT}$  is the convection heat transfer coefficient for the plate and is set equal to  $10 \frac{W}{m^2 K}$ ,  $K_{PT}$  is the

thermal conduction coefficient and is set equal to  $8 \frac{W}{m^2K}$ , and  $C_{PT}$  is the heat capacity coefficient for the plate and is set equal to  $4200 \frac{J}{m^2K}$ .

### 2.2.3 Charring Depth Measurements

Two methods have been used to measure the charring depth from the Compartment Test. The first method directly measures the charring from the ceiling elements, as most of the ceiling elements were cooled down and saved for further measurements after the conducted test. The charring depth measurements were executed by drilling holes through the elements in a grid of 50 cm x 50 cm, as seen in Figure 2.3. Then, brushes were used to scrape around the holes to get rid of char and find fresh wood to measure the depth of the remaining unburned wood. Finally, as seen in Figure 2.4, calipers were used to measure the depth, and the results were put into a table to map how the charring behaved in the elements.



**Figure 2.3 Holes in the ceiling elements from the Compartment Test, in 50 cm x 50 cm grids used for charring depth measurements.**



**Figure 2.4 Caliper used to measure charring depth from ceiling elements used in the Compartment Test.**

The other method used to measure charring from the Compartment Test is using the TCs placed inside the CLT elements to investigate the temperature development inside the elements. The results are illustrated in graphs to present how the temperature develops through the material and is used to calculate charring, considering wood chars at approximately 300 °C (Kleinhenz et al., 2021).

## 2.3 Fire Testing in Cone Calorimeter

The fire testing in the cone calorimeter is based on the test method described in ISO 5660-1 but with some adjustments to achieve the desired data (ISO, 2015). The method is used in fire modeling and engineering to make a prediction model for more extensive fires, product development, and product testing (RISE Research Institute of Sweden, n.d.). The method is cost-effective and time-effective, and therefore easy to test products for control or as preparations for more extensive tests.

To conduct a test in the cone calorimeter, a sample with maximum dimensions of 100 mm x 100 mm x 50 mm of the desired material is inserted below a cone heater at selected heat flux levels (ISO, 2015). The cone calorimeter is equipped with a spark igniter, but it has not been used in the tests. When the material is exposed to a heat flux, it heats up and emits gases, eventually igniting it, as described in Chapter 3.4.1 and Chapter 3.4.3. Gases from the sample is collected in the cone, where it goes through ventilation, cleansing, and measuring to collect data continuously. This data calculates the heat release rate, smoke production, and the content of other gases released during the test. A weight is continuously measuring the mass loss and mass loss rate during the tests.

The purpose of conducting these tests is to understand better how CLT and wood generally react under different conditions and how charring affects the properties of ignition and extinction of timber. During the tests, time to ignition, reignition and extinction is measured in addition to a continuous weighting of the sample and the temperatures within the sample.

### 2.3.1 Cone Calorimeter Setup

The cone calorimeter test machine consists of three parts as shown in Figure 2.5; the computer to the left, the rack in the back, and the cone calorimeter to the right. Figure 2.6 shows the retainer with the sample covered with a gypsum lid, inside the cone.

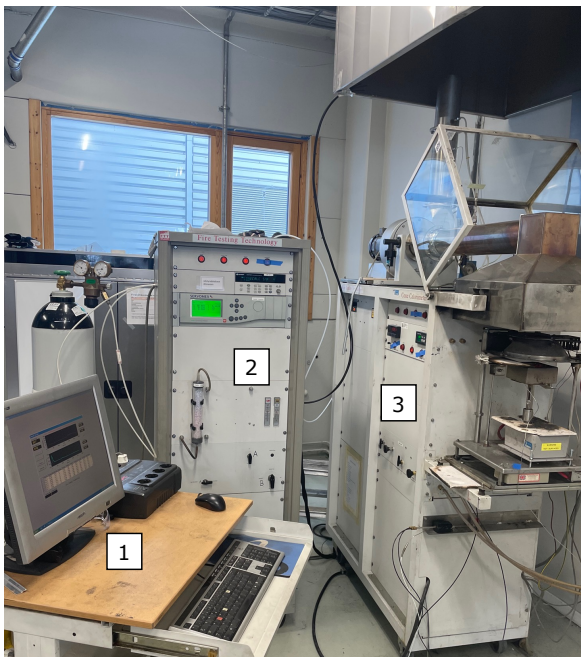


**Figure 2.5 Cone calorimeter. 1: computer. 2: rack. 3: cone calorimeter.**

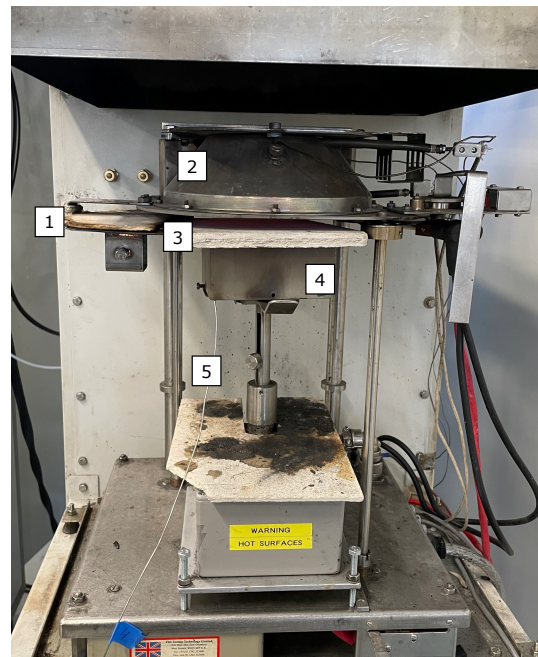


**Figure 2.6 Retainer with a sample covered with a gypsum lid in the cone calorimeter. 1: built-in lid. 2: cone heater. 3: gypsum lid on top of sample. 4: sample inside container. 5: wire from thermocouple.**

The heat flux in the cone is adjusted by changing the temperature in the heater, representing a given heat flux. Some heat fluxes are known from before, as shown below in Figure 2.7 as black dots. These values are used in interpolation on the graph to determine which temperatures represent the desirable heat fluxes used in the experiment, as shown in green below.



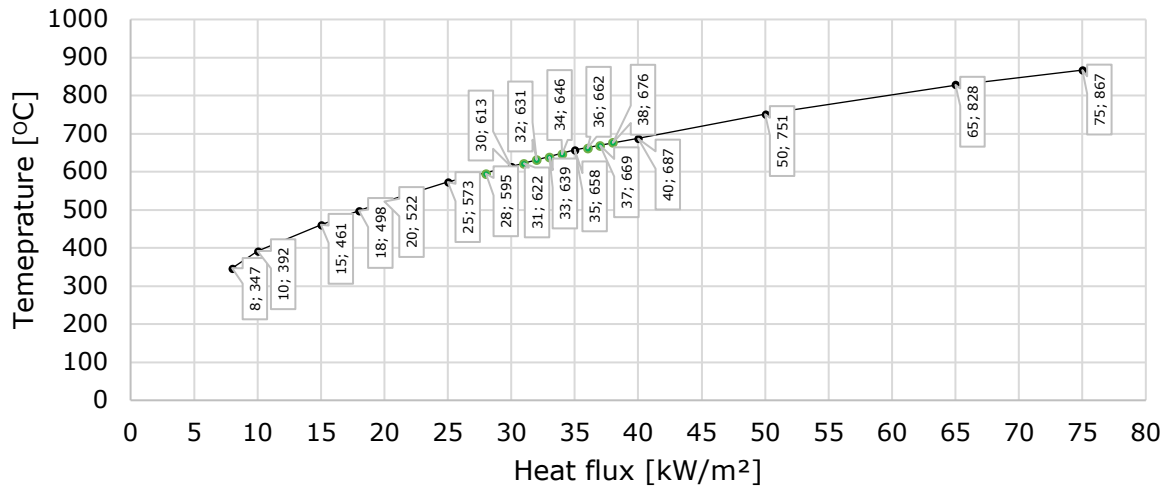


**Figure 2.7** Temperatures with corresponding heat fluxes radiating from the cone towards the sample. The first number represents the heat flux and the last represents the temperatures.

After each test, information tracked continuously during the test is collected and processed, and the desired data is inserted into the system of tables or diagrams. The tables give a systematic overview of the information, while the diagrams illustrate the fire development used to compare the tests against each other.

Looking at trend lines in the diagrams has been used to see if there are some relations between the various factors. The regression number,  $R^2$ , is used to investigate if the trend lines are trustworthy and considered good enough. This number is used to measure how convenient the strength of the relationship between your model and the dependent variable is, from 0 to 1, where a perfect trend line is up against 1 (Frost, 2018). This is related to the variation of the variables spread over a period and how the variables correlate to each other.

### 2.3.2 Temperature Measurements

Thermocouples have been used at different depths inside the samples to measure how temperature develops during the fire. The depths chosen are 15 mm, 20 mm, 25 mm, and 30 mm, in one of the samples in each test situation, and a TC at 25 mm in all the samples. Placements of the TCs in the samples can be seen in Figure 2.8. Further mentioning of the thermocouples goes by *TC15*, *TC20*, *TC25* and *TC30* for each depth. The various depths are chosen because a charred layer of 25 mm will work as insulation for the inner wood (CEN, 2010). It is, therefore, useful to know when the temperature in these depths reaches 300 °C and marks a point for when to reduce the heat flux.

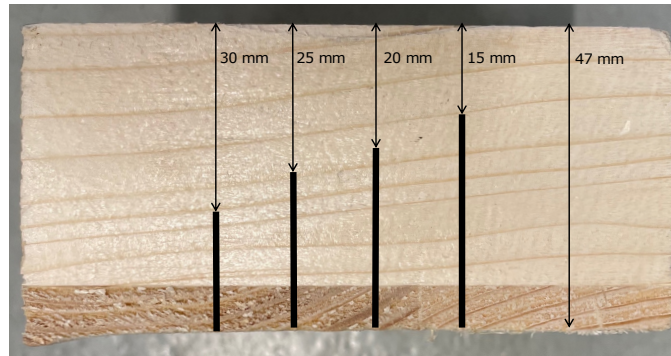


**Figure 2.8 Sample showing TC depths in the samples with four thermocouples. For samples with one thermocouple, only the placement of the TC at 25 mm is valid.**

### 2.3.3 Test Procedure

The test method used in the experiment is inspired by ISO 5660-1 and is based on the same principles but with adjustments (ISO, 2015). This is because there is no standardized test method for adjustments of heat flux during the test period, and changes were required to study the desired outcome. The test procedure for the cone tests is as follows:

#### **Phase 1.1**

The sample was positioned in the cone calorimeter when the desired temperature in the cone was reached, and the countdown to ignition started. If ignition occurred within 15 minutes, the testing went to Phase 2. If ignition did not occur within 15 minutes, the test went to Phase 1.2.

#### **Phase 1.2**

The temperature in the cone was increased to a higher heat flux while the sample remained inside and the countdown to ignition started when the cone had reached the desired heat flux. If ignition occurred within 15 minutes, the testing went to Phase 2. If ignition did not occur within 15 minutes, the sample stayed in the cone and redid Phase 1.2 until TC25 reached 300 °C.

#### **Phase 2**

When TC25 reached 300 °C, the built-in lid was positioned over the sample and the time to extinction was measured. After extinction, the built-in lid was replaced with the gypsum lid to completely cover the sample from the heat exposure. After five minutes with no visible flames, the test continued to Phase 3.

#### **Phase 3**

To continue the test, the temperature in the cone was adjusted to the desired heat flux and the lid was removed. The charred sample remained under the cone and a countdown to ignition started. If ignition occurred within 15 minutes, the testing went to Phase 4. If ignition did not occur within 15 minutes, the test was over, and the sample was removed and cooled down.

#### **Phase 4**

After ignition, the heat flux was adjusted, and the sample burned for the next 15 minutes unless self-extinction occurred. The test ended if extinction happened or if no extinction was observed within 15 minutes.

Twenty-three test samples were used in the tests, divided into seven test groups following the procedure described above. Each test group consists of a minimum of three samples underlying the same process, according to ISO 5660-1 (ISO, 2015). Adjustments from one test group to the next are made by the following principles:

- If the sample ignites → decrease the heat flux for the next group.
- If the sample do not ignite → increase the heat flux for the next group.
- If the sample extinguish → increase the heat flux for the next test group.
- If the sample do not extinguish → decrease the heat flux in the next test group.

To ensure that the samples not only extinguish in Phase 4 because of little to no burnable materials left, some tests are also conducted where Phase 2 is replaced with Phase 4 with a decreased heat flux instead of a lid before it continues in Phase 3. In this case, where no extinction occurs, it returns to Phase 2 with a cover to extinguish the test before continuing as described above. This is stated in the relevant tests.

When the critical heat flux for self-extinction has been tested with the same heat fluxes used for ignition, the time countdown to extinction started to measure from where the HRR is observed to be in a steady-state.

### 2.3.4 Heat Flux Levels Tested in the Cone Calorimeter

An overview of the heat flux levels tested in the cone calorimeter tests for each phase can be found in Table 2.1.

**Table 2.1 Heat flux levels tested in the cone calorimeter tests for each group.**

Test group	Phase 1 Heat flux on fresh timber [kW/m <sup>2</sup> ]	Phase 2 Heat flux for extinction [kW/m <sup>2</sup> ]	Phase 3 Heat flux on charred timber [kW/m <sup>2</sup> ]	Phase 4 Heat flux for extinction [kW/m <sup>2</sup> ]
1	40	0	30	-
2	35	0	50	30
3	30	0	40	40
4	33	0	35	-
5	32	30	38	30
6	31	25	37	37 and 25
7	32, 33 and 34	25 and 28	36 and 37	36 and 37

### 2.3.5 Samples

All the samples used in the experiment are taken from the same ceiling element used in the large-scale test by Andreas S. Bøe, as seen in Figure 2.9. As large parts of the elements are already burnt in the fire, the components used from the elements faced up during the Compartment Test with no direct heat exposure and shows no signs of fire on the small samples. From the time of the test was performed in the fall of 2022, the elements have been stored under a tarpaulin until February 2023. At this time, the samples were cut from one side of the CLT-element and adjusted into smaller samples with dimensions 100 mm x 100 mm x 47 mm, which gives a volume of 0,00047 m<sup>3</sup>. As described in ISO 5660-1, samples thicker than 50 mm shall be cut on the unexposed side to fit the container, and the samples do therefore consist of the outer layer at 40 mm, which contains the surface that will face the cone heater, and a small part of the second inner layer facing down in the retainer. The temperature in the room at the testing time varied between 20,9 – 22,1 °C.



**Figure 2.9 The back of a ceiling element from the compartment test. The unexposed back is used to cut samples used in the cone calorimeter tests.**

After cutting the samples into the right dimensions, the samples were weighed and stored in a climate room with humidity at 50% and temperature at 23 °C for over a month to reach a stable humidity and temperature, as described in NS-ISO 554:1976 (ISO, 1976). Before testing, the samples were regularly weighed to control that the weight remained stable around the time of the test. Each sample was also measured with a moisture meter to verify that every sample had reached approximately the same conditions. The density varied from 377 kg/m<sup>3</sup> to 565 kg/m<sup>3</sup>, and the humidity from 8,0 % to 9,0 %, see Table 2.2.

**Table 2.2 Density and moisture content of the CLT samples.**

Test ID	Weight (g)	Density (kg/m <sup>3</sup> )	Humidity (%)
1-1	223	475	8,6
1-2	224	476	8,5
1-3	266	565	8,3
2-1	228	485	8,9
2-2	194	412	8,1
2-3	198	421	8,9
3-1	206	439	8,0
3-2	184	393	8,0
3-3	206	437	9,1
4-1	178	380	8,2
4-2	193	411	8,5
4-3	209	444	8,5
5-1	177	377	8,3
5-2	242	515	8,9
5-3	193	410	8,3
6-1	183	389	8,4
6-2	225	478	8,7
6-3	202	430	8,5
7-1	181	385	9,2
7-2	183	389	9,0
7-3	205	435	9,0
7-4	184	392	8,8
7-5	184	392	8,5

Before the test, all samples was packed in aluminum foil to avoid heat from anywhere other than the cone above and placed in the retainer with the thermocouples, as seen in Figure 2.10 and Figure 2.11.



**Figure 2.10 CLT sample inside the aluminum foil before testing seen from the side.**

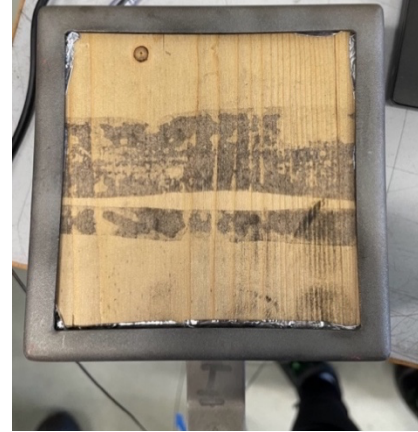


**Figure 2.11 Fresh CLT sample inside the retainer before testing.**

## 3 Literature Review

### 3.1 Fire Development

A fire depends on three factors to burn: burnable material, oxygen, and high temperatures (Reitan et al., 2019). The availability of these factors decides if a fire is fuel-controlled or ventilation-controlled. For example, good access to oxygen gives a fuel-controlled fire where the quantity of fuel determines when the fire decays, while a lack of oxygen provides a ventilation-controlled fire. For the latter, gases and flames are pushed through openings. This may contribute to fire spreading from the initial starting point if the surrounding materials are not adequately protected.

During the growing stage of a fire, the spread will be controlled by the possibility of ignition (Buchanan et al., 2022b). For that reason, it depends on the types of combustible fuel exposed to the fire and how it is distributed in the room. In addition, the burning objects' heat release rate and the surrounding objects' burnability will determine the spread. In this stage, the fire mostly depends on the unburned material already heated from the fire, and initial fire spread may come from heat transfer from one burning material to another.

The spread along the floor surface causes hot gases to spread up toward the ceiling due to buoyancy (Buchanan et al., 2022b). As a result, a layer of gas is formed in the ceiling, radiating heat down towards the unburnt materials. In this process, the temperature will gradually rise and contribute to a faster ignition of the materials, which can lead to a flashover. This process steers a fire from the growth stage to a fully developed fire. At the transition between the growth stage and a fully developed fire, it will go from being fuel controlled to being ventilation controlled. In cases where the walls or ceilings are also in combustible materials, flashovers could occur even earlier in case the amount of available fuel increases. Materials that delaminate can lead to a repetition of this process and lead to second flashovers. In cases with large combustible areas combined with large openings, the lack of oxygen can spread toward nearby buildings of exposed flammable materials. Figure 3.1 shows how the fire develops over time, showing the decay phase in dark grey and the situation where the fire reignites and leading to second flashovers occur in light grey.

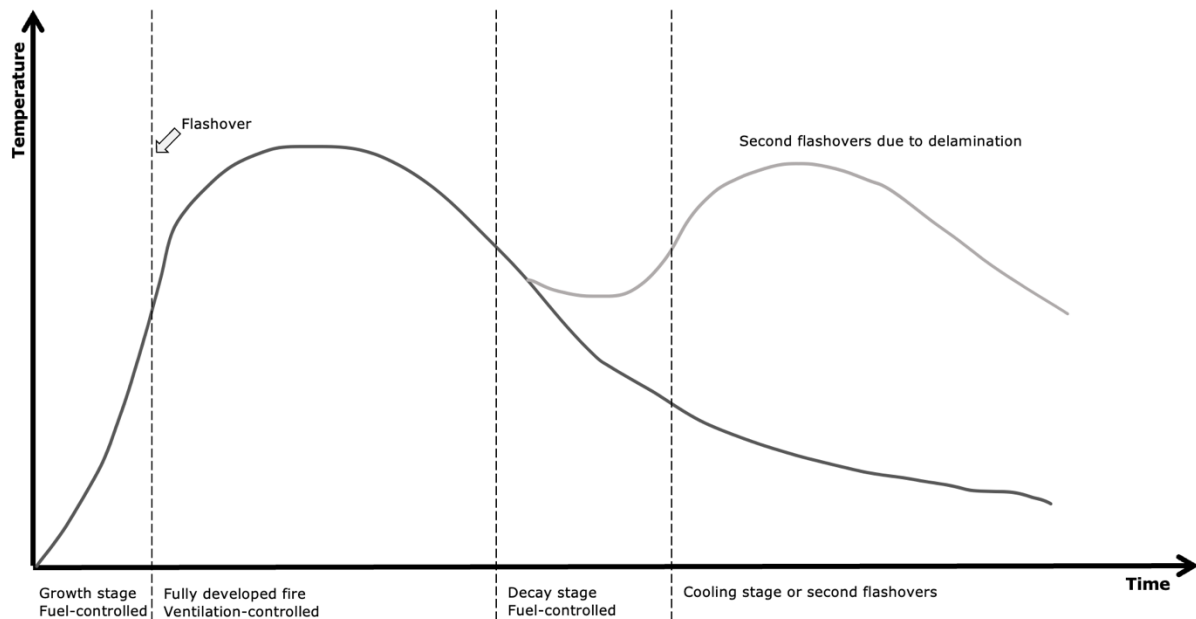


**Figure 3.1 Fire development over time. A fire going to decay is shown in dark grey and a fire that reignites and gets second flashovers is shown in light grey.**

After a while, the supply of combustible material will decrease, and the fire will turn into a fuel-controlled fire (Buchanan et al., 2022b). In an uncontrolled fire, this phase will be called burnout. To achieve adequate fire safety in this phase, it is essential that there has not been a structural collapse or further fire spread to other nearby rooms or buildings. Even though the fire is in the reduction phase, it can continue to crumble into the wood materials. As mentioned earlier, this can contribute to delamination and new contributions to the fire, in addition to a more significant weakening of the bearing capacity. Therefore, it is crucial to extinguish the fire properly for timber materials.

Even though timber materials are not classified as non-combustible, they have traditionally been considered a safer alternative than common plastic materials or synthetic alternatives often seen in furniture (Buchanan et al., 2022b). This is because wood materials have a higher heat flux necessary for ignition and a lower flame spread rate. Another factor that can make wooden materials a good alternative is the possibility for improvements in the fire properties. There are fire-retardant paints or chemical treatments that can be used on timber. Nevertheless, these are not solutions that will work well under flashovers.

### 3.2 Steady-State and Transient State

A fire development can be described in two terms: either as a transient burning fire or a steady burning fire (Emberley, Putynska, et al., 2017). The steady-state describes a period when the heat release is constant over time, and the materials burn consistently and evenly. This often happens when the supply of fuel, oxygen, and other conditions are optimal. The opposite of a steady-state is a transient fire. The fire burns unevenly in this stage, and the heat release changes over time. This is typical at the beginning of a fire when the condition for burning is not optimal, or if changes in the surroundings around the fire occur and can be seen as a peak in the heat release rate. Recognizable signs of a transient fire are changes in temperature, heat release, flame height, or other parameters changing, and is typically observed before the fire reaches steady-state. Earlier research by Emberley, Do, et al. (2017) has shown that samples must burn for about 10-15 minutes



to ensure steady-state conditions. A steady burning fire can be recognized by consistency in HRR, temperature, and flame height.

### 3.3 Theoretical Fire Curves

Theoretical fire curves are mathematical representations or models showing how a fire is expected to behave over time and in terms of temperature (Promat, 2020). It does not necessarily follow the same fire development described in Chapter 3.1, and theoretical fire curves can be nominal or parametric.

#### 3.3.1 Standard Fire Curves

The standard time-temperature curve, or ISO 834-curve, shows the dependency in a fully developed fire (ISO, 1999). It does not represent a real fire but is a nominal curve showing the gas temperature during a fire and is a standardized method for testing the fire resistance of building materials. In addition, the curve is the most common way to classify building materials.

#### 3.3.2 Parametric Fire Curves

In addition to nominal curves, we also have parametric curves. These are meant to create a more realistic picture of fire development concerning time and temperature and are described in NS-EN 1991-1-2, appendix A (CEN, 2008). According to Lucherini et al. (2021), parametric fire curves are the most adopted method to replicate a natural fire exposure for structural elements. These are based on fire loads, geometry, and the thermal properties of the case to be examined and will, in addition to the growth phase, also include the cooling phase of the fire. A numerical analysis to quantify the maximum temperature, duration, and cooling rate for a specific compartment must be conducted to find the natural fire curve for a fire.

### 3.4 Informative Parameters in a Fire

Several parameters will impact the characteristics and behavior of a fire. Understanding these parameters is crucial for analyzing the fire development and investigating how CLT reacts under different fire exposures. The following sections will describe some of these.

#### 3.4.1 Ignition

Ignition can be split up into two different types: piloted ignition and unpiloted ignition, and combustion can be represented as smoldering, glowing, or flaming (Liodakis et al., 2006). A spark or a flame is necessary to start the fire for a piloted ignition. In contrast, an unpiloted ignition only needs heat to gather the energy required to start a fire (Bartlett et al., 2019). The criteria for ignition can be expressed through the critical heat flux or the critical surface temperature, representing the lowest heat flux exposure or the lowest surface temperature needed for ignition. From ISO 5660-1, the critical heat flux for ignition is the average between the highest heat flux that did not cause ignition and the lowest heat flux that caused ignition (ISO, 2015). It is often found during a relevant time interval, where a period of 15 minutes is used for tests following the procedure from ISO 5660-1. Research carried out by Bartlett et al. (2017) has shown that critical heat flux for piloted ignition in timber materials usually varies between 10-13 kW/m<sup>2</sup>, specified by Babrauskas (2002) to 12,5 kW/m<sup>2</sup>. On the other hand, unpiloted ignition needs a heat flux of around 25-33 kW/m<sup>2</sup> to ignite (Babrauskas, 2002).

Nevertheless, DiDomizio et al. (2016) have conducted tests where they found no ignition at heat fluxes as high as 37 kW/m<sup>2</sup> for Canadian pine, where the critical heat flux was found to be 38 kW/m<sup>2</sup>. This was also seen in studies by Emberley, Do, et al. (2017), where the pine and spruce used in the tests needed heat fluxes as high as 43 kW/m<sup>2</sup> to auto-ignite. Opposite, different kinds of piloted ignition also require varied heat exposure to ignite, and studies by Simms and Hird (1958) have shown that impinging ignition needs as little as 4,2 kW/m<sup>2</sup> to ignite for Colombian pine.

For the reignition of charred timber, Terrei et al. (2019) conducted tests to investigate how charred timber reacted to heat fluxes of 55 kW/m<sup>2</sup> and 75 kW/m<sup>2</sup>. It showed that reignition occurred every time for the latter, but no systematic occurrences were found for 55 kW/m<sup>2</sup>. However, the thermal degradation was the same whether the sample flamed or not.

Another way of calculating the critical heat flux for ignition is presented by Janssens (1991). By testing materials in cone calorimeters, the information on the time to ignition at different heat fluxes can be collected. The method shows how the ignition time of a thermally thick material correlates with the heat flux using a piloted ignition. When plotting in the heat flux and the transformed time to ignition,  $t^{0,547}$ , the points will fall on a straight line, showing the approximately critical heat flux for ignition of the material, where the line crosses the x-axis. An example can be seen in Figure 3.2 showing the correlations found by Janssens for some wood species. This makes it possible to predict the critical heat flux for a material using only two parameters. Nevertheless, it should be mentioned that it may be necessary with a slightly higher heat flux than shown in the plotting to make the sample ignite (Babrauskas, 2002). This can be a result of the fact that the critical heat flux is, as already mentioned, the lowest heat flux to make a sample ignite over a long time and that the time to make it ignite is too long to use in a test, causing the result to have a slight margin of error.

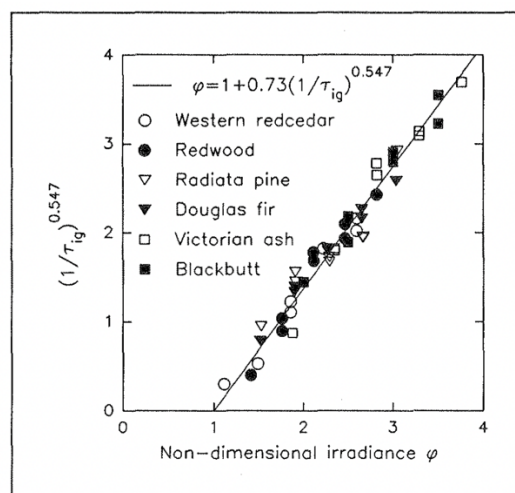


**Figure 3.2 Some of the correlations found by Janssens (1991) for piloted ignition on different oven-dried wood materials.**

While the heat flux is more predictable and often depends on the wood species, the critical surface temperature will vary based on external factors such as density, thickness, moisture content and arrangement, and is harder to predict precisely (Bartlett et al., 2019). Another factor essential for understanding when ignition will occur is the gas phase in the pyrolysis process. In this process, through increasing temperatures, gases from the timber are released, and a flammable mixture is created. Together with the temperature, the volatile composition of gases will create a combination optimal for fire to occur.

### 3.4.2 Extinction

For flames to occur and continue to burn in timber elements, it is necessary with an external heat source high enough to create flames. The most crucial parameter to sustain this burning is the external heat flux and the oxygen concentration around the fire (Buchanan & Östman, 2022). Another factor critical for flaming combustion is enough burnable material left and the size and orientation of the surface towards other surfaces. When large parts of the burnable material are used, the combustion decreases, and the fire goes from flaming to smoldering combustion. Smoldering combustion can sustain smoldering for a long time, whether there is an external heat source or not, as long as there is enough material. Going the other way to a flaming combustion is more complex and cannot be predicted like the opposite. In cases where this transition does occur, flaming combustion is often seen to start at the edges of the material.

For flames to extinguish while there are still materials left to burn, it is necessary to reduce the heat exposure over time, and the same conditions yield both ignition and extinction (Bartlett et al., 2019). Reduction in flames can lead to extinction, either as self-extinction caused by lack of temperature and heat flux, or because of external suppression methods like water or other ways to cool down or suffocate the fire.

Self-extinction can, as already mentioned, occur when the external heat exposure to the material is removed. This happens as the heat flux from the flames itself is not strong enough to sustain the fire over time (Emberley, Putynska, et al., 2017). Critical mass loss and the external heat flux will therefore be two critical and dependent factors in sustaining flames or extinction to occur and is necessary to identify.

During the transient state of the fire, self-extinction can occur at relatively high heat fluxes, while at a steady-state, the flammable fire will continue until the heat flux goes below a critical value (Emberley, Putynska, et al., 2017). On the other hand, the critical mass loss rate will be constant for both the transient and steady-state. Because of these qualities during the steady-state, the most critical phase a fire can reach is the steady-state, as the fire sustains at lower heat exposures.

Bartlett et al. (2016) conducted a series of tests on mass timber to investigate how flames varied under different heat exposures. The samples were exposed to a one-dimensional heat transfer with a constant heat transfer, in addition to a two-phase test where the heat flux was reduced after a time to see how and if the flames sustained with lower heat fluxes. The heat flux used in the tests varied from 14 to 35 kW/m<sup>2</sup>, and the critical heat flux for piloted ignition was between 13 and 14 kW/m<sup>2</sup>. A division at 31 kW/m<sup>2</sup> was found in the tests with constant heat flux. Tests below this number would eventually extinguish, while tests above 32 kW/m<sup>2</sup> sustained flammable until termination. The critical mass loss rate in the same tests was 3,48 g/m<sup>2</sup>s. In the two-phase tests, it began with a heat flux at 40 kW/m<sup>2</sup> and was, after a while, reduced to 15 – 31 kW/m<sup>2</sup>, where extinguishment occurred every time, except for two of the tests with a heat flux at 31 kW/m<sup>2</sup>. Therefore, the critical heat flux for extinguishment in these tests would be 31 kW/m<sup>2</sup>. Bartlett et al. (2019) tested 12 samples at 30 kW/m<sup>2</sup> where all samples self-extinguished. At 40 kW/m<sup>2</sup>, no extinction was seen.

Another test conducted by Emberley, Do, *et al.* (2017) showed that the critical heat flux for self-extinction was as high as 43,6 kW/m<sup>2</sup>. It was also stated that for self-extinction to be consistent and predictable, and a phenomenon that could be used in a design, the CLT should have remained intact during heat exposure to the sample.

### 3.4.3 Charring

Wood exposed to high temperatures undergoes a charring process. Browne (1958) identified different stages of a pyrolysis process. The first stages go up to 200 °C and the wood dehydrates, breaking down cellulose, lignin, and hemicellulose, releasing small amounts of CO<sub>2</sub>, formic acid, and acetic acid. The volatile substances released from the timber are not flammable. Second stage goes from 200 to 280 °C. A slow pyrolysis starts and releases CO<sub>2</sub>, formic acid, acetic acid, and toxic gases like carbon monoxide. Wood begins to char, resulting in a brown color in the wood. The next stage goes from 280 °C to 500 °C, and the pyrolysis intensifies and generates flammable gases like methane and formaldehyde, along with other gases and compounds. Smoke and combustible gases arise from the tar, igniting upon contact with oxygen. The wood continues to char, forming an insulating layer. The last stage goes from 500 °C and above, and the charring starts to penetrate deeper into the wood to access more flammable materials. The remaining cross-section becomes smaller and has reduced bearing capacity compared to its original state. According to Friquin (2011), wood is considered charred when the temperature reaches 280 to 300 °C. This is specified by Kleinhenz et al. (2021) and NS-EN 1995-1-2, who defines 300 °C as the limit for timber to char (CEN, 2010).

Charring, cracks, and irregularities in the surface can affect the mass- and heat transfer from the surface (Frangi et al., 2008). Nevertheless, charring is considered a uniform and constant process for standard wood but does not apply to cross-laminated timber made of wooden planks, considering that the planks are cross-laminated and bonded with glue. Studies by Frangi et al. (2008) have shown that the charring is the same for CLT and regular wood until the first layer is charred. Later, the charring rate increases in the CLT. Char oxidation can occur even in the absence of visible flames, as long as there is a supply of oxygen. The composition and rate of gases present on the surface can also influence the charring rates. Research conducted by Schmid et al. (2019) demonstrates the impact of gas and oxygen concentration, as well as the rate of gas movement across the material's surface, on the contraction of charring. Moreover, the thermal exposure within a room can introduce variations in charring, resulting in uneven charring rates. These findings have implications for the divergent outcomes observed in standard fire tests compared to those conducted under natural fire conditions.

Charring rates for wood can be generalized and taken from NS-EN 1995-1-2, varying from 0,5 mm/min to 0,65 mm/min depending on wood types for one-dimensional charring, where softwood has higher charring rates than hardwood (CEN, 2010). If charring rates should be investigated in a study, cone calorimeter tests in the most common method (Martinka et al., 2018). It is also possible to do large-scale tests. However, these are often expensive and time-demanding and are therefore often not explicitly conducted to investigate only the charring rate but can be a small part of the tests. Even though cone calorimeters are the most used method, they can only measure one-dimensional charring. On the other hand, they enable the investigation of how various factors affect the charring process. A disadvantage of all methods is the lack of opportunities for continuous measuring during a test. The only known methods to get an indication of the charring rate will be by using thermocouples or calculating it from the mass loss rate. Thermocouples will help measure the exact temperature inside the samples at chosen depths. However, they cannot be trusted a hundred percent as the conductivity between the timber and TCs differentiates. The holes drilled to make room for the TCs can also lead heat through the sample differently than the wood itself would do.

Experiments conducted by Martinka et al. (2018) and Xu et al. (2015) both demonstrated that higher heat fluxes corresponded to increased charring rates. This contradicts with values from the European Standards that are constant and independent of the external heat flux (CEN, 2010). It is also seen that charring rates increase in situations where the residual cross-section is less than 50 mm (Frangi & Fontana, 2003). NS-EN 1995-1-2 indicates that a char layer at 25 mm insulates the inner layer and reduces the charring rate (CEN, 2010). Aseeva et al. (2014) briefly summarizes how the char layer works as insulation. The char reduces the release of the combustible gases as a physical barrier, leading to reduced flammable mixture. It also reduces the heat transportation to the inner layers, decreasing the pyrolysis further. Furthermore, it increases the heat loss caused by radiation from the temperatures in the outer char layer.

#### 3.4.4 Heat Release Rate

Heat release rate (HRR) measures the rate of the energy released during a fire per time unit by the combustion of fuel. It is a target describing the intensity of a fire during the different stages, and it is usually measured in watts or watts per square meter (CEN, 2010). Therefore, it is a critical parameter in fire safety engineering as it determines the intensity and spread of a fire. The peak heat release rate (PHRR) illustrates the maximum heat release during a fire and is often seen at the point of ignition as the concentration of energy released is highest at ignition. (Karbhari, 2007). The HRR of a fire depends on various factors, such as the type and amount of fuel, ventilation conditions, and geometry of the enclosure. Findings by Harada (2001) show that higher heat fluxes increase the HRR. It also shows a dependency between the thickness of the material, where a thick material has a lower HRR than a thin material, tested in samples with thicknesses between 10 and 40 mm. Tsantaridis (2003) also found that the HRR would increase as the density increases, especially for solid wood.

#### 3.4.5 Thermally Thin and Thick Materials

Thermally thin materials can be described as an element where the whole material keeps the same temperature and has no significant temperature gradient throughout the sample (El Gazi et al., 2021). A thermally thick material goes for the opposite, where there is a thermal gradient through the material. According to Babrauskas (2002), a material can be said to be thermally thick when the wood sample is over 25 mm thick.

Drysdale (2011) saw differences between thermally thin and thermally thick materials regarding sustained burning. While the thin materials continued to burn without an external heat source, the thick materials self-extinguished when the heat source disappeared. This is also found in tests by Tsantaridis (2003) stating that thicker samples lasts longer during a fire.

#### 3.4.6 Mass Loss

During a fire, when wood goes through pyrolysis, materials char and loses mass continuously. The mass loss can be used to calculate the char depth of timber materials (Martinka et al., 2018). This method is used under cone calorimeter tests, as it makes it possible to weigh the samples continuously under the test. Despite the method being used, there is little to no scientific relationship between mass loss and char depth.

There have been assumptions of how the ratio between mass loss and charring depends on each other. Butler (1971) assumed the density of char to be negligible, giving charring and mass loss to relate directly on each other. Babrauskas (2005) findings, on the other

hand, showed a char fraction of 30 %. Studies by Dupal et al. (2022) investigating bulk density of char concluded that char of spruce had an average density of  $138 \text{ kg/m}^3$ , with an initial density before burning av  $508 \text{ kg/m}^3$ . However, Martinka et al. (2018) carried out a series of tests on Norwegian Spruce and Scots Pine to investigate the charring rate and how this depended on the mass loss, following the procedure from ISO 5660-1 in a cone calorimeter test. From this study, two alignments were made for respectively Norwegian Spruce and Scots Pine with humidity of 0 %:

$1,368 * \text{mass loss} + 3,242$  for Norwegian Spruce (Martinka et al., 2018)

$1,1452 * \text{mass loss} + 4,5924$  for Scots Pine (Martinka et al., 2018)

The equations were based on several tests stopped after 10, 20, and 30 min, measuring the mass loss in terms of the total mass, and the charring depth in terms of the total material depth in percentage.

### 3.4.7 Mass Loss Rate

In addition to measuring the mass loss directly, it can also be referred to as the mass loss rate giving the rate at which the material is lost to the fire. Over time, the mass loss rate can be transient or steady (Emberley, Do, et al., 2017). The transient state usually has a much higher mass loss rate than the steady-state, and the mass loss varies over time without a clear pattern. It also involves the peak mass loss, usually when the char layer begins to form and slowly decreases against a steady-state (Emberley, Putynska, et al., 2017). The steady-state mass loss rate is reached when other fire conditions also reach steady-state, and the fire stabilizes at a constant temperature. This can occur when the char layer thickens and isolates the inner wood, leading to a continuous energy transfer through the charred layer.

Terrei et al. (2019) investigated how mass loss rate and self-extinction correlate with samples under heat exposure of 15, 55 and  $75 \text{ kW/m}^2$ . The tests show that the critical mass loss rate for extinction varied depending on the time from ignition, where the critical mass loss rate were as high as  $7,26 \text{ g/m}^2\text{s}$  and  $5,9 \text{ g/m}^2\text{s}$  for  $55 \text{ kW/m}^2$  and  $75 \text{ kW/m}^2$  five minutes after test start. However, these values decreased to  $3 \text{ g/m}^2\text{s}$  and  $3,7 \text{ g/m}^2\text{s}$ , respectively, explained by the state of the fire. As mentioned in Chapter 3.4.2, the critical mass loss rate for tests conducted by Bartlett et al. (2019) was predicted to be around  $3,48 \text{ g/m}^2\text{s}$ .

### 3.4.8 Orientation, Surface and Scale Effect

Wood as a material is both non-homogenous and non-isotropic, meaning that the material's properties will vary based on orientation and grain direction (Drysdale, 2011). This also complicates the prediction of how a fire degenerates in wood materials.

Studies by Drysdale (2011) showed that auto-ignition happened easier on horizontal than vertical surfaces because a vertical surface is more exposed to convective cooling. Shields et al. (1993) conducted a series of tests in a cone calorimeter to investigate how horizontal and vertical orientation influenced the ignition with gas flame pilot, spark pilot, and spontaneous ignition. A portion of the initially horizontally oriented tests were inverted to simulate a ceiling orientation, while others were conducted to represent a floor orientation. The tests were conducted with three different board materials with 12 mm, 15 mm, and 20 mm thicknesses and were tested on different heat fluxes: 20, 30, 40, 50, 60, and  $70 \text{ kW/m}^2$ . For the ceiling-orientated samples, only the highest heat fluxes were tested. The results showed that vertically oriented samples required longer ignition time than

horizontally oriented samples for heat fluxes between 20 and 40 kW/m<sup>2</sup> for all board materials. For heat fluxes between 50 and 70 kW/m<sup>2</sup>, only minor differences were found. It is also shown that the gas flame required the shortest ignition time independent of the heat flux. Differences between the horizontally orientated samples were also noticed. The samples representing a ceiling ignited faster, especially for spontaneous ignition, which happened five to thirteen times faster than for the floor orientation.

Another factor that can impact the burning of a material is the surface. A known issue for CLT is the splines between the panels (Barber et al., 2022). Deflections in the materials makes room for hot gases to move into the material and could lead to faster charring and flames intruding from several sides of the material.

Furthermore, the scale of the tests is also seen to affect the pyrolysis of timber. Lizhong et al. (2002) found that samples in a cone calorimeter ignited easier than larger samples. This was explained by a more stable and concentrated heat exposure towards the sample. Nevertheless, he also found that the mass loss rate was higher for large scale tests. Findings comparing the peak heat release rate in different scales by Santoni et al. (2015) and Zhou et al. (2023) indicated that small scale tests gave a higher PHRR than larger tests. However, Tsantaridis (2003) conducted tests in a cone calorimeter and a room-corner test, showing good agreement between both methods when it came to charring.

### 3.4.9 Density

A material with low density represents a material with more extensive voids, which leads to reduced thermal conductivity that makes room for more heating inside the material (Bartlett et al., 2019). Differences in the density within the same specie appears and may come from the growth layers existing of a combination of earlywood and latewood (Knapic et al., 2014). The growing conditions of timber regarding climate factors and the soil affects the combination of pith and sapwood, giving different densities in-between the same species.

Bigger voids in the material makes the pyrolysis process go faster, and the charring rate increases in less dense materials. This is seen in several studies, among others from Xu et al. (2015). Tests conducted in five different wood species with three heat flux levels showed that more dense species would have a higher resistance against fire than less dense species. It also showed that a lower density and moisture content led to shorter ignition time. These findings are reinforced by a collection of studies by Friquin (2011), where several studies showed significant correlations between thermal degradation and density. Although some studies did not show correlations between density and charring, it may be explained by minor differences in the density. Correlations between charring rate and density can also be seen in European building regulations, where charring rates are lower for hardwood with a density higher than 450 kg/m<sup>2</sup>, than for other lower dense wood species (CEN, 2010).

On the other hand, Emberley, Do, et al. (2017) examined how critical external heat flux varied in five different wood species with different densities. The results from the study showed no significant dependency between critical heat flux with unpiloted ignition and the density, and instead pointed out that the heat flux is more dependent on the species than the density itself. This agrees well with Frangi and Fontanas (2003) findings from a test following the method from ISO 834, where samples with a density between 340 and 500 kg/m<sup>3</sup> showed no significant pattern between charring rate and density.

### 3.4.10 Moisture Content

During a pyrolysis process, the moisture content in the material slows down the process as the heat is used to heat the water instead of heating the sample simultaneously (Bartlett et al., 2019). This happens when the temperature in the vicinity reaches 100 °C and ceases only after a period within this temperature range, continuing until evaporation is fully accomplished (Di Blasi et al., 2000). Friquin (2011) also demonstrated this phenomenon, indicating that materials with elevated moisture content required more energy for evaporation, resulting in prolonged ignition time and increased emissions of combustible gases.

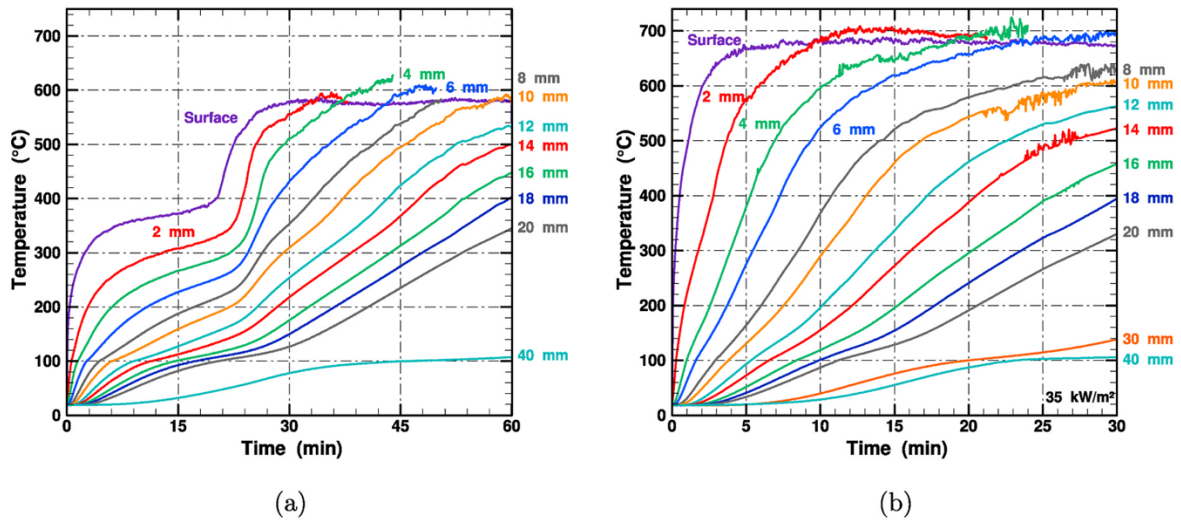
Findings by Atreya & Abu-Zaid (1991) showed the impact moisture content had on the time to ignition with constant heat flux. The wood specie used was Douglas fir, with a constant heat flux at 26,5 kW/m<sup>2</sup> with piloted ignition. They tested four different moisture contents: 0%, 11%, 17%, and 27%, corresponding with times to ignition at 55 s, 100 s, 145 s, and 215 s, respectively. On the other hand, tests by Shi & Chew (2012) showed no significant difference between 0 % and 11 % moisture content for six wood species for autopiloted ignition. This can indicate that the moisture content of wood has a more significant impact on piloted ignition. The latter test showed little to no difference in the mass loss rate between the two moisture contents. Other factors as wood specie, were more critical.

## 3.5 Temperature Measurements inside Timber Samples

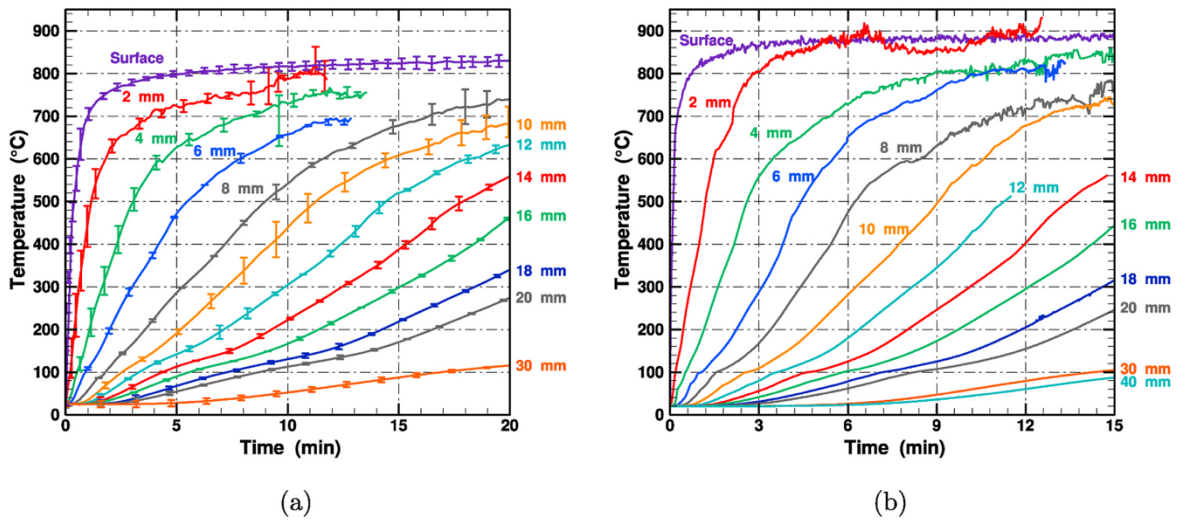
Terrei et al. (2021) conducted a series of tests using a cone calorimeter. First, the samples were split in two to make room for the thermocouples, then inserted the thermocouples, before the samples were glued and pressed together as one block again. These blocks were later put in a cone calorimeter under different heat fluxes to measure temperatures at different depths and mass loss rates. The heat fluxes tested for were 16,5 kW/m<sup>2</sup>, 38,5 kW/m<sup>2</sup>, 60 kW/m<sup>2</sup>, and 93,5 kW/m<sup>2</sup>. Even though it was mentioned that thermocouples could impact the weight negatively, the positive effects were considered worth it. This could come from several factors: thin thermocouples demand little mass reduction through setup in both timber and glue, which also minimizes the conductive heat flux through the wires. The thermal resistance between the sample and wire is negligible.

Figure 3.3 and Figure 3.4 shows how the temperature in the thermocouples develops over time at different heat fluxes. Tests demonstrate a significant pattern indicating that low heat fluxes necessitate the longest time to increase in temperature. The TC at 20 mm needed around 54 minutes to reach 300 °C at 16,5 kW/m<sup>2</sup>, while it only took 14 minutes at 93,5 kW/m<sup>2</sup>. At heat flux level 38,5 kW/m<sup>2</sup>, the TC used a little less than 30 minutes to reach 300 °C at 20 mm.





**Figure 3.3 Figures by Terrei *et al.* (2021) showing temperatures in TCs at different depths for 16,5 kW/m<sup>2</sup> (a) and 38,5 kW/m<sup>2</sup> (b).**



**Figure 3.4 Figures by Terrei *et al.* (2021) showing temperatures in TCs at different depths for 60 kW/m<sup>2</sup> (a) and 93,5 kW/m<sup>2</sup> (b).**

This is also found in tests by Reszka and Torero (2006), where they investigated several heat fluxes and their thermocouple temperatures. Figure 3.5 shows the measurements at 25 kW/m<sup>2</sup>, indicating that it needed around 50 minutes to reach 300 °C at 25 mm.

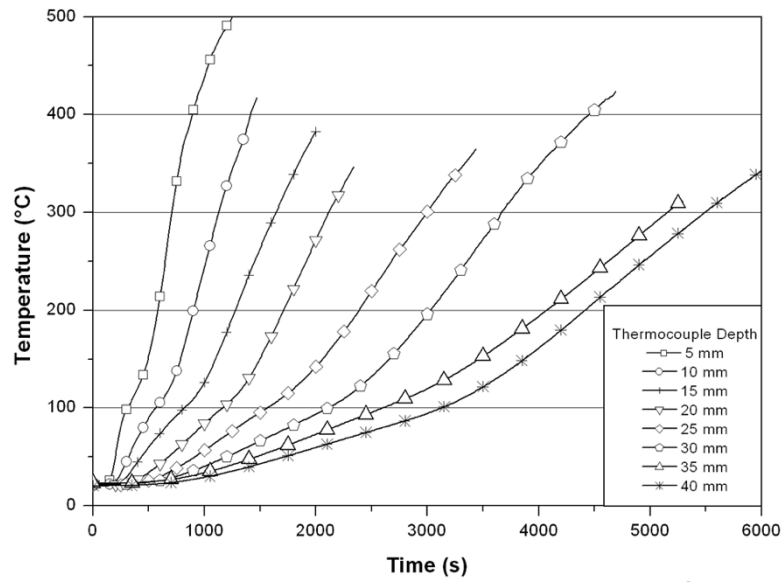


**Figure 3.5 Figures by Reszka and Torero (2006) showing temperatures in TC at different depths at 25 kW/m<sup>2</sup>.**

# 4 Results from the Compartment Test

## 4.1 Results from Compartment Test by Andreas S. Bøe

The following section presents some relevant results from the test conducted by Andreas S. Bøe with exposed CLT in the ceiling. It is prioritized to look at how charring has developed through the compartment over the test period by focusing on the temperatures in the compartment, in addition to char measurements. Figure 4.1 and Figure 4.3, in addition background data to calculate graphs in Figure 4.2, Figure 4.4, Figure 4.5 and Figure 4.6 is received from Bøe et al. (2023).

Observations immediately after the test started showed a rapid burning of fuel in the beginning before the fire almost extinguished when the initial startup fuel was used. It took around one-half hour before the burning in the wood crib increased and stabilized, leading to ignition in the ceiling. When the wood crib eventually burned evenly, more gases were released and collected on the inside of the front beam leading to a flammable mix of gases in the ceiling, eventually leading to burning in the ceiling as well. As seen in Figure 4.1, the fire spread over the wood crib and retreated quickly. This happened several times at different places, as illustrated by the peaks, before it spread and sustained burning until the burnable materials in the wood crib were burned up and approached extinguishment. The compartment self-extinguished before any delamination was observed during the test.

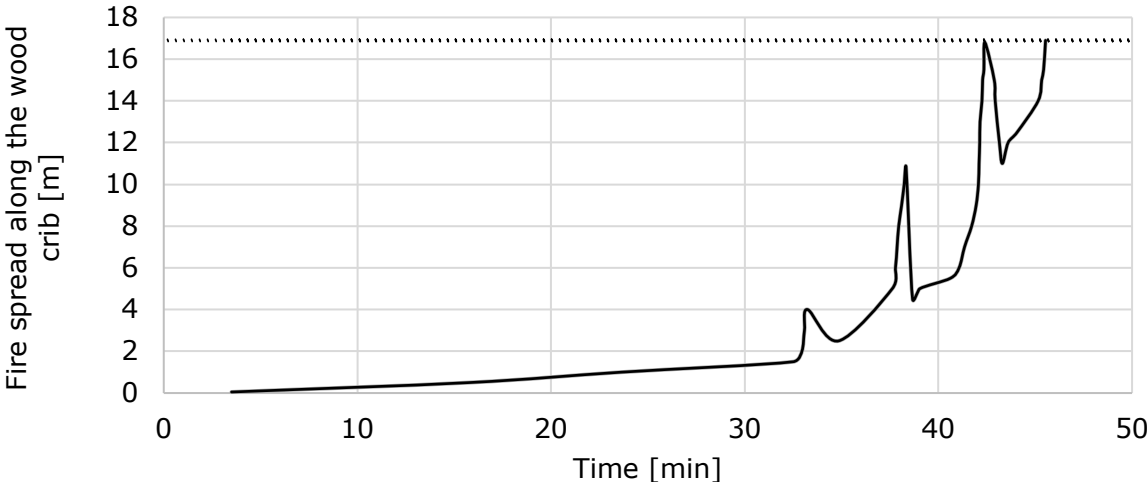


**Figure 4.1 Showing the fire spread along the wood crib over time (Bøe et al., 2023). The stippled line shows end of crib.**

The temperature from the plate thermocouples was measured at three locations in the ceiling, as shown in Figure 2.1. The temperatures were then calculated to represent heat fluxes at the locations, using the method described in Chapter 2.2.2, resulting in the graphs shown in Figure 4.2, presenting the heat flux levels at the three locations. It shows a slow burning the first 31 minutes, before it increases with higher peaks four times. The heat flux is highest in the middle of the compartment, reaching up against 160 kW/m<sup>2</sup> at a point but decreases as the fire does not sustain burning. The time of the peaks correlated to the peaks seen in Figure 4.1.

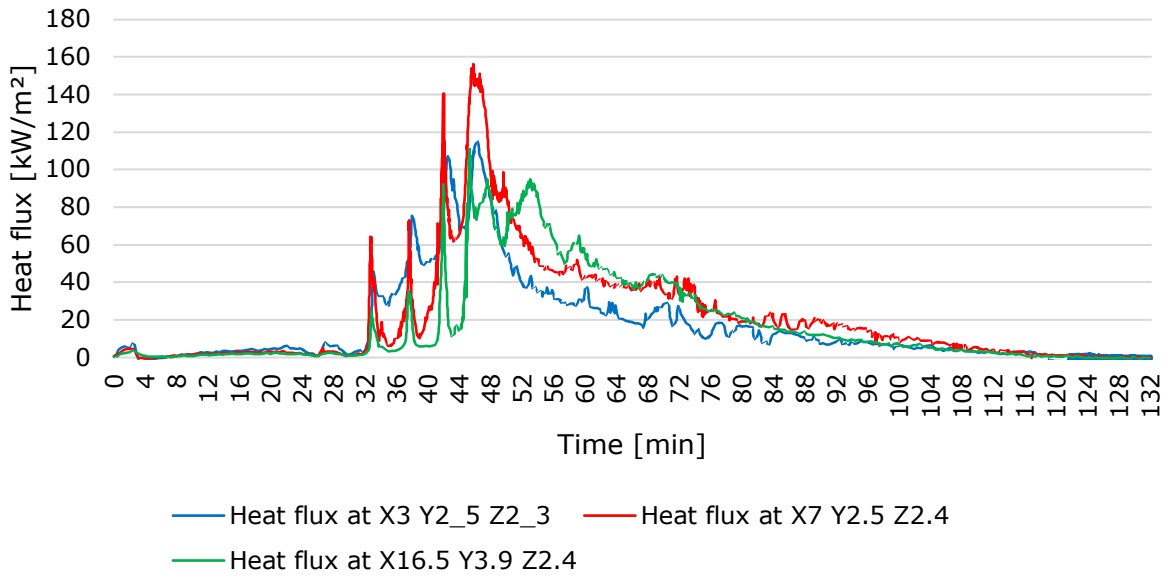


**Figure 4.2 Heat flux in PTs at three different locations in the compartment.**

The charring depth is calculated from the remaining uncharred wood and an average value of the four remaining lamellas possible to measure. These remaining lamellas showed a depth of 102,5 – 103,5 mm after the test when the charring depth measurements were conducted, where an average depth of 103 mm is chosen as a base. The depth of the remaining wood and the char depth can be seen from Figure 4.3. Findings from the measurements show that the charring is highest 2,3 to 2,8 meters from the window side and lowest near the window. Element 5 and 7 have the highest charring depths, and at most 40 mm charring at 14,3 from ignition side.

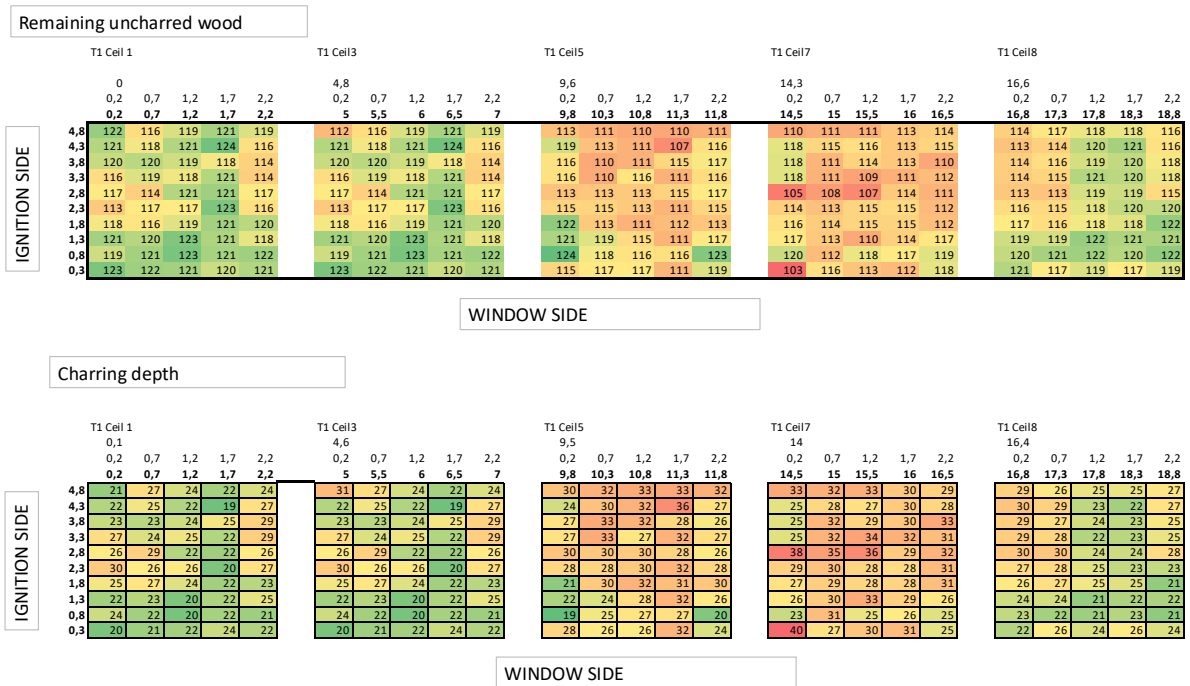


**Figure 4.3 Results from char measurements, reused from (Bøe et al., 2023).**

Through the measurements, lamellas that have partly loosened because of delamination are not considered if they have not fallen off. Therefore, it is a considerable risk that the bearing of the element cannot be predicted from the charring depths shown in this task, as the load-bearing properties are lower than may be shown here due to pyrolysis and further heating in the lamellas. However, clear signs of delamination have been observed in ceiling element 5 and 7 through loose boards showing that the adhesive has released, but they have not fallen completely off.

Diagrams in Figure 4.4, Figure 4.5 and Figure 4.6 presents temperatures in the TCs placed inside the ceiling elements at three different locations, 4,7 m, 9,5 m, and 14,3 m from the ignition side. As shown in the figures, the black graph is an average between the temperature at 20 mm and 30 mm to find the time to reach a 25 mm charred layer, representing the char layer thick enough to isolate the inner wood.

From these diagrams, observations shows that the ignition of the wood crib burned slowly for the first 31 minutes, before the fire increased and spread along the compartment. This can be seen by the rapid increase in the temperature in the TC at 0 mm. After a period of even burning, the fire decreased before it was extinguished after 122 minutes, shown in the graphs as a sudden temperature fall. This gives a period of 91 minutes where the fire can cause damage through pyrolysis of the material. However, it is evident that the fire does not burn at a consistent rate throughout this time. This can be observed in the fire spread diagram, which displays variations in flaming combustion within the compartment. Additionally, the diagrams below demonstrate the temperature decrease at 0 mm, providing an insight into the temperatures inside the compartment.

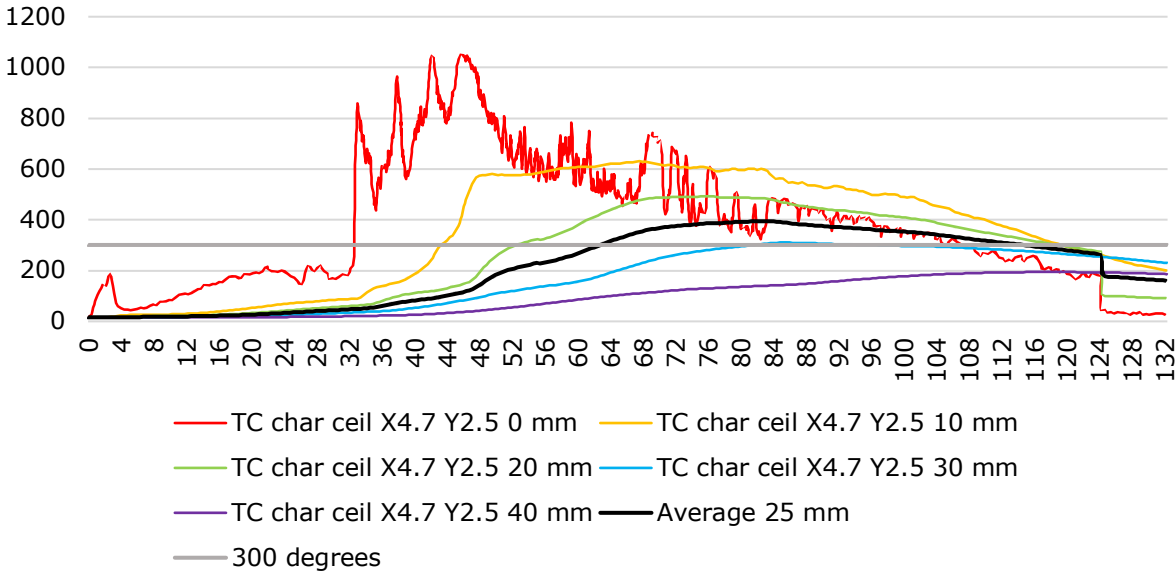


**Figure 4.4 Thermocouples placed in ceiling element at different depths, 4,7 m from the ignition source.**

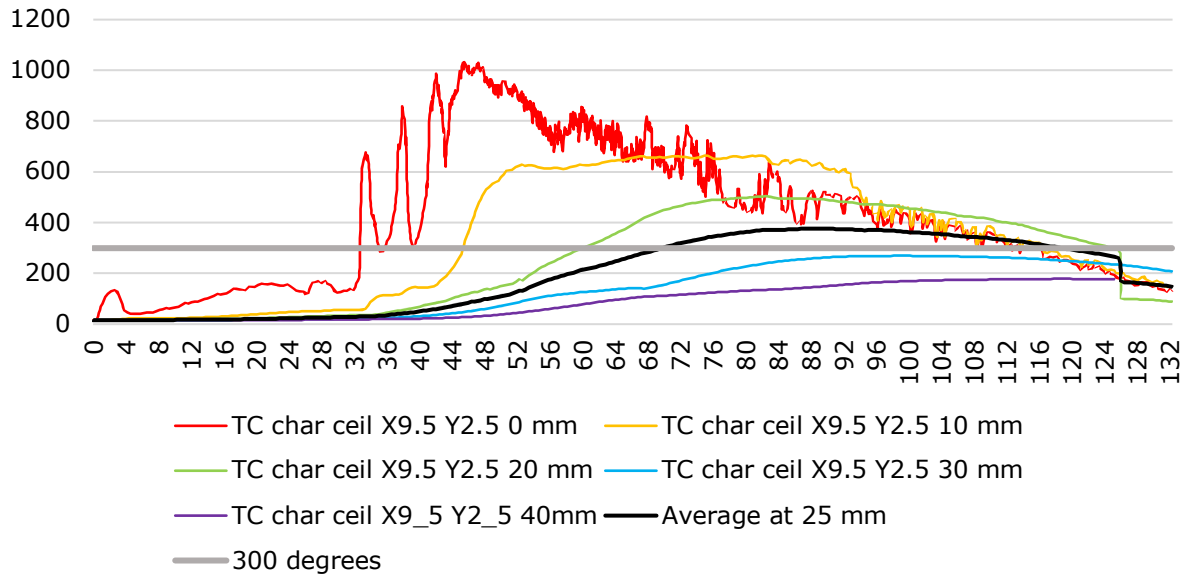


**Figure 4.5 Thermocouples placed in ceiling element at different depths, 9,5 m from the ignition source.**

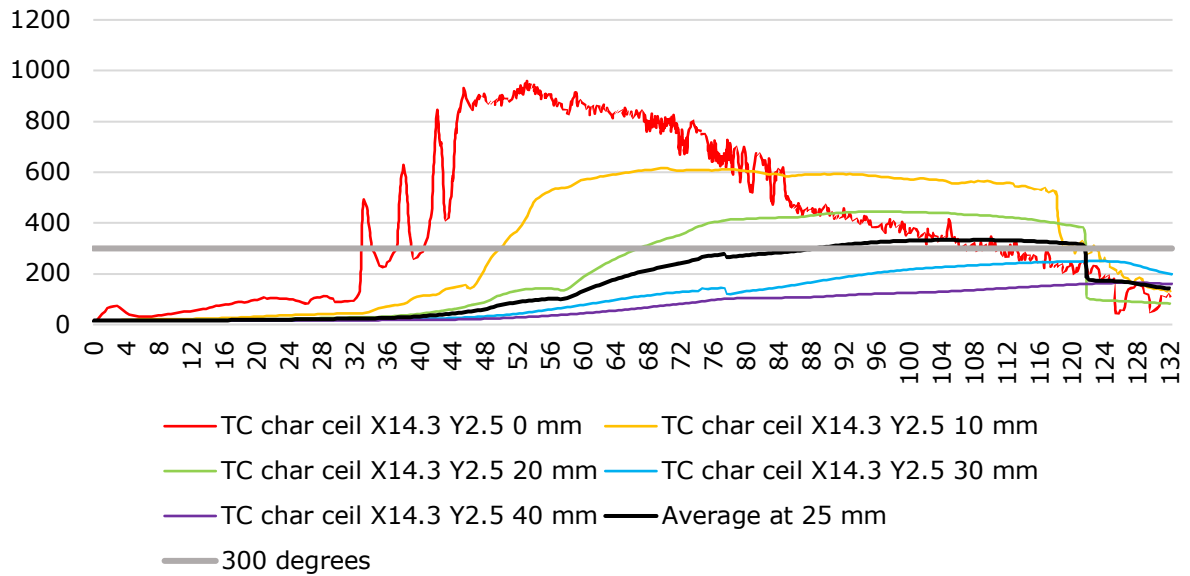


**Figure 4.6 Thermocouples placed in the ceiling elements at different depths, 14,3 m from the ignition source.**

Based on the information in the diagrams above and the literature stating that wood chars at 300 degrees, charring depths for the three locations in found and presented in Table 4.1. These charring depths is used to calculate the charring rates in the same locations, based on a fire duration of 122 minutes measured from the beginning, and on a fire duration of 91 minutes measured from the temperature increase.

**Table 4.1 Charring depth and corresponding charring rate based on temperatures in the thermocouples inside the ceiling elements in the Compartment Test.**

	4,7 m from ignition side	9,5 m from ignition side	14,3 m from ignition side
Approximate charring depth [mm]	30	28	26
Charring rate based on a 122 min fire duration [mm/min]	0,25	0,23	0,21
Charring rate based on a 91 min fire duration [mm/min]	0,33	0,31	0,29

## 5 Results from Cone Calorimeter Testing

The following section presents the results from the cone calorimeter tests. The first thing presented in the subsections is the heat flux setup used in the tests, followed by results in a table or as observations presented in text or figures. Next, graphs representing heat release rate and temperature development during the experiment are displayed, in addition to the mass loss rate. Furthermore, other results relevant from the tests is presented. The description of each test group in the header represents the heat fluxes in each phase.

### 5.1 Test Group 1: 40 kW/m<sup>2</sup> – 0 kW/m<sup>2</sup> – 30 kW/m<sup>2</sup>

This subsection presents the main results from three of the twenty-three samples tested. The procedure followed through testing is described in Chapter 2.3.3, with the heat fluxes tested in the different phases presented in Table 5.1.

**Table 5.1 Test group 1: set up.**

Test ID	Phase 1.1 Heat flux [kW/m <sup>2</sup> ]	Phase 1.2 Heat flux [kW/m <sup>2</sup> ]	Phase 2 Heat flux [kW/m <sup>2</sup> ]	Phase 3 Heat flux [kW/m <sup>2</sup> ]	Phase 4 Heat flux [kW/m <sup>2</sup> ]
1-1	40		0	30	-
1-2	40		0	30	-
1-3	40		0	30	-

Table 5.2 summarizes the time needed for ignition and extinction at different conditions, in addition to charring rates for each sample. All samples ignited within a minute at the given heat flux. Test 1-1 and Test 1-2 used nearly the same time until TC25 reached 300 °C, while Test 1-3 differs and needed longer time than the others, as shown in Figure 5.1. This results in lower charring rates for this sample as well. Another thing seen in Figure 5.2, showing the HRR and temperature from Test 1-3, is that TC30 reached 300 °C before TC25 and had approximately the same temperatures through the entire test.

**Table 5.2 Test group 1: results.**

Test ID	1-1	1-2	1-3
Density [kg/m <sup>3</sup> ]	475	476	565
Weight [g]	223	224	266
Humidity [%]	8,6	8,5	8,3
Time to ignition from start of Phase 1 on fresh wood [s]			
- 40 kW/m <sup>2</sup>	40	53	46
Time to extinction from start of Phase 2 with no heat flux [s]	68	66	580
Time to ignition from start of Phase 3 on charred wood [s]			
- 30 kW/m <sup>2</sup>	No ignition	No ignition	No ignition
Time to reach 300 °C [s]			
- 15 mm			2130
- 20 mm			2985
- 25 mm	2640	2409	3681



- 30 mm			3637
Charring rate [mm/min]			
- 15 mm			0,42
- 20 mm			0,40
- 25 mm	0,57	0,63	0,41
- 30 mm			0,49

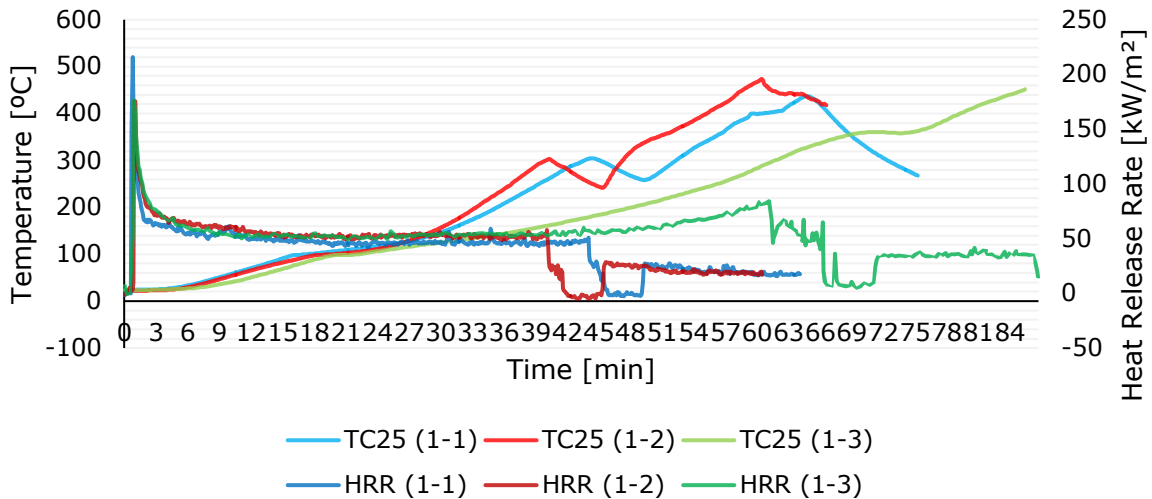


**Figure 5.1 Test group 1: HRR and temperature.**

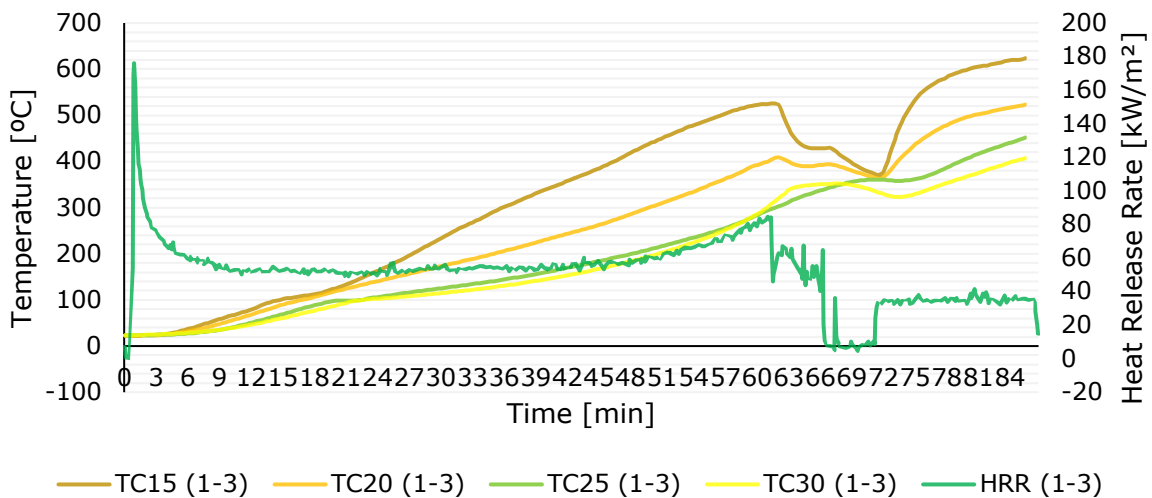


**Figure 5.2 Test 1-3: HRR and temperature.**

Another observation worth noticing for Test 1-3 is that the sample did not extinguish within five minutes with the build-in lid, which can be seen from Figure 5.2 around 60 minutes where the HRR gets two sudden drops; the first when the build-in lid is used, and the second where the gypsum lid suffocates the flames, but the temperature do not decrease as for the other tests. Observations during the period showed that the flames went around the lid towards the cone, as shown in Figure 5.3. Since no signs of extinction were observed, the gypsum lid was necessary to smother the flames and continue the test.

None of the tests reignited with a heat flux at 30 kW/m<sup>2</sup>, but there are observed movements of glow in the charred layer.



**Figure 5.3 Observations from Test 1-3, when the flames went around the lid in Phase 2.**

The mass loss rate has been tracked continuously through the test. Graphs shown in Figure 5.4 summarize this to illustrate how the mass loss rate has developed continuously. To avoid significant interruptions followed by off and on with lids during the tests, the periods where the lids have interrupted the mass loss have been deleted from the graph. This can be seen in all the following graphs by the periods where the average mass loss rate lies at zero. Some other interferences from thermocouples may also have occurred, where some of the apparent interruptions have been removed from the graph to avoid unrealistic high and low values. Other minor deviations may come from this, and not the sample's mass loss. It is still considered valuable to use the values when looking at the total and not only at one specific point of the graph. Therefore, an average value is taken every 30 seconds to avoid significant deviations at specific points.

Especially Test 1-2 has shown massive deviations in the mass loss rate and may come from interferences on the weight from the thermocouples. Aside from this, Test 1-1 and Test 1-3 has a general mass loss rate varying evenly between 3,7-5,6 g/m<sup>2</sup>s during the constant burning at 40 kW/m<sup>2</sup>. In Phase 3 where no reignition occurred, the mass loss rate is more unstable making it harder to investigate the exact values. However, the mass loss rate in Phase 3 is observed to be higher for Test 3-3 than for Test 3-1, even though none of them ignited.

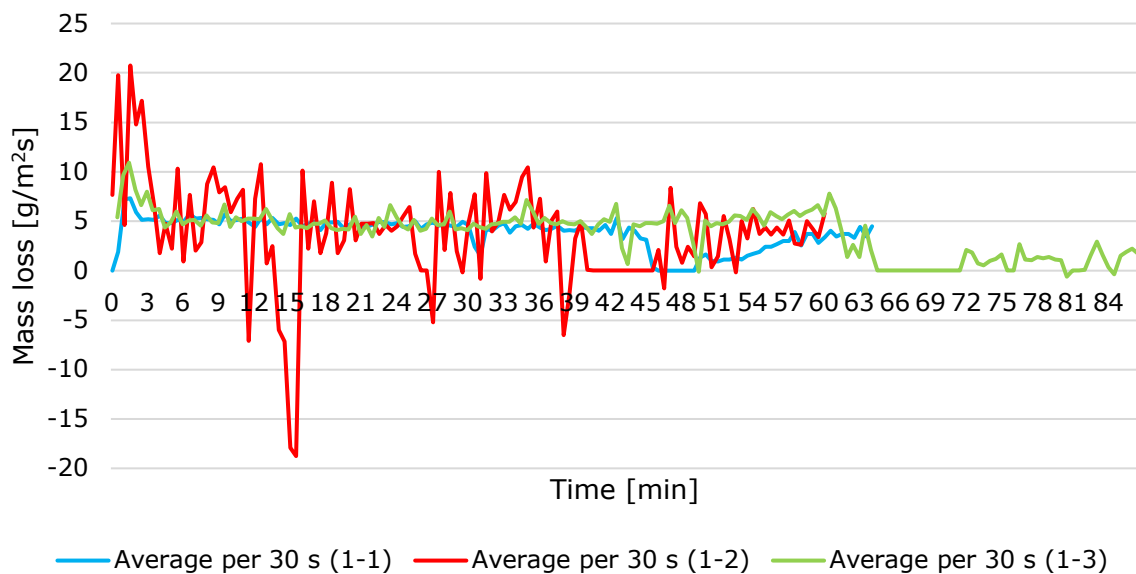


**Figure 5.4 Test group 1: mass loss rate.**

## 5.2 Test Group 2: 35 kW/m<sup>2</sup> – 0 kW/m<sup>2</sup> – 50 kW/m<sup>2</sup> – 30 kW/m<sup>2</sup>

Samples in Test group 2 follows the same test procedure as described in Chapter 2.3.3, and the chosen heat fluxes can be seen in Table 5.3.

**Table 5.3 Test group 2: setup.**

Test ID	Phase 1.1 Heat flux [kW/m <sup>2</sup> ]	Phase 1.2 Heat flux [kW/m <sup>2</sup> ]	Phase 2 Heat flux [kW/m <sup>2</sup> ]	Phase 3 Heat flux [kW/m <sup>2</sup> ]	Phase 4 Heat flux [kW/m <sup>2</sup> ]
2-2	35		0	50	30
2-3	35		0	50	30
2-4	35		0	50	30

Table 5.4 summarizes the time needed for ignition and extinction at different heat fluxes, in addition to charring rates for each sample. Test 2-1 and Test 2-2 ignited within 1,5 minutes, while Test 2-3 did not ignite during the 15 minutes, and the heat flux was then increased to 50 kW/m<sup>2</sup>. However, even with this heat flux, no flaming ignition was observed within the next 15 minutes. The sample used nearly 32 minutes before flaming ignition occurred.

All tests self-extinguished within 2,5 minutes with no heat flux and reignited at 50 kW/m<sup>2</sup> relatively quick. When the heat flux was reduced to 30 kW/m<sup>2</sup> in Phase 4, the fire continued to burn in Test 2-1 and Test 2-3 before it eventually extinguished within the 15-minutes time frame. It is especially observed remaining flames on the edges of the samples, as shown in Figure 5.5, capturing Test 2-2 that did not extinguish during Phase 4. Figure 5.6 shows the cooled-down sample from Test 2-2, which also showed a crack at the part where the burning continued until it was extinguished manually after the test ended.

**Table 5.4 Test group 2: results.**

Test ID	2-1	2-2	2-3
Density [kg/m <sup>3</sup> ]	485	413	421
Weight [g]	228	194	198
Humidity [%]	8,9	8,1	8,9
Time to ignition from start of Phase 1 and 1.2 on fresh wood [s]			
- 35 kW/m <sup>2</sup>	85	45	No ignition
- 50 kW/m <sup>2</sup>			1012
Time to extinction from start of Phase 2 with no heat flux [s]	143	81	146
Time to ignition from start of Phase 3 on charred wood [s]			
- 50 kW/m <sup>2</sup>	82	123	140
Time to extinction from start of Phase 4 with heat flux [s]			
- 30 kW/m <sup>2</sup>	859	No extinction	410
Time to reach 300 °C [s]			
- 15 mm		1592	
- 20 mm		2245	
- 25 mm	3170	2375	2501
- 30 mm		3079	
Charring rate [mm/min]			
- 15 mm		0,56	

- 20 mm		0,53	
- 25 mm	0,47	0,63	0,6
- 30 mm		0,58	

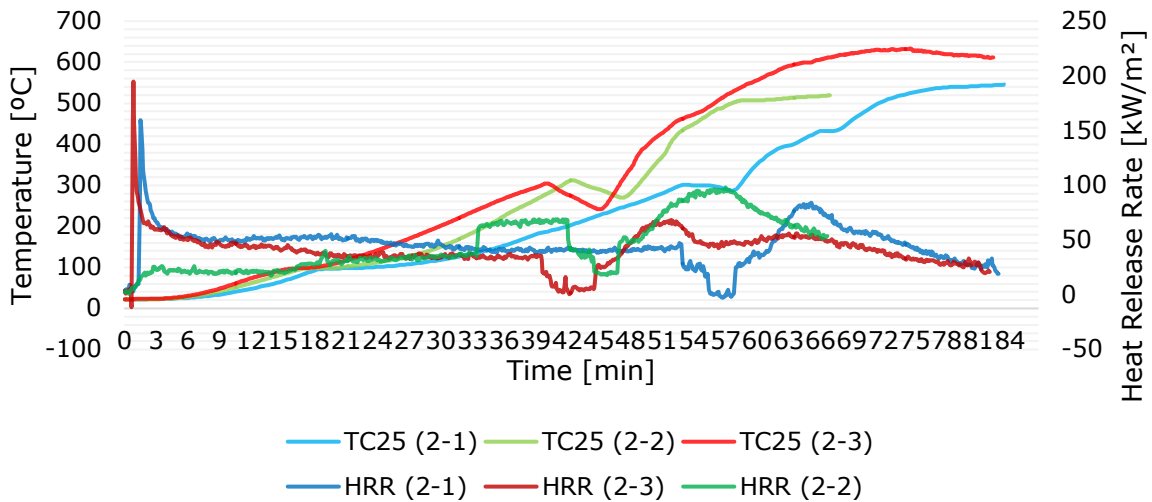


**Figure 5.5 Test 2-2 shows burning in one side in Phase 2.**



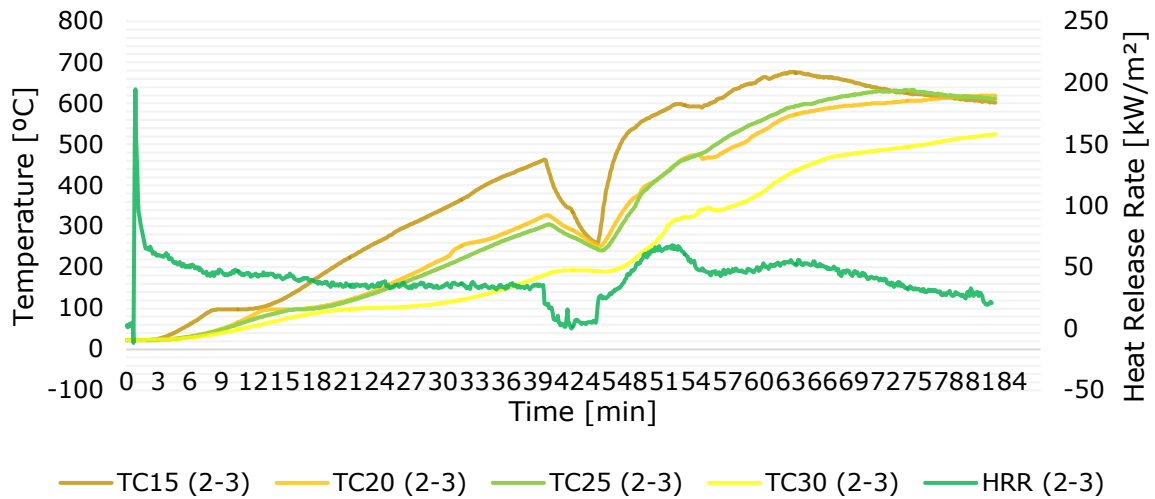
**Figure 5.6 Test 2-2 showing cracks of char on the same side as the burning continued.**

As seen from the first 30 minutes on the graph in Figure 5.7 comparing HRR and temperature from Test 2-1 and Test 2-2, the temperature inside the sample increased faster in Test 2-2 than Test 2-1. This happened even though Test 2-2 did not ignite within the initial time, and Test 2-1 ignited and burned steadily during the same period.



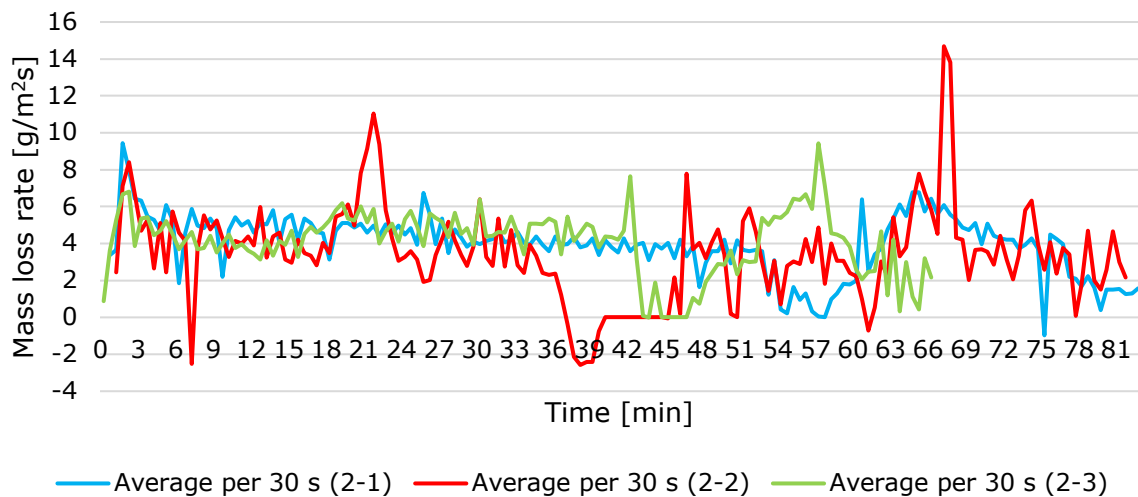
**Figure 5.7 Test group 2: HRR and temperature.**

Figure 5.8 shows that the temperature in TC20 and TC25 are nearly identical from start to finish. It also shows that the temperature in TC30 is more stable and less affected by external variations, and flattens out instead of dropping fast as the others did.



**Figure 5.8 Test 2-3: HRR and temperature.**

Even though one of the tests did not ignite simultaneously as the others, the mass loss rate for all tests is almost similar for the first 20 minutes, as shown in Figure 5.9. However, after reignition with 50 kW/m<sup>2</sup> in Phase 3, the mass loss rate is higher than in Phase 1 with 35 kW/m<sup>2</sup> for all tests.



**Figure 5.9 Test group 2: mass loss rate.**

### 5.3 Test Group 3: 30 kW/m<sup>2</sup> – 0 kW/m<sup>2</sup> – 40 kW/m<sup>2</sup> – 40 kW/m<sup>2</sup>

This group of tests follows the same procedure as described in Chapter 2.3.3. Heat fluxes used in these tests is described in Table 5.5. These tests started with the lowest initial heat flux of all 23 tests, and none of the three samples ignited at 30 kW/m<sup>2</sup>. The cone was then heated to 50 kW/m<sup>2</sup> to reensure ignition.

**Table 5.5 Test group 3: setup.**

Test ID	Phase 1.1 Heat flux [kW/m <sup>2</sup> ]	Phase 1.2 Heat flux [kW/m <sup>2</sup> ]	Phase 2 Heat flux [kW/m <sup>2</sup> ]	Phase 3 Heat flux [kW/m <sup>2</sup> ]	Phase 4 Heat flux [kW/m <sup>2</sup> ]
3-1	30	50	0	40	40
3-2	30	50	0	40	40
3-3	30	50	0	40	40

Table 5.6 shows that Test 3-1 ignited when the cone reached 48 kW/m<sup>2</sup>, Test 3-2 ignited at 35 kW/m<sup>2</sup>, and Test 3-3 needed almost two minutes at 50 kW/m<sup>2</sup> to ignite.

In Phase 3, all three tests ignited within two to four minutes at 40 kW/m<sup>2</sup>. In these tests, the same heat flux as for reignition in Phase 3 was used to investigate if extinction occurred in Phase 4. This is because a crucial part of investigating the boundary conditions is knowing whether the fire decays because of little to no burnable materials left or by the lack of an external heat source. As Phase 3 and 4 had the same heat flux, the transition between the phases happened when the samples burned in a steady-state and was observed by the HRR during the test. None of the tests self-extinguished within 15 minutes and the tests was ended manually.

Test 3-2 shows a deviation in the graph for HRR, as seen in Figure 5.10 and Figure 5.11. This comes from a mistake during testing, where the rack was not ready and adjusted properly before testing.

**Table 5.6 Test group 3: results.**

Test ID	3-1	3-2	3-3
Density [kg/m <sup>3</sup> ]	439	393	437
Weight [g]	206	185	206
Humidity [%]	8,0	8,0	9,1
Time to ignition from start of Phase 1 and 1.2 on fresh wood [s]			
- 30 kW/m <sup>2</sup>	No ignition	No ignition	No ignition
- 30-50 kW/m <sup>2</sup>	130 (ignition at 48 kW/m <sup>2</sup> )	125 (ignition at 45 kW/m <sup>2</sup> )	245
Time to extinction from start of Phase 2 with no heat flux [s]	106	120	80
Time to ignition from start of Phase 3 on charred wood [s]			
- 40 kW/m <sup>2</sup>	215	198	244
Time to extinction from start of Phase 4 with heat flux [s]			
- 40 kW/m <sup>2</sup>	No extinction	No extinction	No extinction
Time to reach 300 °C [s]			
- 15 mm		1035	
- 20 mm		1804	
- 25 mm	2928	2187	2477
- 30 mm		2794	
Charring rate [mm/min]			
- 15 mm		0,87	
- 20 mm		0,66	
- 25 mm	0,51	0,69	0,61
- 30 mm		0,64	

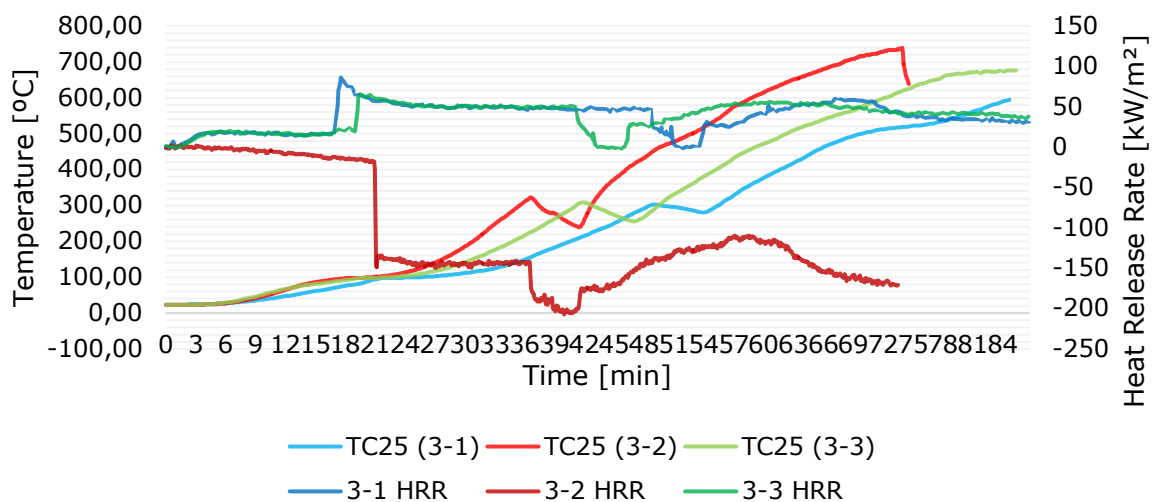


**Figure 5.10 Test group 3: HRR and temperature.**

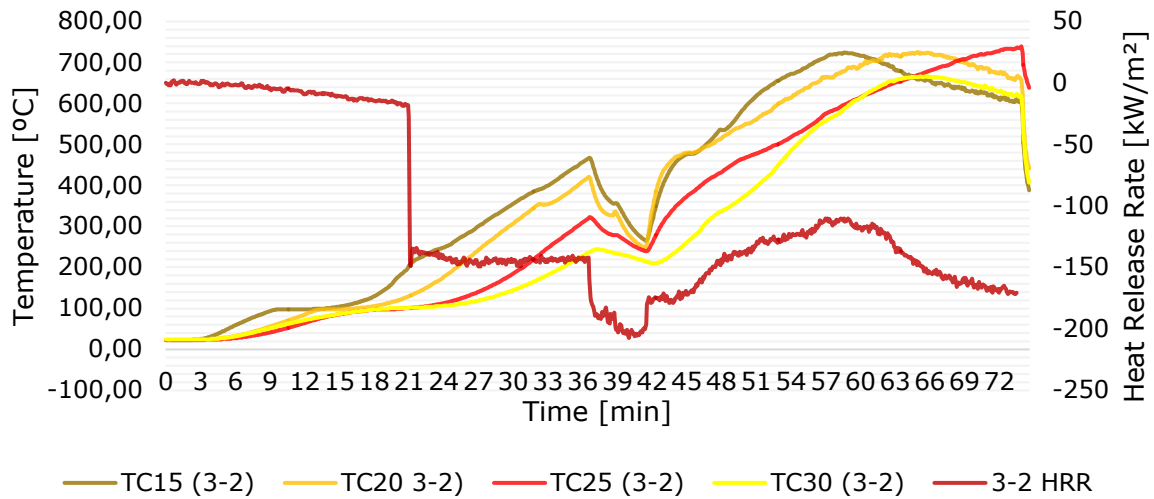


**Figure 5.11 Test 3-2: HRR and temperature.**

The mass loss rate for Test 3-1, Test 3-2, and Test 3-3 can be seen in Figure 5.12. The mass loss rate for all samples is higher in the beginning before it slowly decreases until ignition. At ignition, it increases to 7 g/m<sup>2</sup>s before stabilizing at a level higher than before ignition. Test 3-1 and Test 3-2 varies slightly after ignition, while Test 3-3 is more even and stabilizes at values between 4 and 5 g/m<sup>2</sup>s. This trend continues throughout the test, showing a more stable line for Test 3-3 than the others, indicating that these tests may have been disturbed during the period.

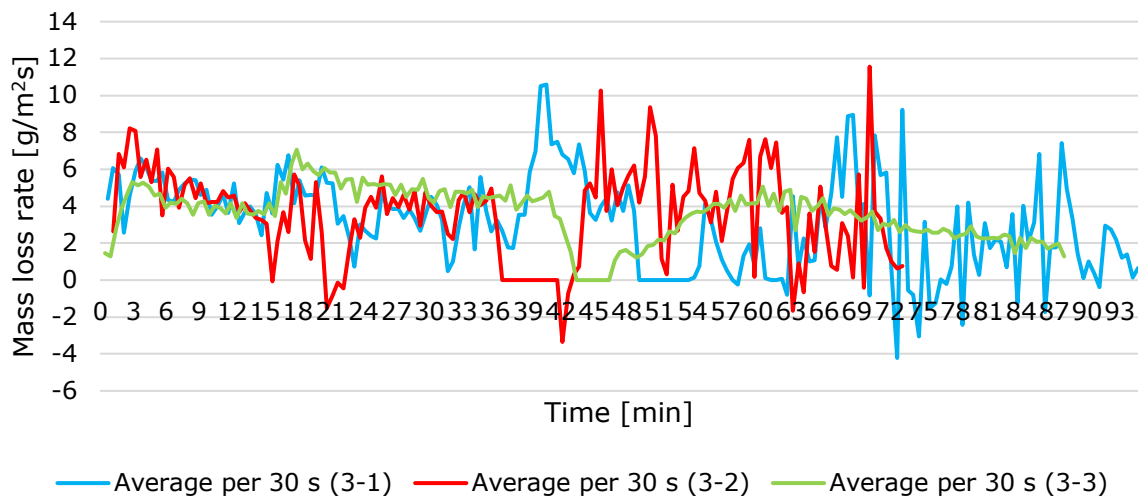


**Figure 5.12 Test group 3: mass loss rate.**

#### 5.4 Test Group 4: 33 kW/m<sup>2</sup> – 0 kW/m<sup>2</sup> – 35 kW/m<sup>2</sup>

Tests in Test group 4 follows the described procedure in Chapter 2.3.3, with chosen heat fluxes described in Table 5.7. Heat flux at 33 kW/m<sup>2</sup> is chosen because no samples ignited at 30 kW/m<sup>2</sup> in the previous tests, but all samples ignited at 35 kW/m<sup>2</sup> for fresh wood. All samples ignited at 40 kW/m<sup>2</sup> in the previous tests for charred wood, and lower heat fluxes must be tested.



**Table 5.7 Test group 4: setup.**

Test ID	Phase 1.1 Heat flux [kW/m <sup>2</sup> ]	Phase 1.2 Heat flux [kW/m <sup>2</sup> ]	Phase 2 Heat flux [kW/m <sup>2</sup> ]	Phase 3 Heat flux [kW/m <sup>2</sup> ]	Phase 4 Heat flux [kW/m <sup>2</sup> ]
4-1	33		0	35	-
4-2	33	50	0	35	-
4-3	33		0	35	-

Results from Test group 4 are stated in Table 5.8. This shows that only two out of three fresh samples ignited at 33 kW/m<sup>2</sup>. Test 4-2 did not ignite at the initial heat flux and did not ignite when increased to 50 kW/m<sup>2</sup>. It was then increased to 56 kW/m<sup>2</sup> to ignite. These increases in the heat flux can be observed in Figure 5.18 as small increases in HRR 15 minutes into it. As shown in Figure 5.13 and Figure 5.14, sample 4-3 had a hole in the surface, which could have impacted their ability to ignite, whereas sample 4-2 had a smooth surface besides a spline in the middle. Even though no ignition occurred in Test 4-2, Figure 5.15 shows glowing and smoldering in the container the entire time before ignition in Phase 1 and Phase 1.2. No reignition happened at 25 kW/m<sup>2</sup> in any of the tests.

**Table 5.8 Test group 4: results**

Test ID	4-1	4-2	4-3
Density (kg/m <sup>3</sup> )	380	411	444
Weight [g]	178	193	209
Humidity [%]	8,2	8,5	8,5
Time to ignition from start of Phase 1 and 1.2 on fresh wood [s]			
- 33 kW/m <sup>2</sup>	104	No ignition	93
- 50 kW/m <sup>2</sup>		No ignition	
- 56 kW/m <sup>2</sup>		40	
Time to extinction from start of Phase 2 with no heat flux [s]			
	154	116	257
Time to ignition from start of Phase 3 on charred wood [s]			
- 35 kW/m <sup>2</sup>	No ignition	No ignition	No ignition
Time to reach 300 °C [s]			
- 15 mm			2175
- 20 mm			2994
- 25 mm	2552	2214	3002
- 30 mm			2964
Charring rate [mm/min]			
- 15 mm			0,41
- 20 mm			0,50
- 25 mm	0,59	0,68	0,50
- 30 mm			0,60

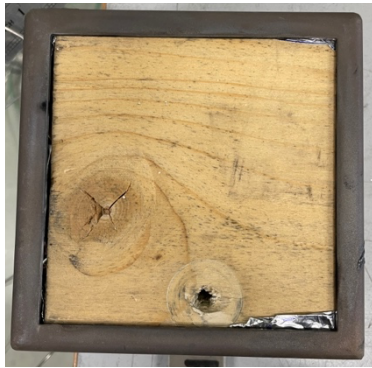


**Figure 5.13 Sample 4-3 showing holes in the surface.**

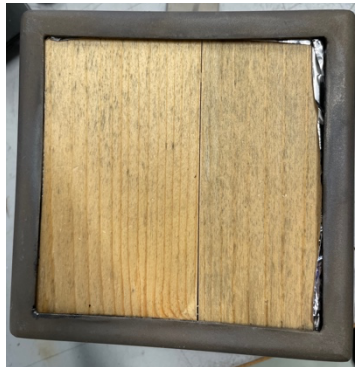


**Figure 5.14 Sample 4-2 showing a spline in the middle.**



**Figure 5.15 Sample 4-2 during the test with no ignition in Phase 1 and 1.2.**

Another interesting factor that can be seen from Figure 5.18 is that TC25 in Test 4-2 reached 300 °C before the other tests, even though it did not ignite. Test 4-3 needed as much as 51 minutes for TC25 to reach 300 °C, 32 minutes for Test 4-2 and 42 minutes for Test 4-1. It is observable that even though the sample did not flame, smoldering ignition degraded the sample. The time for TC25 in Test 4-3 to reach 100 °C is faster than the others but slows down after this point, and the other tests move past Test 4-3. It also shows some differences in the HRR compared to Test 4-1, where the HRR continues to increase for a more extended period after the first peak, indicating a slower burning process. However, it increased just before the test was extinguished. For Test 4-1, the heat release rate in Phase 1 and Phase 3 is the same 15 and 55 minutes into the test, even though there was no ignition in Phase 3.

High heat release rates in the beginning for Test 4-1 and Test 4-3 can also be observed during the tests by high flames, shown in Figure 5.16. However, ten minutes into the test, the flames are significantly lower when the HRR has decreased and stabilized into a steady state, as shown in Figure 5.17.

Figure 5.19 shows HRR and temperature for Test 4-3. This shows that TC15 follows the other TCs until 100 °C is reached. After this point, the other TCs slows down and increases at the same rate for the rest of the test. Only TC15 gets an apparent dip when extinction occurs.



Figure 5.16 Flames right after ignition and Test 4-3.



Figure 5.17 Test 4-3 10 minutes after ignition.

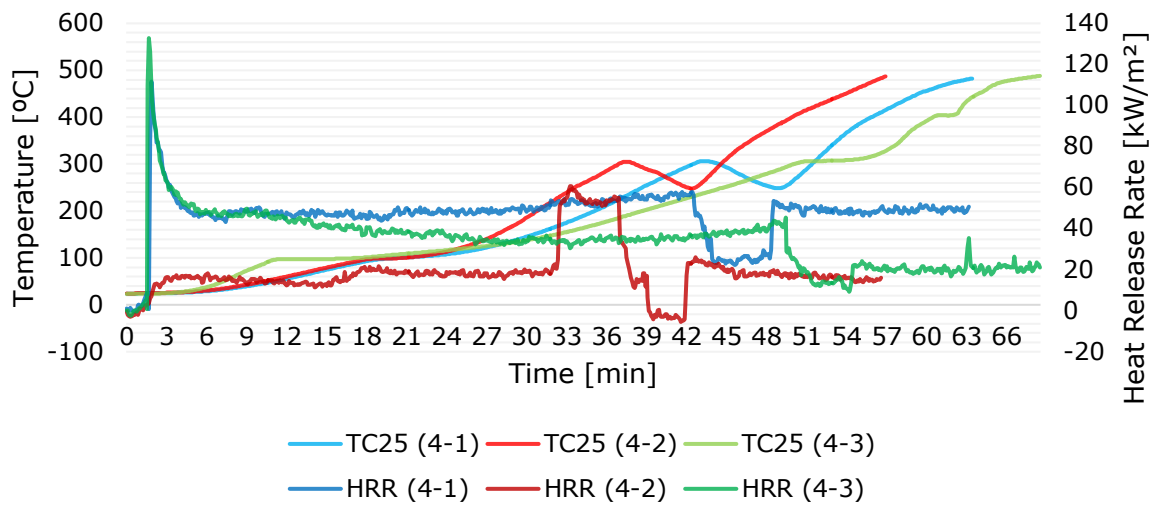
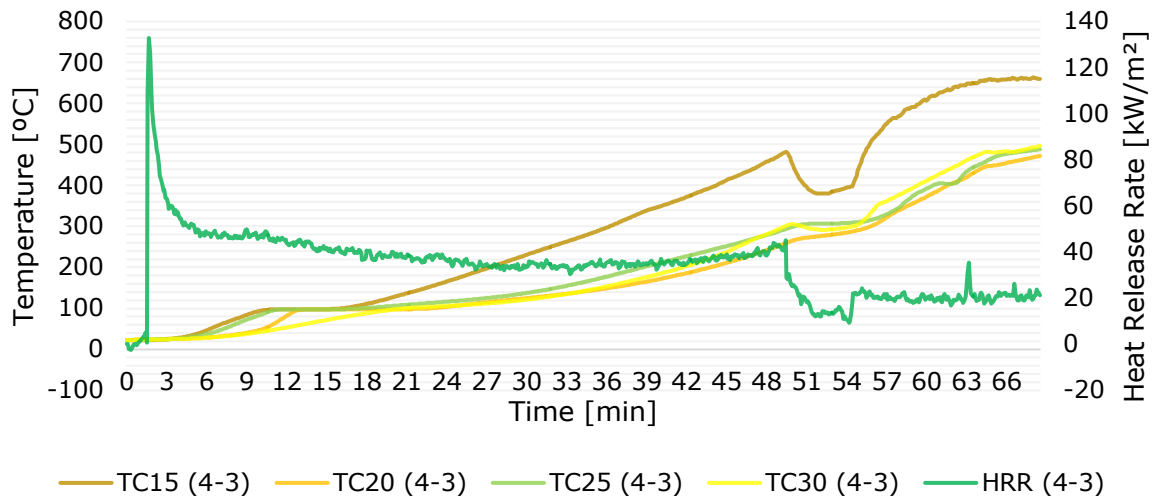
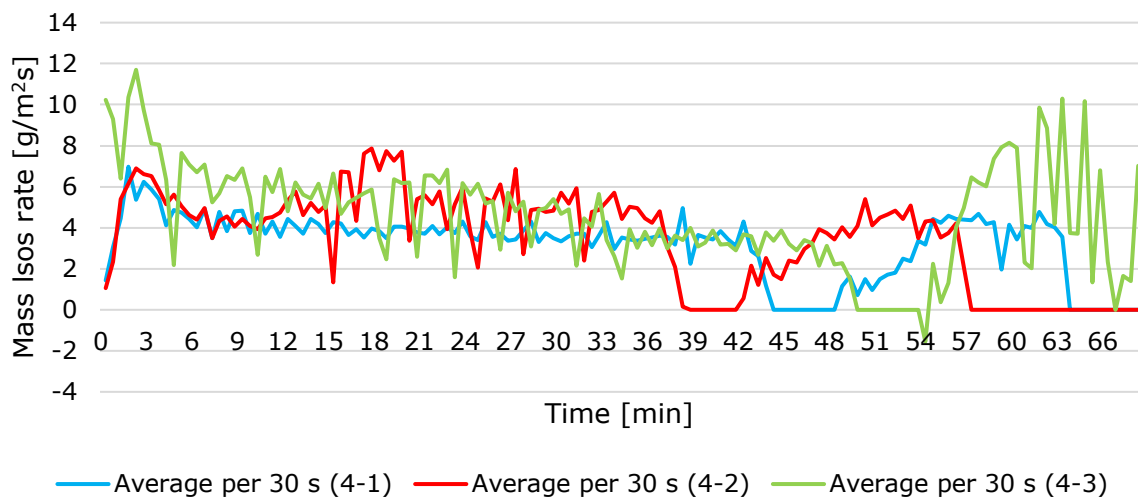


Figure 5.18 Test group 4: HRR and temperature.



**Figure 5.19 Test 4-3: HRR and temperature.**

Even though Test 4-1 ignited at the very beginning and Test 4-2 did not ignite within 30 min after the start, the mass loss in the first 15 minutes is about the same, varying from the peak at 7 g/m<sup>2</sup>s and decreasing to a value between 4-5 g/m<sup>2</sup>s, see Figure 5.20. As seen in Figure 5.18, a slow increase in HRR was observed at 15 minutes for Test 4-2. This shows the increase in heat flux from 30 to 50 kW/m<sup>2</sup> and correlates with the increase in mass loss rate simultaneously in Figure 5.20. When Test 4-2 did ignite after 32 minutes, no differences were seen in the mass loss rate other than a slight decrease from the small peak at 19 min until extinction. After removing the lid in Phase 3, Test 4-1 and Test 4-2 approached a mass loss rate slight above 4 g/m<sup>2</sup>s, while Test 4-3 had a more uneven mass loss with peaks and dips between 10 and 2 g/m<sup>2</sup>s.



**Figure 5.20 Test group 4: mass loss rate.**

## 5.5 Test Group 5: 32 kW/m<sup>2</sup> – 30 kW/m<sup>2</sup> – 38 kW/m<sup>2</sup> – 30 kW/m<sup>2</sup>

The procedure described in Chapter 2.3.3 is followed, besides some changes in Phase 2, where heat flux adjusts to 30 kW/m<sup>2</sup> instead of 0 kW/m<sup>2</sup> to investigate critical heat flux for self-extinction for samples with more materials left than in the earlier tests. Heat fluxes for Test group 5 are presented in Table 5.9.

**Table 5.9 Test group 5: setup.**

Test ID	Phase 1.1 Heat flux [kW/m <sup>2</sup> ]	Phase 1.2 Heat flux [kW/m <sup>2</sup> ]	Phase 2 Heat flux [kW/m <sup>2</sup> ]	Phase 3 Heat flux [kW/m <sup>2</sup> ]	Phase 4 Heat flux [kW/m <sup>2</sup> ]
5-1	32		30 → 0	38	-
5-2	32	50	30 → 0	38	30
5-3	32		30 → 0	38	30

Results from the tests is presented in Table 5.10. As for the tests with heat flux at 33 kW/m<sup>2</sup> for fresh samples, only Test 5-1 and Test 5-3 did ignite at 32 kW/m<sup>2</sup>. Test 5-2 needed over 15 minutes to ignite at 50 kW/m<sup>2</sup> in Phase 1.2. The time to ignition for the tests that did ignite is nearly the same. The surfaces of all the three samples are shown in Figure 5.21, Figure 5.22 and Figure 5.23. Test 5-1 had a spline in the surface, while Test 5-2 has no splines or twigs, and Test 5-3 had a twig. For charred samples at 38 kW/m<sup>2</sup>, two samples did ignite. The density for the sample that did not ignite is higher than for the others.

The same heat flux was tested for extinction in Phase 2 and 4, to investigate if the samples were extinguished because of lack of mass left or removal of the heat flux source. As seen from Table 5.10, none of the tests in Phase 2 extinguished at 30 kW/m<sup>2</sup>, while it happened for two of them in Phase 4. After 15 minutes in Phase 2 with no extinction, lids were used to suffocate the flames.

**Table 5.10 Test group 5: results**

Test ID	5-1	5-2	5-3
Density [kg/m <sup>3</sup> ]	377	515	410
Weight [g]	177	242	193
Humidity [%]			
Time to ignition on fresh wood [s]			
- 32 kW/m <sup>2</sup>	81	No ignition	108
- 50 kW/m <sup>2</sup>		191	
Time to extinction from start of Phase 2 with heat flux [s]			
- 30 kW/m <sup>2</sup>	No extinction	No extinction	No extinction
Time to ignition from start of Phase 3 on charred wood [s]			
- 38 kW/m <sup>2</sup>	No ignition	241	101
Time to extinction from start of Phase 4 with heat flux [s]			
- 30 kW/m <sup>2</sup>		317	231
Time to reach 300 °C [s]			
- 15 mm			2290
- 20 mm			2610
- 25 mm	2893	2853	3050
- 30 mm			3184
Charring rate [mm/min]			
- 15 mm			0,34
- 20 mm			0,46
- 25 mm	0,52	0,43	0,5
- 30 mm			0,57

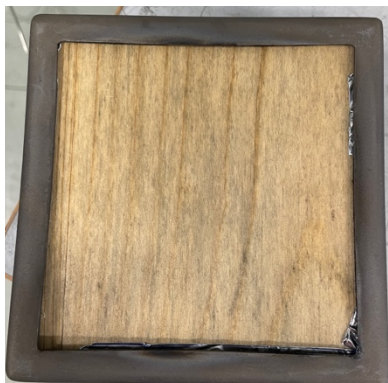


**Figure 5.21 Surface of sample 5-1 showing a spline at the left side.**



**Figure 5.22 Surface of sample 5-2 showing no twigs or splines.**



**Figure 5.23 Surface of sample 5-3 showing a twig in the middle of the sample.**

The time for all samples to get a charred insulating layer at 25 mm is approximately the same in all tests, even though ignition happened at different times for one of them. It can also be seen in Figure 5.24 that the peaks in the tests that ignited right after the test started are much higher than Test 5-2 that ignited after 18 minutes, but it remains higher until the heat flux is reduced to 30 kW/m<sup>2</sup>. When TC25 reaches 300 °C, the heat flux is reduced to 30 kW/m<sup>2</sup> in all tests, and Phase 2 has started. This reduction is not observed as any significant drops in HRR for Test 5-1 and Test 5-3, as the difference in heat flux between the phases is low. A fellow observation at around 50 minutes is that the HRR is

increasing instead of extinguishing for both graphs. For Test 5-2, a decrease in the HRR is observed at 45 minutes when the heat flux is reduced but increases and stabilizes after 10 minutes.

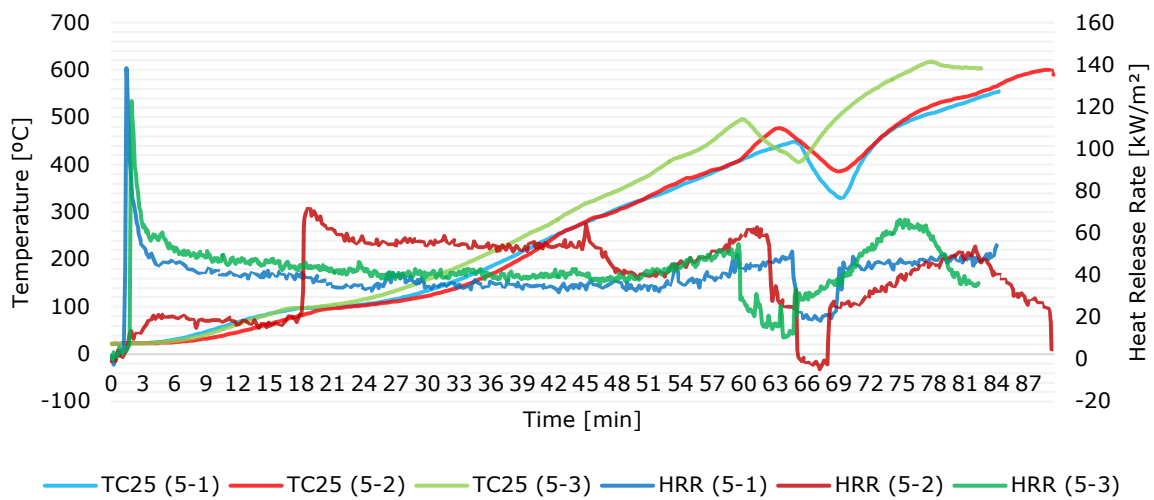


**Figure 5.24 Test group 5: HRR and temperature.**

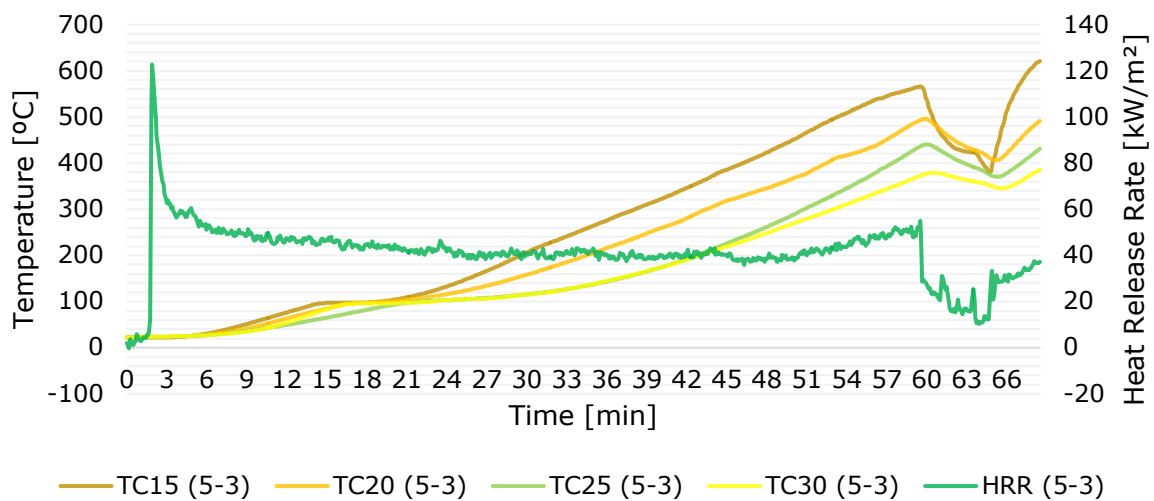


**Figure 5.25 Test 5-3: HRR and temperature.**

Even though Test 5-2 did not ignite initially, the mass loss rate lies on the same level as for Test 5-1 for the first 15 minutes. Test 5-3 has higher peaks but stabilizes at the same level as Test 5-1. The mass loss rate for Test 5-2 increases as the heat flux increases. In contrast to the HRR, it can be observed a slight decrease in the mass loss rate easiest observed for Test 5-1 in Figure 5.26, where it slowly moved from 4 g/m<sup>2</sup>s to slightly above 2 g/m<sup>2</sup>s.

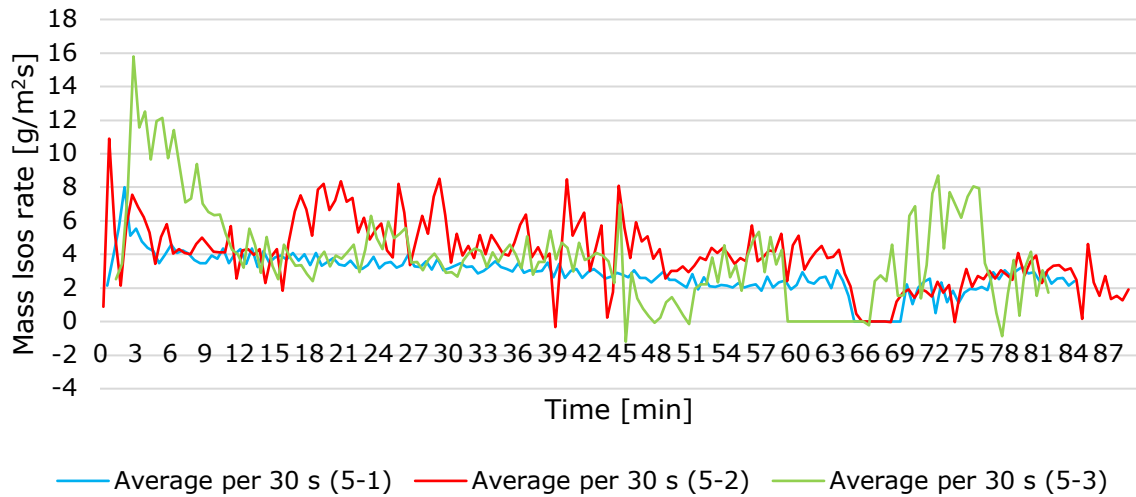


**Figure 5.26 Test group 5: mass loss rate.**

## 5.6 Test Group 6: 31 kW/m<sup>2</sup> – 25kW/m<sup>2</sup> – 37 kW/m<sup>2</sup> – 25 and 37 kW/m<sup>2</sup>

Test group 6 follows the same procedure as Test group 5 but with a reduction in heat flux in Phase 2 instead of zero heat flux exposures, following the setup described in Table 5.11. All tests in this group have only one TC inside of them placed at 25 mm from the exposed side.

**Table 5.11 Test group 6: setup.**

Test ID	Phase 1.1 Heat flux [kW/m <sup>2</sup> ]	Phase 1.2 Heat flux [kW/m <sup>2</sup> ]	Phase 2 Heat flux [kW/m <sup>2</sup> ]	Phase 3 Heat flux [kW/m <sup>2</sup> ]	Phase 4 Heat flux [kW/m <sup>2</sup> ]
6-1	31	50	25	37	-
6-2	31	50	25 → 0	37	25
6-3	31	50	25	37	37

As seen from Table 5.12 none of the tests ignited at the initial heat flux. Test 6-1 ignited after 15 minutes at 50 kW/m<sup>2</sup>, while the others ignited three minutes after the increase in Phase 1.2. In contrast to all other tests in Phase 2, extinction with a sustained heat flux at 25 kW/m<sup>2</sup> occurred for two of the tests. Two tests reignited at 37 kW/m<sup>2</sup>, while one of them extinguished at the same heat flux in Phase 4.



**Table 5.12 Test group 6: results.**

Test ID	6-1	6-2	6-3
Density [kg/m <sup>3</sup> ]	389	478	430
Weight [g]	183	225	202
Humidity [%]	8,4	8,7	8,5
Time to ignition on fresh wood [s]			
- 31 kW/m <sup>2</sup>	No ignition	No ignition	No ignition
- 50 kW/m <sup>2</sup>	925	181	165
Time to extinction from start of Phase 2 with heat flux [s]			
- 25 kW/m <sup>2</sup>	119	No extinction	20
Time to ignition from start of Phase 3 with heat flux [s]			
- 37 kW/m <sup>2</sup>	No ignition	249	12
Time to extinction from start of Phase 4 with heat flux [s]			
- 37 kW/m <sup>2</sup>		268	-
Time to reach 300 °C [s]			
- 15 mm			
- 20 mm			
- 25 mm	2503	2650	2670
- 30 mm			
Charring rate [mm/min]			
- 15 mm			
- 20 mm			
- 25 mm	0,6	0,57	0,56
- 30 mm			

HRR and temperatures is presented in Figure 5.27. All tests started with the same heat flux, but the HRR for Test 6-1 stands out compared to the others because it sustains or increases the first 15 minutes, while the others decrease during the same period. The PHRR occurs at the time of extinction, and unlike Test 6-2 and Test 6-3, the HRR stays high and increases even more during the next 10 minutes after ignition.

Before Phase 2 and the first extinction in Test 6-1, the flames went smaller before they extinguished within two minutes after reduction in heat flux. This is seen in Figure 5.27 with a drop in the HRR. Although, it should be noted that the HRR is significantly higher at extinction than it is for the other tests. In Test 6-3, the flames went smaller already when the heat flux was reduced and extinguished immediately after the cone had reached 25 kW/m<sup>2</sup>, shown in the drop that nearly goes to zero. The same was observed in Test 6-2, but it managed to stabilize the flame eventually, so it did not extinguish, and the flame increased and stabilized after a short time. This is seen as the first drop of HRR (6-2), while the second drop shows when the lid extinguished the fire. In between the two drops, an increase in the HRR is observed while the flame stabilizes and reaches steady-state 10 minutes after the heat flux reduction.

Two of the tests reignited at 37 kW/m<sup>2</sup>. An important aspect found in Test 6-2, is that the test self-extinguished at 37 kW/m<sup>2</sup>, the same heat flux necessary for ignition on the same sample. This shows the importance of not assuming that every test extinguishes because of reduced heat flux but also considering the mass left in the sample.

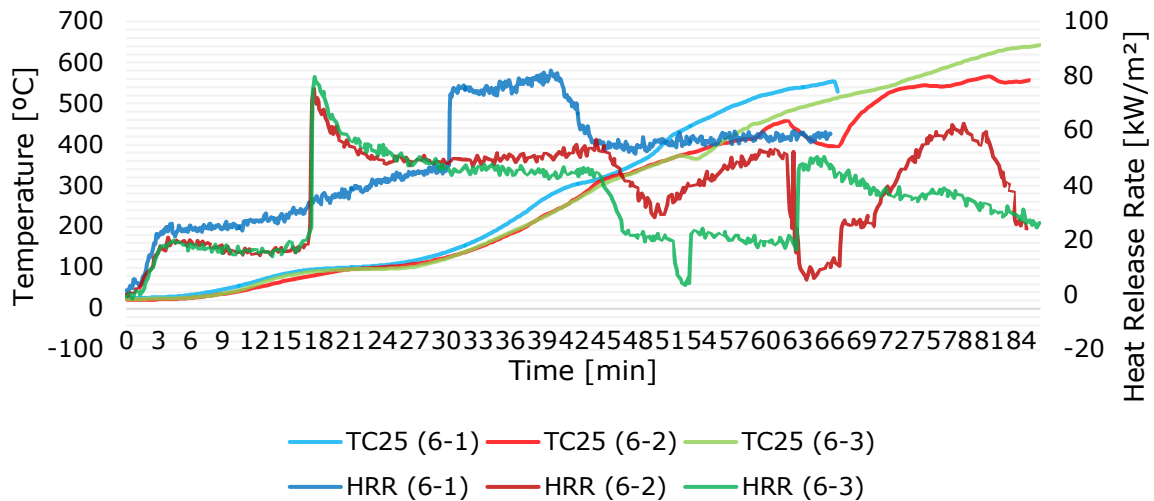


**Figure 5.27 Test group 6: HRR and temperature.**

The mass loss rate in Figure 5.28 follows the same lines during the first 40 minutes, independent of when they ignite. Comparing the mass loss rate to the points where two of the tests extinguished and one sustained burning shows that the mass loss rate for the test that sustained burning is higher than the others. Before extinction, all tests had a mass loss rate between 4 and 5 g/m<sup>2</sup>s. After the reduction in heat flux, the mass loss rate for Test 6-2 had a low point at 3 g/m<sup>2</sup>s, while the others fell to 2 g/m<sup>2</sup>s.

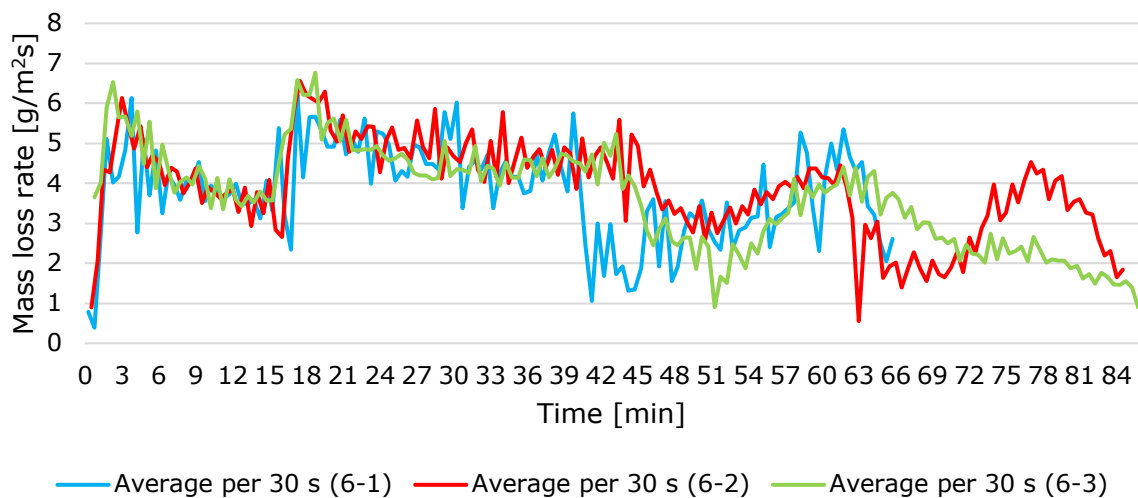


**Figure 5.28 Test group 6: mass loss rate.**

## 5.7 Test Group 7: a Combination of Different Heat Fluxes

Test group 7 has combined heat flux levels from the other tests to fill in where there is seen necessary to get more results and is presented in Table 5.13. As all tests have different heat flux combinations for the different phases, one diagram per test has been made, besides the mass loss rate where it has been possible to present it all combined.

**Table 5.13 Test group 7: setup**

Test ID	Phase 1.1 Heat flux [kW/m <sup>2</sup> ]	Phase 1.2 Heat flux [kW/m <sup>2</sup> ]	Phase 2 Heat flux [kW/m <sup>2</sup> ]	Phase 3 Heat flux [kW/m <sup>2</sup> ]	Phase 4 Heat flux [kW/m <sup>2</sup> ]
7-1	32	50	28 → 0	36	-
7-2	33	50	28 → 0	36	36
7-3	34	40 – 50	28 → 0	36	-
7-4	34		28 → 0	36	-
7-5	34	40 – 50	25	37	37

Test results is presented in Table 5.14. Test 7-1 and Test 7-2 did not ignite at 32 kW/m<sup>2</sup> and 33 kW/m<sup>2</sup>, and it was only Test 7-4 that ignited at 34 kW/m<sup>2</sup>.

In Phase 2, the heat flux was reduced to 25 kW/m<sup>2</sup> for Test 7-5 and 28 kW/m<sup>2</sup> for the others. No extinction occurred in any of them. However, observations showed that all tests almost extinguished as only small flames on the edges was observed after adjustment. After approximately 5 minutes, the flames increased and stabilized. The test was then extinguished with a lid to continue to Phase 3. Reignition occurred in two out of three tests at 36 kW/m<sup>2</sup>, in addition to the test exposed to 37 kW/m<sup>2</sup>.

**Table 5.14 Test group 7: results.**

Test ID	7-1	7-2	7-3	7-4	7-5
Density [kg/m <sup>3</sup> ]	385	389	435	392	392
Weight [g]	181	183	205	184	184
Humidity [%]	9,2	9,0	9,0	8,8	8,5
Time to ignition on fresh wood [s]					
- 32 kW/m <sup>2</sup>	No ignition				
- 33 kW/m <sup>2</sup>		No ignition			
- 34 kW/m <sup>2</sup>			No ignition	70	No ignition
- 40 kW/m <sup>2</sup>			No ignition		No ignition
- 50 kW/m <sup>2</sup>	923	360	365		No ignition
Time to extinction from start of Phase 2 with heat flux [s]					
- 25 kW/m <sup>2</sup>					No extinction
- 28 kW/m <sup>2</sup>	No extinction	No extinction	No extinction	No extinction	
Time to ignition from start of Phase 3 on charred wood [s]					
- 36 kW/m <sup>2</sup>	No ignition	682	No ignition	No ignition	
- 37 kW/m <sup>2</sup>					287
Time to extinction from start of Phase 4 with heat flux [s]					
- 36 kW/m <sup>2</sup>		496			No extinction
- 37 kW/m <sup>2</sup>					
Time to reach 300 °C [s]					
- 25 mm	2468	2430	2877	2792	2642
Charring rate [mm/min]					
- 25 mm	0,61	0,62	0,52	0,54	0,57

The surface of the sample in Test 7-3, Test 7-4 and Test 7-5 is presented in Figure 5.29, Figure 5.30 and Figure 5.31. The surface of sample 7-3 and 7-4 had a spline in the surface, in addition to torn of pieces, leading to new, fresh timber in the surface. Sample 7-5 is mostly smooth, with a few pieces torn of on the edge.



**Figure 5.29 Sample 7-3 showing a spline in the surface.**



**Figure 5.30 Sample 7-4 showing irregularities in the surface.**



**Figure 5.31 Sample 7-5 showing a smooth surface, besides a few irregularities on the bottom edge.**

HRR and temperatures for all tests in group 7 is presented in Figure 5.32, Figure 5.33, Figure 5.34, Figure 5.35 and Figure 5.36. Here again, tests that ignited right after the test started got a high PHRR at the time of ignition and stabilizes at a lower level. Tests that used some time to ignite had sustained high HRR, but at a lower level than the PHRR for rapid ignition.

HRR and temperatures for all tests in group 7 is presented in Figure 5.32, Figure 5.33, Figure 5.34, Figure 5.35 and Figure 5.36. Here again, tests that ignited right after the test started got a high PHRR at the time of ignition and stabilizes at a lower level. Tests that used some time to ignite had sustained high HRR, but a lower level for the PHRR.

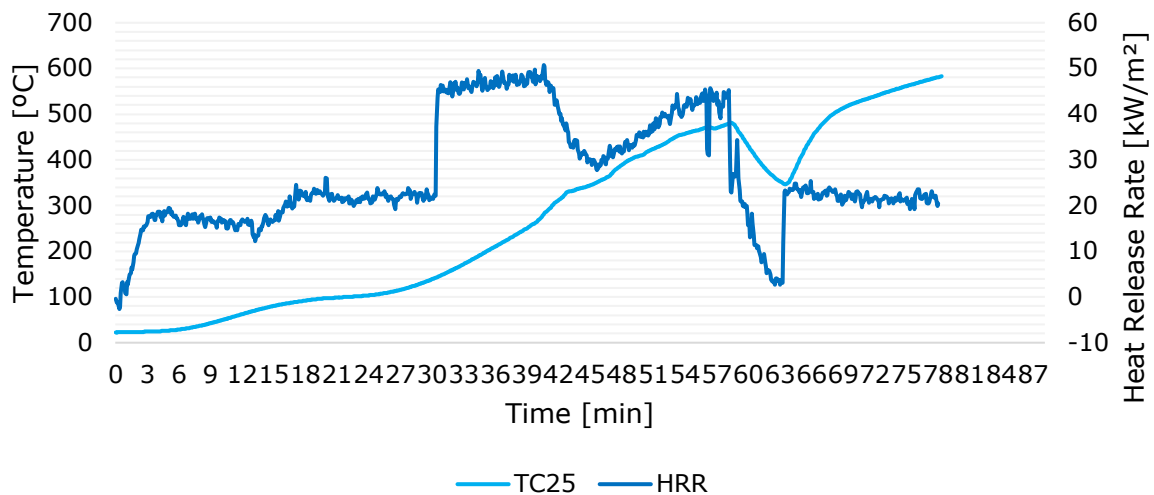


**Figure 5.32 Test 7-1: HRR and temperature.**

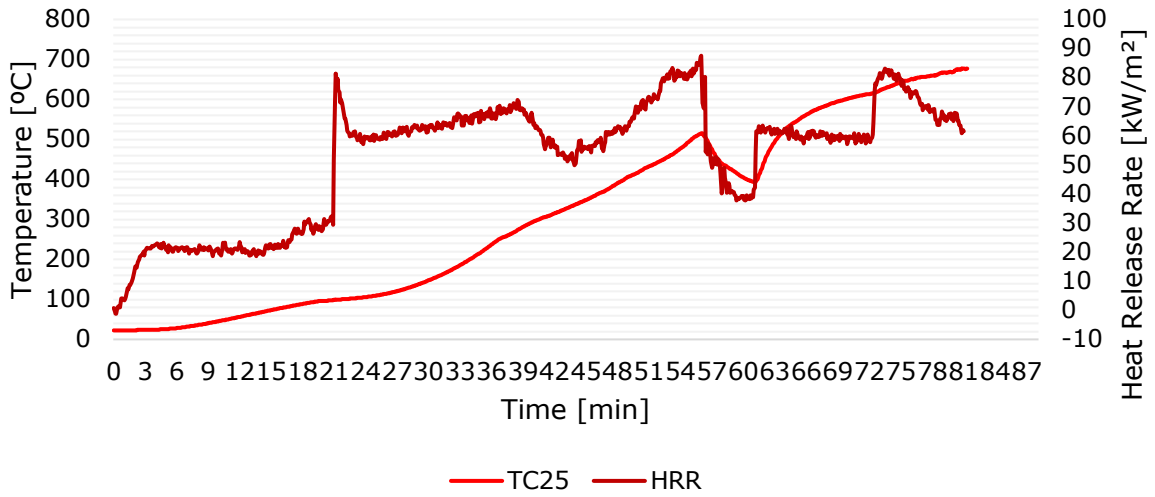


Figure 5.33 Test 7-2: HRR and temperature.

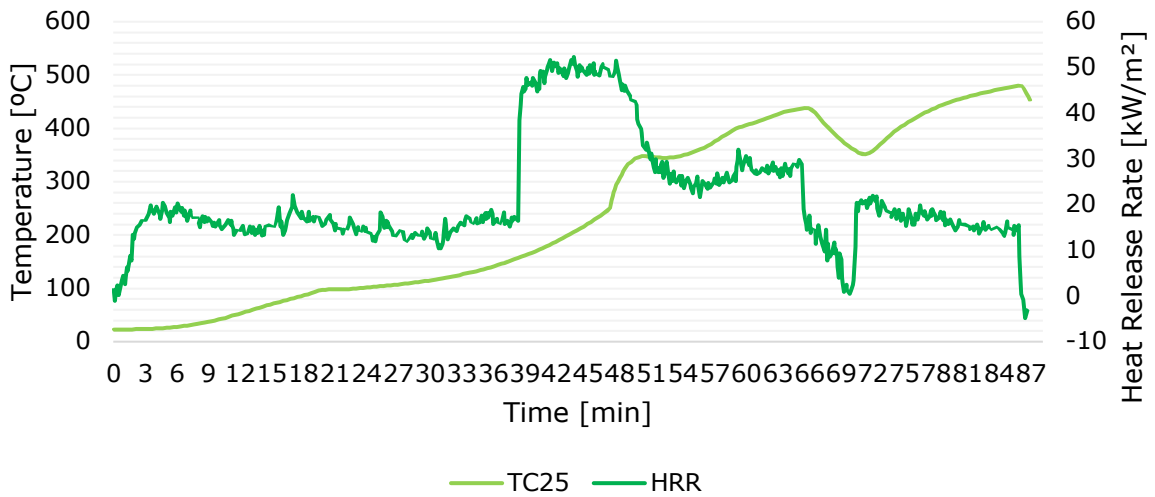


Figure 5.34 Test 7-3: HRR and temperature.

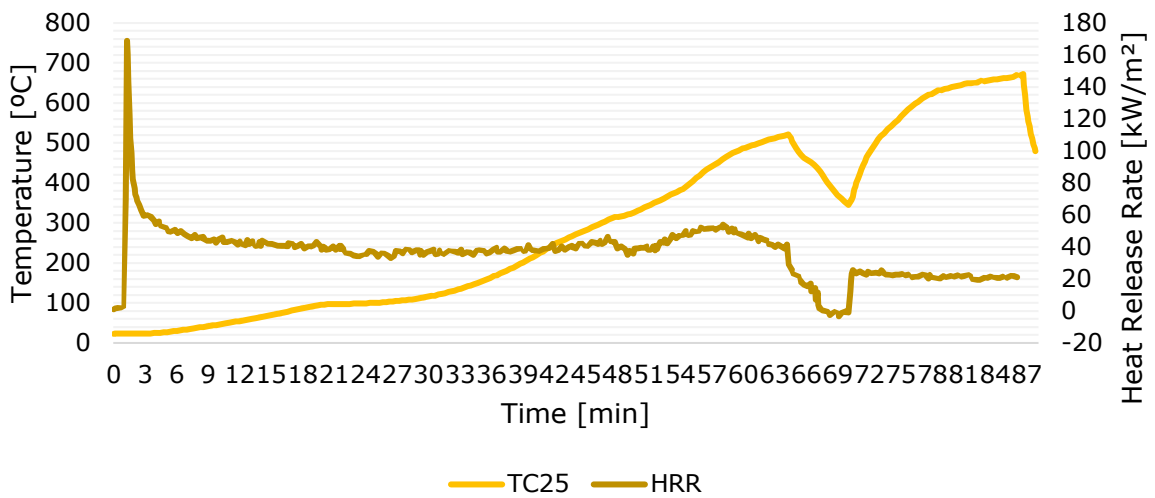
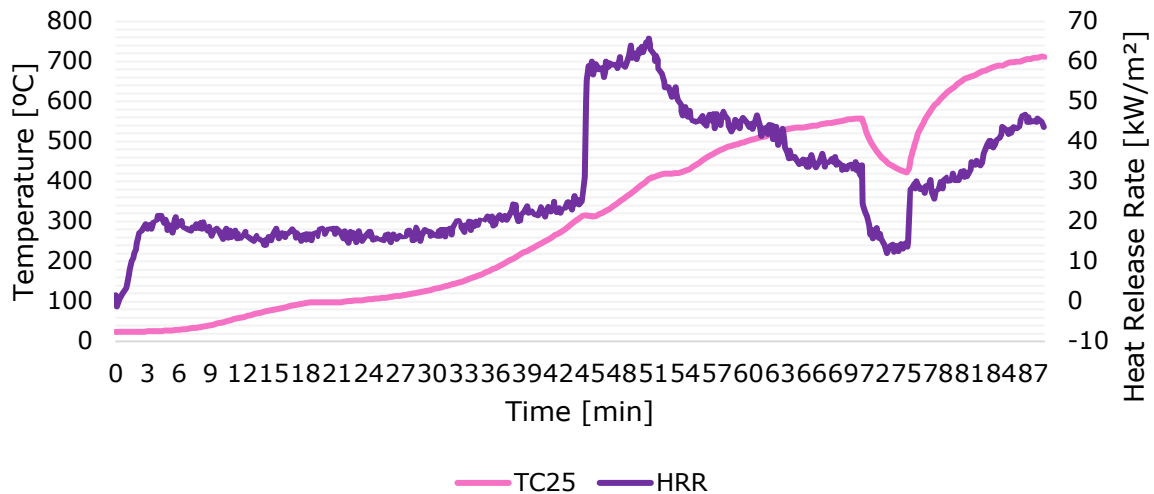
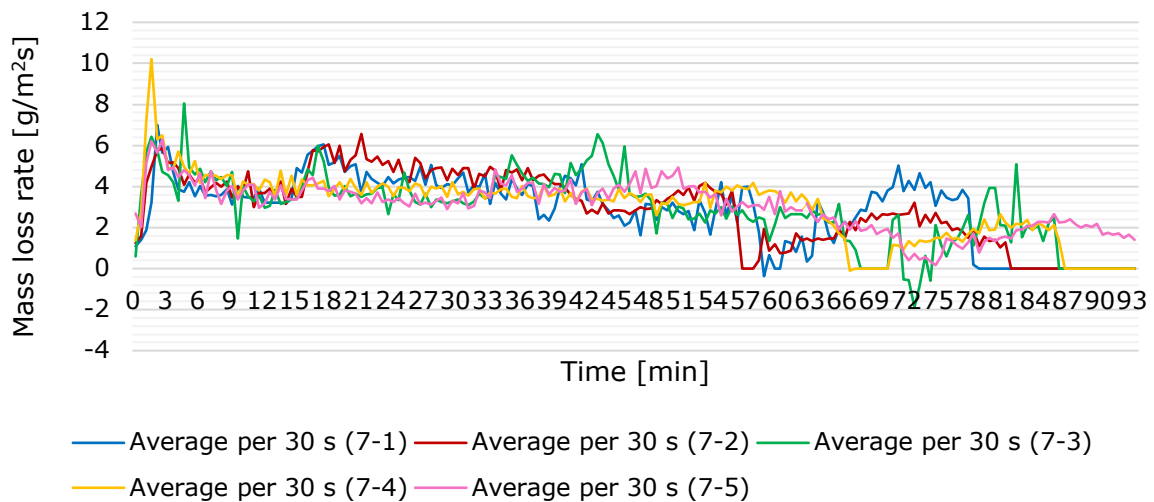


Figure 5.35 Test 7-4: HRR and temperature.



**Figure 5.36 Test 7-5: HRR and temperature.**

The mass loss rate for all tests in Test group 7 shown in Figure 5.37. A significant peak can be seen for the mass loss rate for Test 7-4, which corresponds to the peak of HRR from Figure 5.35. All the other tests that did not ignite at the initial heat flux does also have a peak in the beginning, but slightly lower than for the ignited sample. After the peak, it decreases and stabilizes at around 4 g/m<sup>2</sup>s, until an increase is observed at the time of ignition. For Test 7-5, that extinguished at 28 kW/m<sup>2</sup> at 72 minutes, had a mass loss rate as low as 0,17 g/m<sup>2</sup>s at the time of extinction. Test 7-2 that did not extinguish, but managed to stabilize had a slightly higher mass loss rate at 0,4 g/m<sup>2</sup>s.



**Figure 5.37 Test group 7: mass loss rate.**

## 5.8 Critical Heat Flux for Ignition

Based on the definition for calculating the critical heat flux in ISO 5660-1 as presented in the method, the critical heat flux is the average between the lowest heat flux for ignition and the highest heat flux for no ignition within 15 minutes. This gives a critical heat flux at 31,5 kW/m<sup>2</sup> for fresh wood and 35,5 kW/m<sup>2</sup> for charred wood.

## 5.9 Critical Heat Flux for Extinction

It is observed that all samples besides one extinguished within 5 minutes with no heat flux radiation. For a reduced heat flux in Phase 2, one sample extinguished at 25 kW/m<sup>2</sup>, while all other samples sustained burning. In Phase 4 with a reduced heat flux, several samples extinguished within 15 minutes at 30, 36 and 37 kW/m<sup>2</sup>.

## 5.10 Critical Heat Flux for Ignition According to Janssens Method

As described and presented in the earlier chapters, the time for ignition on fresh wood was measured in all tests. The results from these measurements can be used to predict the critical heat flux for the ignition of the material by using Janssens procedure (Janssens, 1991). The method is described in more detail in Chapter 3.4.1.

To include that some of the samples did not ignite at all at the given heat flux, the time to ignition is set unrealistically high to imply that they do not ignite. These samples can be seen as the dots nearest the x-axis in Figure 5.38. Together with the samples that ignited and are plotted in the transformed formula for ignition time,  $t^{-0,547}$ , they create the basis for a linear line crossing the x-axis in the point that is assumed to be the critical heat flux for the material. The line crosses the x-axis at 29,87 kW/m<sup>2</sup>.

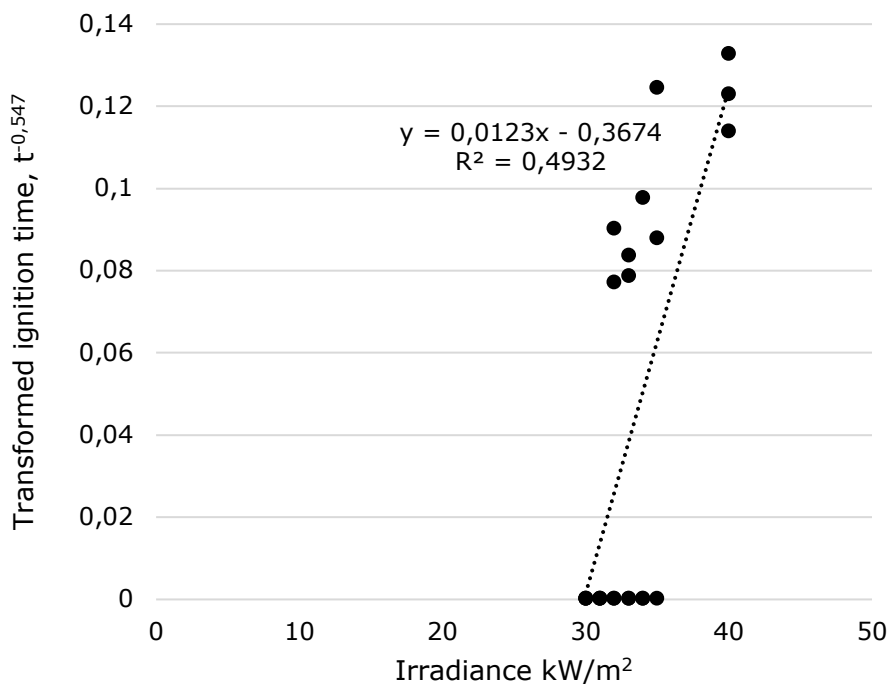


**Figure 5.38 Janssens method for predicting critical heat flux the CLT samples.**



## 5.11 Calculation of Char Depth from Mass Loss

Tests in the cone calorimeter have given results regarding continuous tracking of mass loss and temperatures inside the samples. This information is used to investigate if there is possible to find an equation that can calculate the char depth in the material during a test if the mass loss is known. Parts of the result can be seen in Figure 5.39 and Figure 5.40. In Figure 5.39, the mass loss is calculated as a percentage of the total mass of the sample, and the char depth is calculated as a percentage of the total thickness of the sample. In Figure 5.40, the mass loss is presented in grams and the char depth is presented in millimeters.

The mass loss is based on the average mass loss in all the samples. It is found by taking the average mass loss every fifth second in all samples, divided by the number of samples. When a sample has reached 300 °C in TC25, the sample is removed from the calculation, and the number divided on the mass loss decreases with one. This is repeated until all samples have reached 300 °C in TC25.

The method used to deduce equations in percentage, and grams and millimeters, is the same. At first, the average mass loss over time from all the samples is found and inserted into a diagram seen as the blue solid line in Figure 5.39 and Figure 5.40. Secondly, the time for all TC25 to reach 300 °C is inserted as red crosses in the figure. One linear trend line is found for the blue line and, and one is found for the red crosses, shown as a blue dotted line for mass loss and a red dotted line for TC25 to reach 300 °C, with corresponding equations for each. The equations are framed in blue for mass loss (ML) and red for char depth (CD), in terms of the time (t).

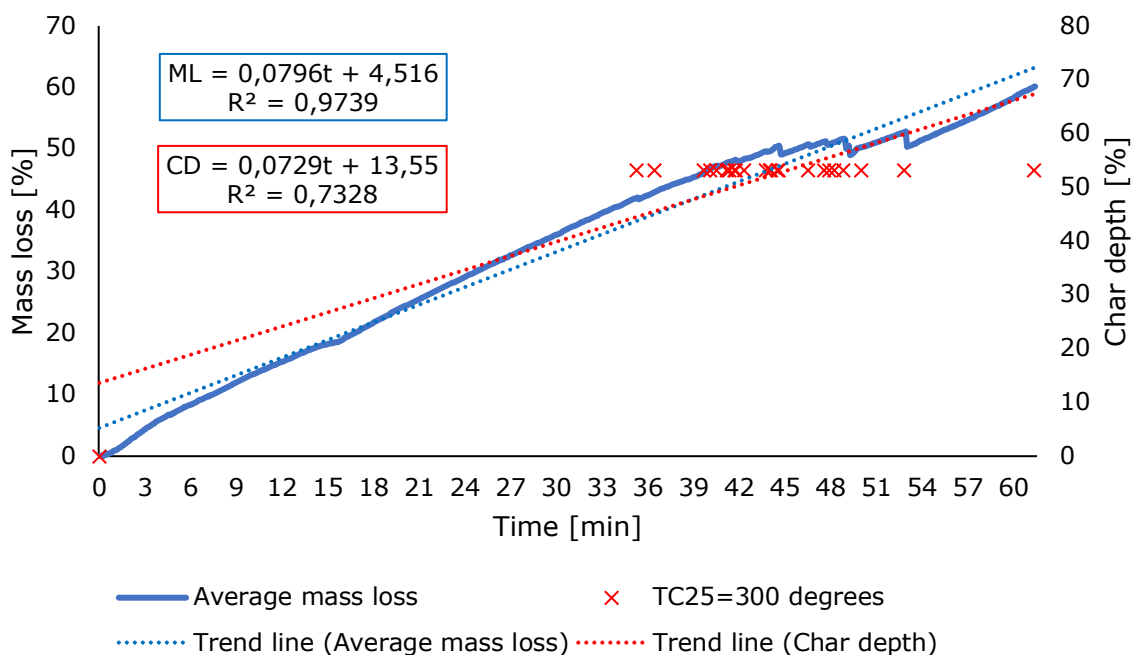


**Figure 5.39 Average mass loss and char depth in percentage.**

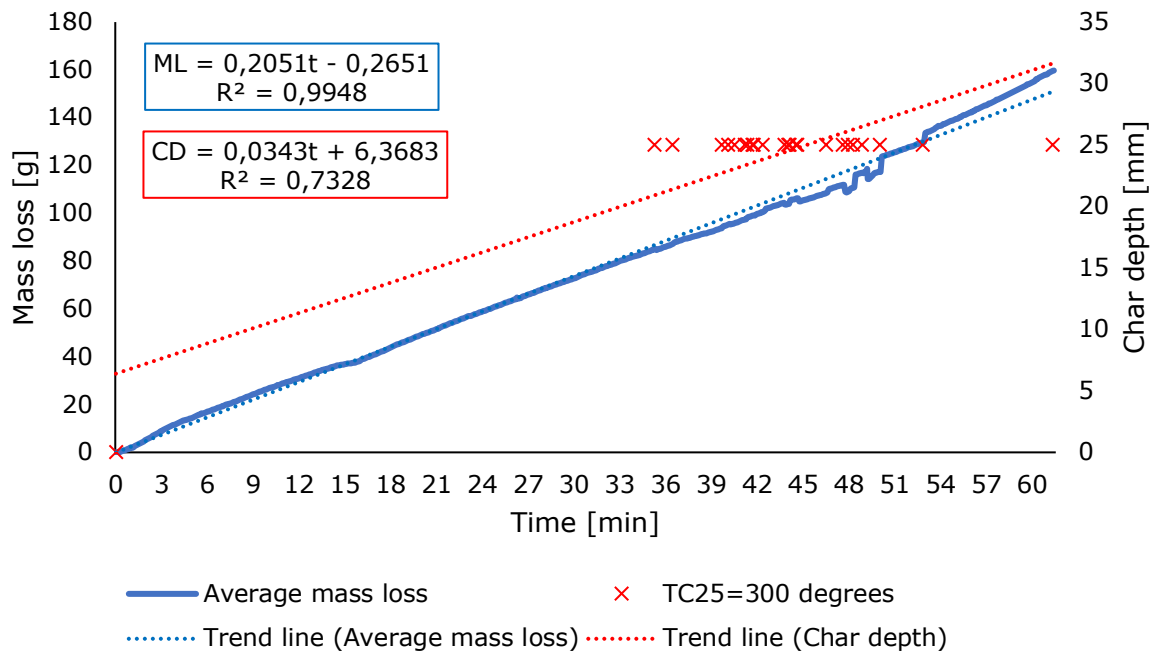


**Figure 5.40 Average mass loss and char depth in grams and millimeters.**

These diagrams have given us four equations, two per diagram. By combining these two, an equation for finding the char depth by knowing the mass loss is found. The calculation of the final equation in percentage is called *Equation 1*, and the one in grams and millimeters is called *Equation 2*.

Equation 1: development of equation for depth and mass loss in percent:

$$CD = 0,0729 * t + 13,55$$

$$ML = 0,0796 * t + 4,516$$

$$t = \frac{ML}{0,0796} - \frac{4,516}{0,0796} = \frac{ML}{0,0796} - 56,7337$$

$$CD = 0,0729 * \left( \frac{ML}{0,0796} + 56,7337 \right) + 13,55 = 0,9158 * ML - 4,1359 + 13,55$$

$$\underline{CD = 0,9158 * ML + 9,4141}$$

Equation 2: development of equation for char depth in mm and mass loss in g:

$$CD = 0,0343 * t + 6,3683$$

$$ML = 0,2051 * t - 0,2651$$

$$t = \frac{ML}{0,2051} + \frac{0,2651}{0,2051} = \frac{ML}{0,2051} + 1,2925$$

$$CD = 0,0343 * \left( \frac{ML}{0,2051} + 1,2925 \right) + 6,3683 = 0,1672 * ML + 0,0443 + 6,3683m$$

$$\underline{CD = 0,1672 * ML + 6,4126}$$

## 6 Discussion

The discussion aims to have a discourse about the results from the literature review, the Compartment Test and the cone calorimeter tests presented in Chapter 3, 4 and 5. The cone calorimeter test results create the basis for the discussion. Next, the results are compared with the Compartment Test and existing literature. It discusses the sources of errors and uncertainties during the preparations, the methods employed in the testing, and the limitations and simplifications undertaken in the analysis. Finally, it attempts to find relations between small-scale testing and a large-scale compartment fire, and how temperatures and charring in CLT timber behave for each situation. To discuss the results presented in the previous chapters, results from a few test groups or tests is chosen under each section. The chosen results are either standing out from the rest of the group or gives a representation of how the timber behaves during a fire.

### 6.1 Criticism of the Methods

#### 6.1.1 Uncertainties with ISO 5660 Adjustments

Chapter 2.3 mentions that the method used in the cone calorimeter tests partly follows the procedure described in ISO 5660-1. After Phase 1, the principles from the standard is followed, but some heat flux adjustments are made throughout the test. The method used for the testing is adjusted for these exact tests to make it possible to measure the desired outcome. Therefore, it is not validated by any authorization and does not follow any standardized method, making it easier to make mistakes during the testing and allowing adjustments in the test procedure throughout the testing. It is pursued avoided by planning the tests in advance and running the same procedure for several tests. However, it does not follow the same method as accredited tests does.

Each test situation used three samples besides a few additional tests at some heat fluxes in Test group 7. From Chapter 2.3.3, ISO 5660-1 demands that a minimum of three similar samples should be tested in each situation. In situations where ignition has occurred two out of three times, it has not been conducted more tests for the same exposure for further investigations. It could have been tested more to get a more representative result. The reason for not conducting more tests, is the need for more test materials and time; it has been prioritized to try different heat fluxes instead. This has given more unprecise but general results, showing that the validity of the tests is ok, but has yet to give as reliable results as desired.

As mentioned in Chapter 2.3.3, each phase has a time limitation of 15 minutes to ignite or extinguish at the given heat flux, depending on the phase, based on the instructs for critical heat flux for ignition given in ISO 5660-1. After 15 minutes of no ignition or extinction, the heat flux is adjusted, and a new countdown for the next 15 minutes starts before the situation repeats until ignition or extinction. Based on this, it assumes that the samples do not ignite or extinguish at the given heat flux at all if it does not ignite or extinguish within 15 minutes when calculating the critical heat flux. For ignition, it assumes that the material has lost its properties for a fresh sample and the char will insulate the inner layers and protect it from further ignition after 15 minutes, and a more extended period does not lead to ignition.

A negative factor about this approach is that it does not consider the difference between if the sample had ignited at 16 minutes or not at all. Therefore, the definition of critical heat flux saying that it is the lowest heat flux necessary for ignition, may not be fulfilled by only 15 minutes of testing time, and the results given from the cone calorimeter tests could be slightly lower if the testing time lasted longer.

Another example of why it could have been necessary to use a few more samples at each test situation is for Test 3-2, where the measurements in the HRR did not start at the correct baseline before ignition occurred. As a result, it has a negative HRR for the first 30 minutes. In this case, it was evaluated if throwing away the sample and starting over was necessary. However, further testing concluded that the heat fluxes used in the test did not form the boundary conditions for ignition or extinction, and the test would not be decisive for the result.

### 6.1.2 The Impact of Lids and Thermocouples

During testing, there is a continuous weight measuring the mass loss of the samples. The thermocouples can affect the weighting because of the wires, but also because parts of the wood are replaced with thermocouples instead. Still, experiments by Terrei et al. (2021) with thermocouples in timber samples tested in a cone calorimeter have shown that the difference in mass loss rate with and without thermocouples was not that big.

However, findings from the cone calorimeter testing have shown interferences in the weight caused by the thermocouples. This has significantly impacted the mass loss rate, together with the interferences caused by the lids. As described in the previous chapters, some values collected from continuous weighting during the tests have been removed from the diagrams. These changes were necessary to get readable information from the diagrams of the mass loss rate. Original data from Test 4-2 is shown in Figure 6.1. The big dip at the start shows where the gypsum lid has laid on the sample before the test started, to prevent heat exposure on the sample, while the dips and peaks during the test shows where lids have been used throughout the test, in addition to smaller deviations caused by the thermocouples. It is on this behalf chosen to remove values that cause massive deviations to get an overall picture of how the mass loss rate has developed. The impact of thermocouples can also be seen in Figure 5.12, showing the mass loss rate for Test 3-1 and Test 3.2. Negative values are observed at three points, which is impossible if the tests were burning undisturbed and not touched.

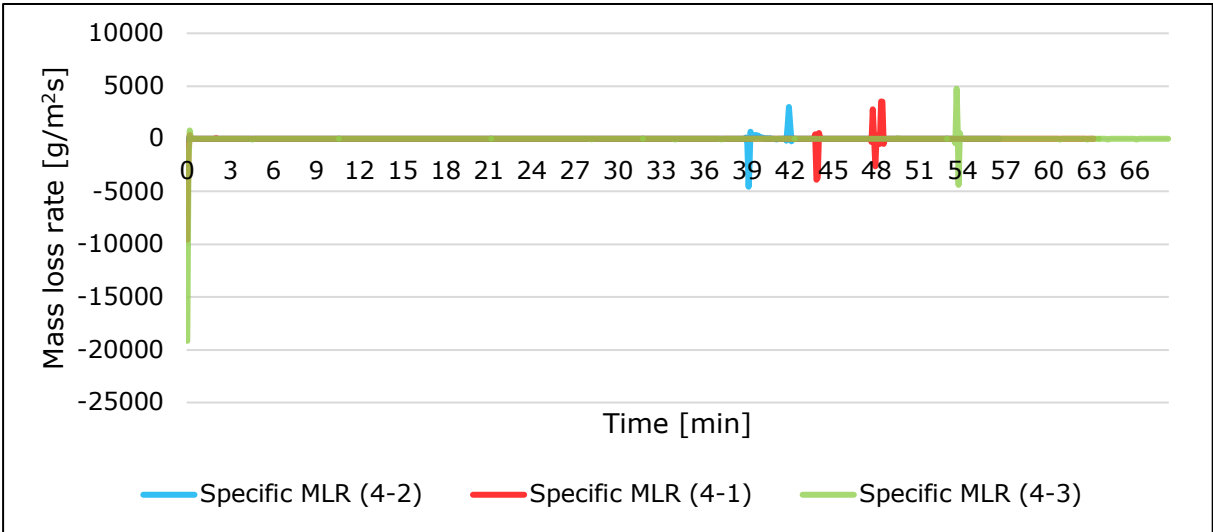


Figure 6.1 Mass loss rate with original data.

The thermocouples can also interfere with the mass loss, so the wires impact the weight differently after movements. As the lids go on and off the sample, movements, and changes in the retainer's position with the belonging TCs lead to weight variations if the wires are lifted more or less than before the movements. This again affects the results when calculating the charring rate and charring depth based on the mass loss. It can explain the dips when calculating the charring depth based on the mass loss in Chapter 5.11.

Even though the wires and the wood have different conductivity, the positive effects found by Terrei et al. (2021) of using thermocouples were more extensive than the uncertainties they created. This could come from several factors: thin thermocouples demand little mass reduction through setup in both timber and glue, which also minimizes the conductive heat flux through the wires. The thermal resistance between the sample and wire could be assumed negligible. Nevertheless, it should be noted that thermocouples will be affected by the radiation as the charring goes deeper into the wood. It will, therefore, not be a specific measurement for the gas temperature inside the wood when the layer between the heat source and the thermocouples reduces.

Implementing thermocouples inside a sample requires preparations of the samples in the form of drilling holes to make room for the thermocouples. These holes are supposed to lay at 15 mm, 20 mm, 25 mm, and 30 mm depth from the exposed surface. However, since these are inside the sample, some deviations from the exact values may have occurred as to errors in the measurements. Therefore, uncertainties are tried to prevent by double measuring the depths in all the samples.

In some tests with multiple thermocouples at different depths, the temperature has not developed as linearly as the theory may imply. For example, in Test 4-3, TC20, TC25, and TC30 follow nearly the same temperature increase the entire time, even though the most natural development would be that TC20 increases first, then TC25 and TC30. A reason for this is that the burning of wood is inhomogeneous. As seen earlier, when wood gets heated, water vaporizes, and the remaining solid contracts. The char creates holes at sometimes random places in the wood, and irregularities in density, cracks, or holes in the surface make room for the heat to develop unevenly through the wood sample. When these holes coincide with the TCs, the temperature in the TC may not necessarily apply to the whole sample but at the exact point. The drilled hole for the TC to fit in may amplify the probability of coinciding cracks as it will make room for air in the hole and makes the density at the point lower.

In Test group 1, Test 1-2 is seen to have the highest charring rate of the three samples tested. A crack is observed at the same point the TC lays for this sample, that can be seen in Figure 6.2. The cracks in the charred layer have coincided with the TC, which could have impacted the time for TC25 to reach 300 °C. This can also lead to a wrong basis for comparing charring rates against other tests directly. Nevertheless, performing multiple tests will still provide an accurate depiction of how wood responds to heat exposure. Another noteworthy aspect is that this occurrence in a small cone calorimeter test highlights the unpredictable nature of wood. It would also exhibit a different and non-uniform behavior during an actual fire, especially when larger and more significant elements are involved.



**Figure 6.2 Showing cracks at the same place a TC in Test 1-2.**

## 6.2 Differences in the Material

As mentioned in Chapter 1.1, CLT as a material does consist of several layers of lamellas using glue between the cross layers. This leads to splines between the planks, both in between the different layers and within the same layer. Figure 6.3 shows a spline in the surface from the side, and Figure 6.4 shows a spline in the surface from above. Splines like these could, according to Barber et al. (2022), make the heat move more accessible through the timber and lead to a faster burning rate and multidimensional charring from several sides. It can especially be critical in compartment fires leading the heat further in than for the rest of the material, causing weak spots where the timber has charred more than the rest, resulting in worse bearing capacity than expected.

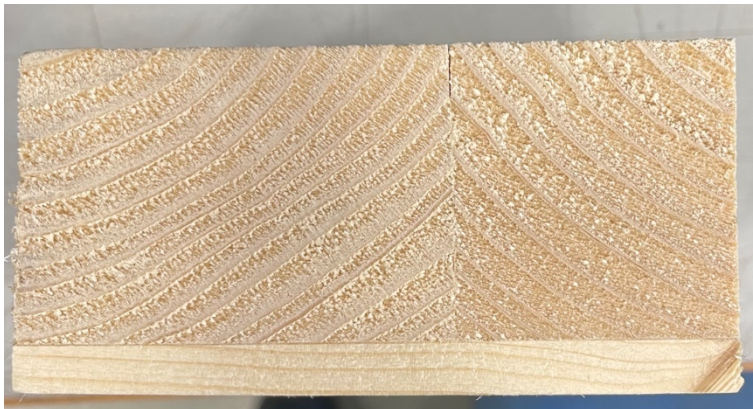


**Figure 6.3 Splines between two planks glued together.**



**Figure 6.4 Splines between two planks glued together.**

Another thing that is inevitable in timber materials is twigs. As for splines, holes in the samples would lead the hot gases further into the wood and cause faster charring. Figure 6.5 shows a twig on the left side of the material in sample 4-3. Other irregularities as scratched and ripped timber, as shown in Figure 6.6 from sample 7-4, could also impact the ignition and burning. From Test group 4, there is not found any relationship between the surfaces of the samples. The same yields Test group 7, where the splines in the surface, and its ability to ignite and its charring rate, shows no dependency. Test group 5 found that two out of three samples ignited with the initial heat flux, and the same tests that ignited had a spline or a twig in the surface, in contrast to the smooth surface for the sample that did not ignite. However, even though earlier research has indicated that splines, and therefore also twigs, could impact the burning, no significant dependencies

have been observed between ignition and twigs or other irregularities in the cone calorimeter tests, as the tests have shown conflicting results.



**Figure 6.5 Holes and twigs in the surface in sample 4-3.**



**Figure 6.6 Irregularities and a spline in the surface in Test 7-4.**

In addition to these differences, there have been some variations in humidity and density in the samples. However, all the samples have had a humidity between 8 and 9 %, which is a relatively small difference, and it is seen as irrelevant to investigate the impact it has had, as the differences are most likely too small to show obvious signs, and trends taken from these values will most likely just be a coincidence. Nevertheless, the theory from the literature states that moisture content will affect the burning in the way that water evaporates when it reaches 100 °C. This is observed in the HRR and temperature graphs for all test groups when the temperature gradient reaches 100 °C and flats out for a period when the water vaporizes before it continues to rise.

Even though all samples are taken from the same CLT element, there still are some differences in density between the samples. An explanation could be that CLT elements consist of many lamellas glued together and the composition of the material in each lamella varies. Another factor that may have impacted the elements is that it has laid outside under a tarpaulin between September and March, exposing it to cold and wet weather and affecting the material.

The impact densities have had on the cone calorimeter testing will be discussed further in the chapter.

### 6.2.1 Orientation

Samples tested in the cone calorimeter lays horizontally, orientated as a floor. Shields et al. (1993) stated that a floor-orientated sample ignited faster than a vertically-orientated sample. However, ceiling-orientated samples ignited drastically faster than both, especially for spontaneous ignition. It should be noted that exposed CLT often is desired to use in ceilings in buildings, and ignition could occur faster than shown in the cone tests. Given that the time to ignition is faster for ceilings than floors and the testing time only gives 15 minutes to ignite, it could also be possible that the critical heat flux for ignition may have been lower if the cone calorimeter tests were orientated differently.

### 6.2.2 Premises for Calculating Charring Rate

The basis for determining when the charred layer has reached the insulating 25 mm limit mentioned in Chapter 3.4.3 is when TC25 reaches 300 °C. Therefore, to find the charring rate in millimeter per minutes, 25 mm has been divided by the time necessary for this to happen.

A possible error using this approach is the assumption that the heat moves linearly through the sample. As shown earlier in the section, the position of the TC could impact the time for it to reach 300 °C. If cracks appear at the same place as the TCs, the calculated charring rate would be higher than for the rest of the sample. Nevertheless, cracks and irregularities causing heat to move differently in a CLT element would appear in CLT elements used in bigger compartments or buildings and shows that the charring rate would vary even within the same element with the same preconditions.

The other premise used for calculation is that timber chars at 300 °C, but this is not an accurate value, as it could vary between 280 and 300 °C according to literature. These differences could impact the charring rate but give minor errors compared to the impact of the TCs mentioned above.

## 6.3 Heat Release Rate and Temperature Development

From the diagrams presenting HRR and temperature in Chapter 5, it is typical with a peak right after ignition, before the HRR stabilizes. This shows how the fire goes from a transient state and stabilizes in a steady-state. The transient state can also be observed by the high flames from test in Figure 5.16 that occur right after ignition when the HRR in Figure 5.19 peaks in the beginning before it decreases. The flames shown 10 minutes into the test can be seen in Figure 5.17, showing the smaller flames in steady-state, with a corresponding lower HRR level. These findings correlate with findings in the literature review.

Findings presented by Harada (2001) indicated that the heat release rate also depends on the heat flux exposed to the sample. This is also found from the cone calorimeter tests, presented as green columns in Figure 6.7 and Figure 6.8 below, to show the maximum peak heat release rate for each heat flux level where the fresh samples ignited within 15 minutes. The lowest maximum PHRR is seen at 33 kW/m<sup>2</sup>, slightly higher than for 32 kW/m<sup>2</sup>, while it increases for 34, 35, and 40 kW/m<sup>2</sup>, indicating that the HRR increases with higher heat fluxes.

By comparing the HRR within the same heat flux level with the density in Figure 6.7, no significant relationship is observed. However, Figure 6.8 comparing time to ignition with the PHRR, indicates that there might be some dependencies between them. As every column with the lowest time to ignition gives the highest PHRR within the same heat flux levels, it may look like a more rapid ignition releases more energy. This could be explained by the literature stating that fresh timber releases combustible gases, and that a char layer would reduce the flow from the fresh inner wood. Whether ignition occurs before the char layer has begun to form, could possibly impact the PHRR. Though, one thing to notice is that for some of the samples, only seconds separate them, and it can be questioned if this is related or just a natural variation between the samples.



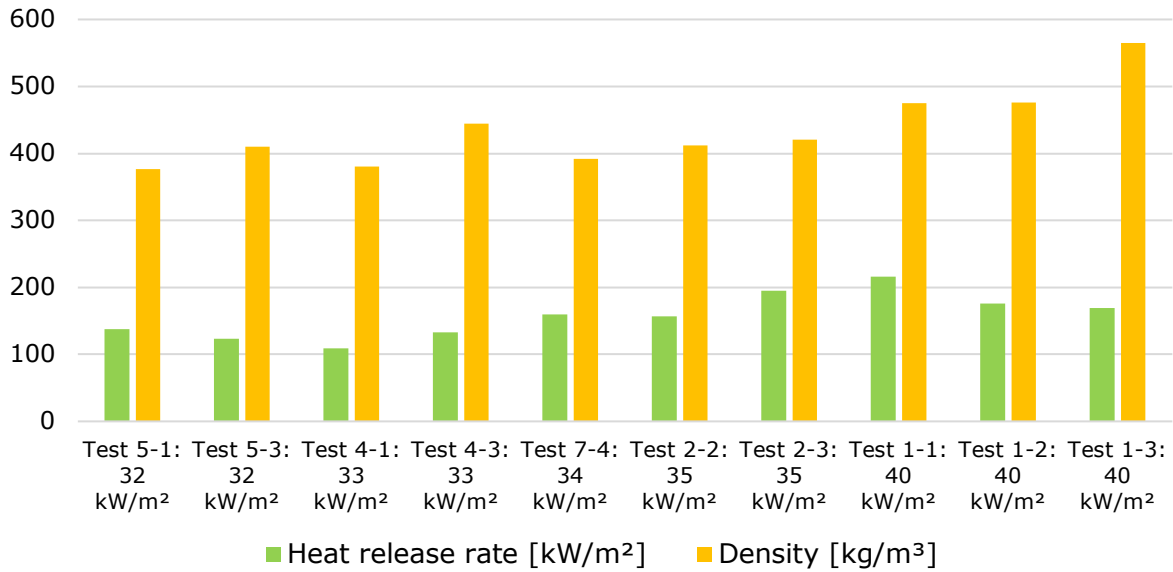


**Figure 6.7 Peak heat release rate and density for samples that ignited within 15 minutes.**

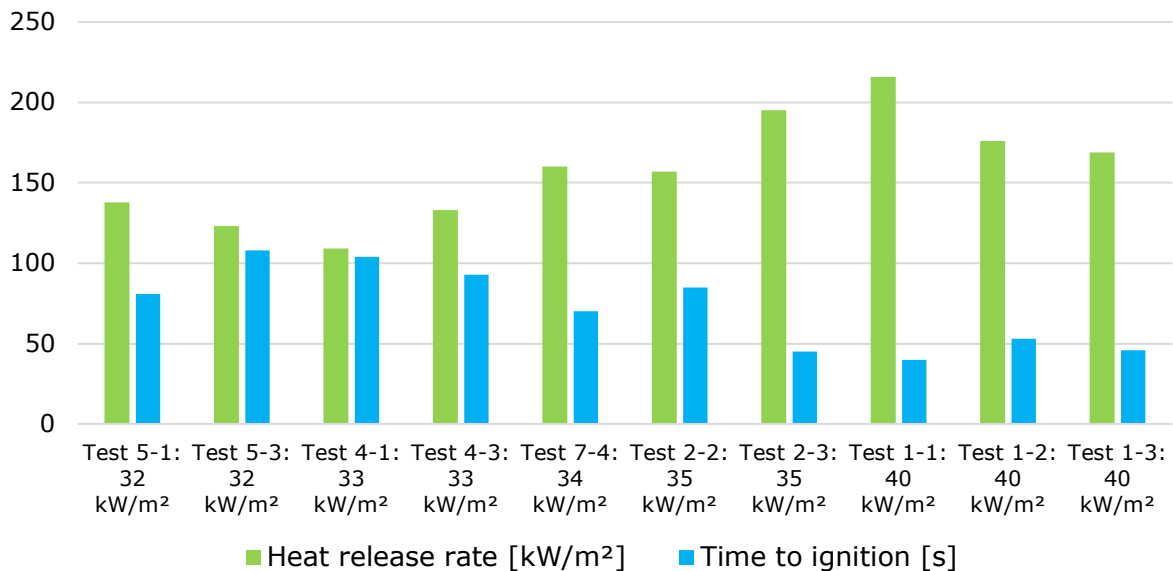


**Figure 6.8 Peak heat release rate and time to ignition for samples that ignited within 15 minutes.**

In Test group 6, none of the tests ignited within 15 minutes with the initial heat flux of 31 kW/m<sup>2</sup>. However, after 15 minutes, the heat flux was increased to 50 kW/m<sup>2</sup>, and Test 6-2 and Test 6-3 ignited. Test 6-1 needed as much as 15 minutes of exposure at 50 kW/m<sup>2</sup>. Diagrams in Chapter 5.6 shows that the HRR for the two samples that did ignite had approximately the same HRR for the first 15 minutes, while Test 6-1 had a higher HRR during the same period. If this is a coincidence and just a result of natural variation or a pattern cannot be concluded. However, it should be mentioned and maybe speculated if this relates to the same theory saying that a steadier fire, even though it only smolders, needs more severe changes to affect the burning.

Another finding from the results can be seen between Test 2-1 and Test 2-3. Test 2-1 ignited after 85 seconds, while Test 2-3 needed almost 32 minutes to ignite, even though

the heat flux was adjusted to 50 kW/m<sup>2</sup> after 15 minutes. By comparing the temperature graphs of the two tests, Test 2-3 increased faster than 2-1, only by smoldering ignition. Therefore, it can assume that it is not necessarily the flames that cause the pyrolysis through the wood but the heat exposure. The same findings was also found by Terrei et al. (2019). This indicates that even though reignitions and second flashovers may not occur in a real fire, continuous charring can be just as big of a threat to the structural system in a building of massive timber where burning materials are exposed to heat.

## 6.4 Critical Heat Flux for Ignition

Test results presented in the previous chapters have shown that the critical heat flux for unpiloted ignition in fresh wood is 31,5 kW/m<sup>2</sup>. None of the fresh samples ignited at 30 and 31 kW/m<sup>2</sup>. All samples ignited at 35 kW/m<sup>2</sup>. At 32 and 33 kW/m<sup>2</sup>, two out of three samples ignited at each level, while at 34 kW/m<sup>2</sup>, only one out of three ignited. This shows that there are some coincidences or irregularities when investigating wood materials. For charred samples, none ignited at 30 and 35 kW/m<sup>2</sup>, while all tests ignited at 40 and 50 kW/m<sup>2</sup>. The lowest heat flux that led to ignition was 36 kW/m<sup>2</sup>, giving a critical heat flux for unpiloted ignition in charred wood of 35,5 kW/m<sup>2</sup>.

For fresh samples, this correlates with the interval at 25-33 kW/m<sup>2</sup> found by Babrauskas (2002) for unpiloted ignition but is lower than what DiDomizio et al. (2016) found for Canadian pine. It is still considered realistic as other studies have found approximately the same results. For charred timber, Terrei et al. (2019) showed that a heat flux as high as 55 kW/m<sup>2</sup> gave no systematic results regarding reignition. This contradicts to the findings in this thesis, as all tests reignited at 40 and 50 kW/m<sup>2</sup>. However, based on literature of the material properties of timber and char presented in Chapter 3.4, it is expected that a charred sample needed higher heat flux exposures to ignite.

These results show that charred timber's critical heat flux for ignition is higher than fresh timber. Nevertheless, the difference is minor. Values described in Figure 2.7 show the corresponding temperatures for each flux. For example, 31 kW/m<sup>2</sup> is the same as 622 °C, and 36 kW/m<sup>2</sup> is 662 °C. This gives a difference at 40 °C, a relatively small difference in a real fire. Comparing this to the highest temperatures in the compartment fire, which was around 1050 °C, a difference at 40 °C will most likely not keep it not from reigniting because of the insulation of the wood during a fully developed fire.

When the fire spread and detracted in the compartment test, the first spread led to a heat flux from 24 kw/m<sup>2</sup> to 62 kW/m<sup>2</sup> dependent on the location and then back to a slightly higher level than before the peak. With continuous exposure, the ceiling would probably ignite immediately based on the critical heat flux but needed a higher exposure as it only happened over a short period. For the PT placed 2,3 from the fire, a sustained heat flux at 30 kW/m<sup>2</sup> should lead to ignition according to the findings from the cone calorimeter tests, as it did.

For ignition of charred wood, tests have ignited between 0 and 15 minutes from the start of the phase. It can therefore be questioned if some of the tests that did not ignite within 15 minutes would have ignited if the sample got a little longer time under the same heat exposure and would impact the results.

A noteworthy aspect from the cone calorimeter testing, is that all samples reignited within 140 seconds with a heat flux exposure at 50 kW/m<sup>2</sup> in Phase 3. However, in the tests on fresh wood in where the heat flux was increased to 50 kW/m<sup>2</sup> after no ignition at the initial

heat flux in Phase 1, there were several situations where it did not ignite or needed as long as 18 minutes to ignite. This is observed in Test 2-3, who needed over 15 minutes at 50 kW/m<sup>2</sup> in Phase 1.2, and only 140 seconds to reignite at the same heat flux in Phase 3. The same applies to Test 5-2, where it did not ignite at 50 kW/m<sup>2</sup> within 15 minutes in Phase 1.2 but did reignite at 38 kW/m<sup>2</sup> in Phase 3. A possible explanation can be the conditions for a fire to burn properly. When the pyrolysis process goes on, burnable gases are released and collected in the area around the fire, making the conditions for a fire to develop better. However, in the early stage of the fire, these conditions have yet to get the time to develop and the necessary high temperatures, as it has when the fire has burned for a while in Phase 3. These questionable findings indicate that a char layer will insulate the inner wood, even though if the layer is thin, especially when the conditions for a fire development are not optimal.

Janssens's method for predicting critical heat flux has given a value a little below the values from the cone calorimeter testing at 29,87 kW/m<sup>2</sup>. As some tests did not ignite, a fictional time to ignition was given to represent no ignition in these cases. This may not give a correct value for the critical value, but compared to not considering them, it would have given a misleading value for the critical heat flux. The linear trend line has an R<sup>2</sup>-value of 0,4932. This is slightly low, as comes from the spread in values. However, comparing the two values from cone calorimeter tests and from the literature that states a value between 25 and 33 kW/m<sup>2</sup> shows that all values lay around the same area.

More samples at these heat fluxes should have been tested to get more precise answers, in addition to more tests at higher heat fluxes to get more points of reference over larger areas on the graph. As only a few tests at the different heat fluxes were conducted, other results may have been found if more testing had been examined. It should also be mentioned that because the cone calorimeter tests only observe the test for 15 minutes, it is possible that the tests would have ignited if they got a longer exposure time. Nevertheless, as seen from the results presenting the time to ignition, it is especially seen for fresh wood that if the sample does not ignite within the first 2 minutes, it does not ignite at all within 15 minutes. Considering this, it can be assumed that as soon as the outer layer gets charred and the fresh timber surface is gone, the wood can be considered charred because some of the properties of fresh wood have disappeared.

## 6.5 Critical Heat Flux for Extinction

Measurements for extinction are conducted for two cases: zero heat flux and reduced heat flux. As described in Chapter 2.3.3, a built-in lid is used when the heat flux is reduced to zero to cover the sample from the radiation. However, as the cone heater still radiates toward the sample, the lid will eventually heat up and radiate heat to the sample after a period. Therefore, the built-in lid is replaced by a thicker gypsum lid when the samples have self-extinguished.

From the literature, Emberley, Do, et al. (2017) stated that it took between 10-15 minutes for a fire to reach steady-state. By comparing the HRR in the samples after a reduction in heat flux, it is possible to see how the HRR drops before it increases and stabilizes. The time needed for stabilizing in a steady-state agrees with the literature, where Test 6-2 began to stabilize 10 minutes after heat flux reduction. The same is observed in Test 7-2, to mention some of them.

Samples with no external heat flux extinguished within 5 minutes every time besides one. Figure 5.3 shows that the flames went around the lid towards the heat flux, and an

assumption for this is if the lid radiated heat downwards. The flames searched for the best conditions to sustain around the lid. Besides this, all samples self-extinguished, consistent with the theory that thermally thick materials need an external heat source to sustain burning.

To find the critical heat flux for self-extinction, the heat flux was reduced in either Phase 2, Phase 4, or both. As seen from the tests where extinction with heat flux was tested in the middle of the procedure, the samples sustained burning at lower heat fluxes than for the tests where extinction was measured at the end. This is because fire needs fresh and burnable materials to sustain burning. A good example of this is for Test 6-2, where the charred sample ignited at  $37 \text{ kW/m}^2$  in Phase 3 but did also extinguish at the same heat flux in Phase 4 within 5 minutes from the HRR was in a steady state. This contradicts to the theory described in Chapter 3.4.2 by Bartlett et al. (2019), stating that the same conditions yield for both ignition and extinction. As all the other factors affecting the fire remained the same, the most reasonable explanation for extinction was the lack of materials.

Considering these observations, the results for extinction in Phase 4 cannot be trusted when it comes to finding the critical heat flux for extinction. Therefore, the only useful results regarding self-extinction to analyze are those from Phase 2. As this observation was made halfway through the testing, only a few samples were left to test on. All samples sustained burning at 28 and  $30 \text{ kW/m}^2$ , and the same yields for  $25 \text{ kW/m}^2$  besides two out of four samples that extinguished.

Some tests, in example Test 7-1 and Test 7,2, almost extinguished when the heat flux was adjusted in Phase 2 but stabilized after a few minutes. This can be explained by a fire's steady state and transient state, where a reduction in the heat flux leads the fire from a steady state to a transient state. This can also be seen in the first drop in HRR from the tests, that reaches the relatively lowest point and slowly increases before the lid is used to extinguish the fire. As Chapter 3.2 mentions, a transient fire is more susceptible to changes and extinguishment than a fire in a steady state that can continue to burn under worse circumstances. Therefore, after a period of burning in a transient state, the fire will eventually stabilize, go over to a steady state, and increase the HRR and flames. This agrees with literature from Emberley, Do, et al. (2017) who stated that it took between 10-15 minutes for a fire to reach steady-state. The time needed for stabilizing in a steady-state correlates with the literature, where Test 6-2 began to stabilize 10 minutes after the heat flux reduction. The same is observed in Test 7-2.

Suppose the statement of Bartlett et al. (2019), stating that the same conditions yields extinction and ignition of wood, is correct. In that case, the critical heat flux for extinguishment should be the same as the critical heat flux for ignition but for piloted ignition. Unfortunately, this has not been investigated during this thesis, and the predicted critical heat flux for ignition has not been tested properly. However, the literature found by Bartlett et al. (2016) assumes that the critical heat flux for piloted ignition, and therefore also extinction, lies around  $10\text{-}13 \text{ kW/m}^3$ .

Comparing this to the one sample that extinguished at  $25 \text{ kW/m}^2$ , the difference is big. Nevertheless, like some of the others, this sample could also extinguish because of the lack of materials left, as only two samples extinguished. It can therefore be assumed that the critical heat flux is slightly lower than this value but cannot be stated by a given value in this thesis.

From the Compartment Test, it is seen repetitive fire spreads along the compartment. As the peaks in Figure 4.2 show, as well as the heat flux, the fire in the ceiling elements do not sustain burning, and the material self-extinguishes after a period when the wood crib is burned out.

### 6.6 Relationship between Ignition Time and Density for Fresh and Charred Timber

The results regarding time to ignition from Chapter 5 is plotted into Figure 6.9 and Figure 6.10, showing how the time to ignition on fresh and charred wood depends on the density of the wood. Only the samples that ignited within the first 15 minutes are shown in the figures.

All samples were weighted several times in the days and weeks before the test to ensure the moisture content was as similar as possible. However, even though the samples were taken from the same element, there were some differences in the weight, which also resulted in various densities, as the volume for all samples was the same.

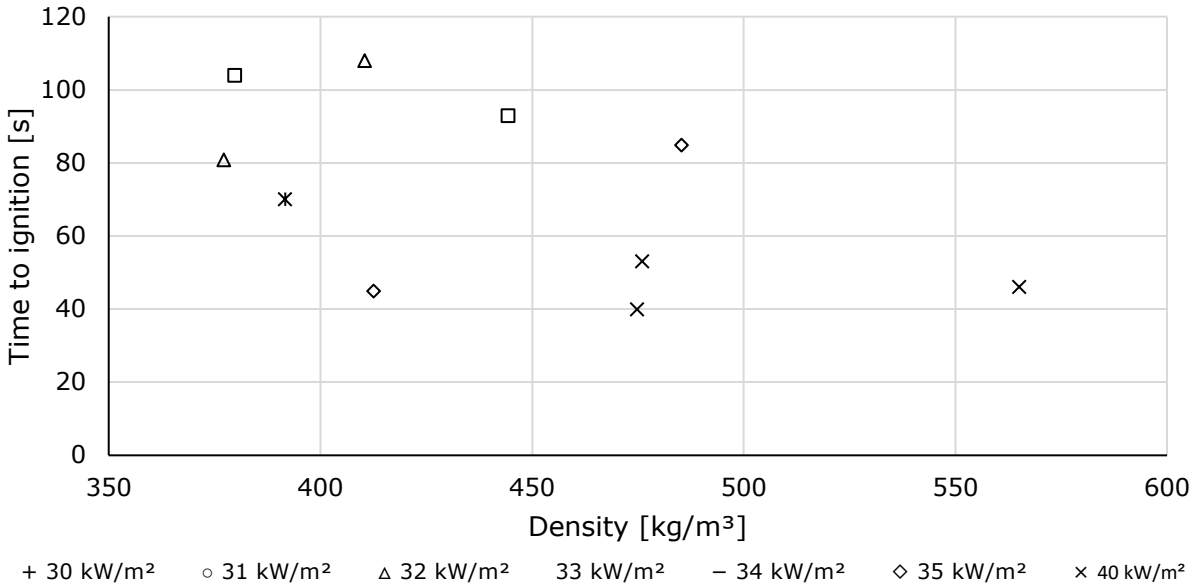


**Figure 6.9 Relationship between ignition time and density for fresh wood.**

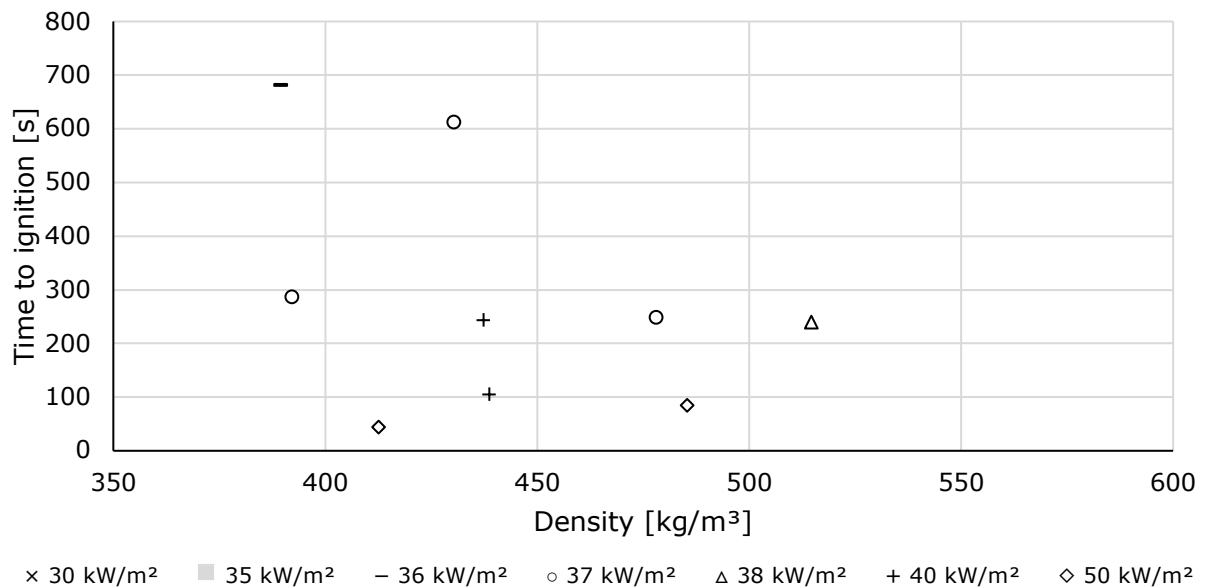


**Figure 6.10 Relationship between ignition time and density for charred wood.**

Findings from the tests indicate no correlation between density and time to ignition for fresh or charred wood.

The theory from Chapter 3.4.9 states that density will impact fire behavior and that wood with higher densities could better resist a fire. Although, it is not mentioned if it affects the ignitability or just the burning and charring of the material. Another factor that can impact the results is that all samples consist of the same specie and that the difference in density needs to be more significant to impact the time to ignition. It may also be other factors impacting the time to ignition. As mentioned earlier in the discussion, irregularities, cracks, or twigs in the surface may impact the burning and ignition properties of the material. Although many factors may impact the time to ignition, the main parameter important for ignition in these tests has been heat flux exposure.

## 6.7 Charring Rate Depending on Heat Flux and Density

As the samples have been exposed to different heat fluxes and have different densities, it is also interesting to investigate if these factors affect the charring rate. This can be seen in Figure 6.11 and Figure 6.12, showing charring rates for all samples, whether they ignited within 15 minutes or not. The charring rate is based on the time for TC25 to reach 300 °C and shows only the charring rate for the first 25 mm of the sample. The average charring rate for all samples is calculated from the values presented in Chapter 5 to 0,57 mm/min.

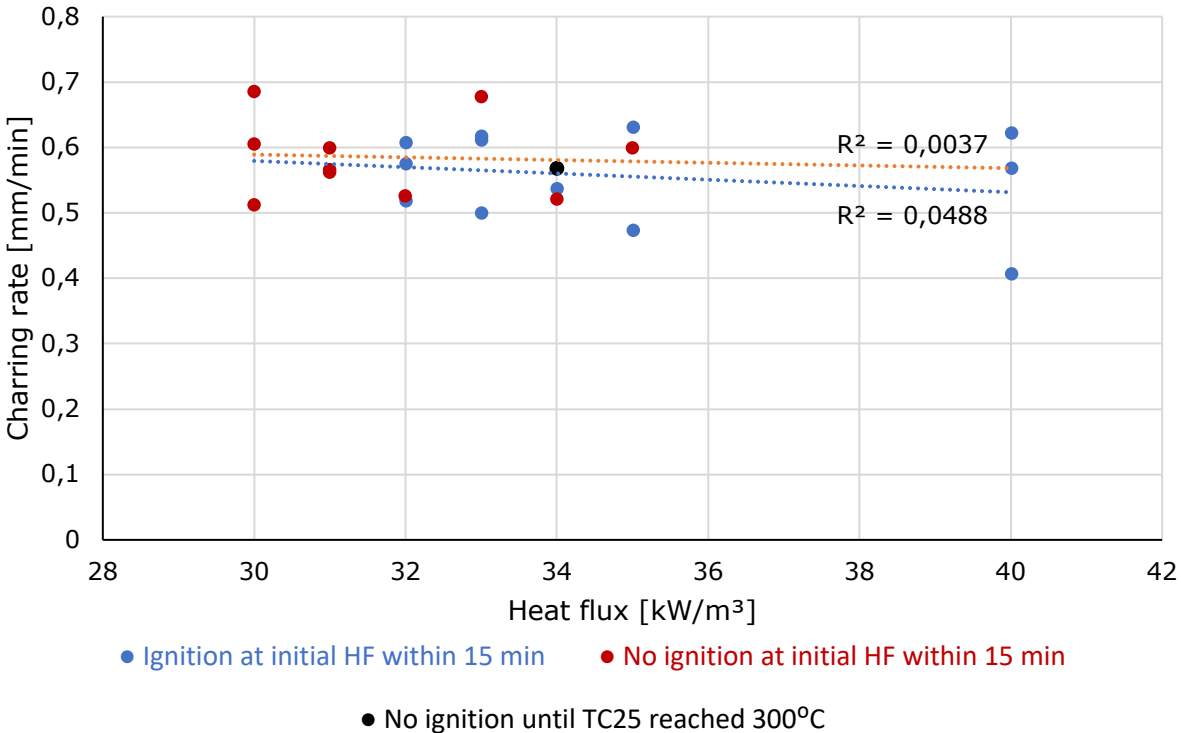
The red dots illustrate the samples that did not ignite within the first 15 minutes, and the heat flux was increased. However, these dots cannot clearly indicate if heat flux has impacted the charring, as it has not been continuous at one heat flux level. The black dot illustrates a sample that did not ignite within the time to TC25 reached 300 °C, and the blue dots indicate the ones that ignited with the initial heat flux exposure.

Figure 6.11 shows the dependency between charring rate and heat flux. Trend lines for each category is inserted in the diagram and show no significant patterns. As mentioned earlier, the regression number should lay between 0,5 to 1 to imply clear correlations between the two factors. These numbers are as low as 0,05 and 0,004, with a slight trend going against that higher heat flux leads to slower charring, which is unlikely to be true. It

can, though, be seen from the diagram that one of the samples at 40 kW/m<sup>2</sup> stands out with a lower charring rate than all the others and impact the trend line.

The regression number for the samples that ignited with the initial heat flux within 15 minutes was slightly higher than those with no ignition with the initial heat flux. However, they cannot be said to be dependent on each other. As seen in the theory from Terrei et al. (2021) and Reszka and Torero (2006) showing the temperature in the TCs inside the samples, it could be expected to see some relations between the two variables, where the temperatures at some depths increased drastically faster for higher heat fluxes. However, these correlations are opposite of the trend lines in Figure 6.11. Moreover, Martinka et al. (2018) stated that the charring rate increased with higher heat flux exposures. Even though no trends between heat flux and the charring rate were found in the cone calorimeter tests, relations between them are expected to occur if the differences between the heat flux levels were bigger.

The red line representing non-igniting samples appears above the blue dots indicating ignited samples, suggesting the possibility of faster charring. However, further investigation is needed to confirm this. Compared to the ignited samples, prolonged exposure to increased heat flux after the initial 15 minutes may contribute to a higher charring rate. These assumptions contradict the diagram's findings, which show no correlation between heat flux and charring rate. One possible explanation for this discrepancy is the absence of heat flux deviations in initially ignited samples. In contrast, the non-igniting samples experienced consistent heat fluxes at 50 kW/m<sup>2</sup>, potentially influencing the charring rate. The black dot, which smoldered without flaming igniting, lies amidst them.



**Figure 6.11 Charring rate dependent on heat flux.**

Figure 6.12 shows how the charring rate has varied for the different sample densities. It shows some correlations between the two parameters and yields the samples that ignited within 15 minutes and those that did not ignite within 15 minutes. Even though the

regression numbers do not reach above 0,5, it still indicates a certain trend. This reinforces the theory by Bartlett et al. (2019) saying that lower density creates lower thermal conductivity, allowing more heat inside the material.

The same findings are also presented in other studies and stated among others by Friquin (2011) and Xu et al. (2015). However, in contrast to those, Emberley, Do, et al. (2017) saw no dependencies between the density itself but between different species. As all these samples come from the same CLT-element and consist of the same material, this does not imply in this case and goes against the findings from the cone tests.

Another interesting thing to mention is that no matter if the samples did ignite or not within the given 15 minutes or ignited at all before extinction, there are no significant differences in the charring rate for either heat flux or density.

Charring rates from European standards are presented earlier in the literature review and gave charring rates at 0,65 mm/min for softwood and 0,5 mm/min for hardwood. Comparisons with these values shows that the average value at 0,57 mm/min lies below what is expected for softwood but higher than hardwood. It should also be noted that even though the specie goes under the softwood category, some of the samples have a relatively high density with associated low charring rates, which impact the average charring rate.

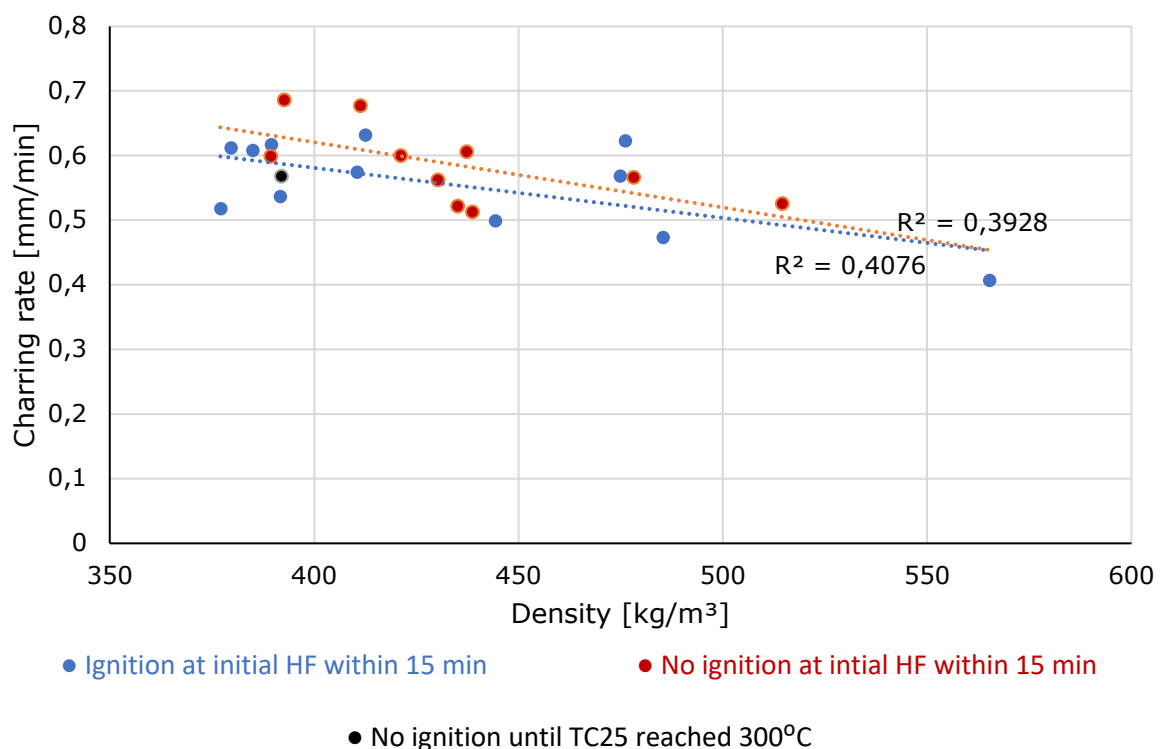


**Figure 6.12 Charring rates at various densities.**

## 6.8 Mass Loss and Mass Loss Rate

As mentioned earlier in the chapter, some values from the mass loss and the mass loss rate have been removed from the graphs due to interruptions from the lids and the TCs to avoid severe deviations that will make the results impossible to present. Removing the deviations has led to some incorrect values. However, it is pursued to avoid significant sources of error by making the graph linear between the points where values are removed. This is not observable in the graphs, besides the period with the lid on, but may have led



to different trend lines than initially if the mass loss and mass loss rate had been measured undisturbed. To even out the differences, it is chosen to use the mass loss rate for an average of 30 seconds. This will also relate better with the reasonable level of precision presented in the thesis, as the precision level of the results also should reflect the precision level in the input. The mass loss has used the original values besides some deviations during the first minutes. These results have not been affected in the same way as for the mass loss rate.

Considering that none of the results perfectly represents the mass loss rate during a fire as to significant interruptions, it is still possible to see some relations.

Comparisons between Test 4-1 and Test 4-2 show that the mass loss rate for the first 15 minutes follows the same pattern even though only Test 4-1 ignited immediately. Both peaks at around  $7 \text{ g/m}^2\text{s}$  at the beginning before it decreases to  $3,5\text{-}4,5 \text{ g/m}^2\text{s}$ . 15 minutes into the test, the mass loss rate for Test 4-2 increases to almost  $8 \text{ g/m}^2\text{s}$  at the most as the heat flux increases. Nevertheless, the peak happens immediately after the increase, reducing to an average of  $5,5 \text{ g/m}^2\text{s}$  and remains the same after ignition at 30 min. Test 4-1 continues stabilizing at approximately  $4 \text{ g/m}^2\text{s}$  until extinction. This correlates with findings in the literature stating that the mass loss rate is highest in the transient state and decreases towards a steady burning as the heat transfer through the samples approaches a continuous rate. Test 4-3, however, lie at a higher level but has more significant variations than the others, either from interruptions or natural variations without a clear pattern.

Test 4-2 shows that the mass loss rate depends more on the heat flux and not if the sample ignites, which contradicts to theory giving a value for the critical mass loss rate for extinction. The same observations are seen for Test 2-3, which also did not get any increase at the time of ignition. If no dependencies exist between ignition and mass loss rate, as seen in this test, the critical heat flux would not have been possible to calculate based on extinction itself but more on the radiating heat flux, as the same conditions must be fulfilled for ignition and sustained burning.

To investigate if there is possible to find a specific value for extinction to occur, the mass loss rate from Test group 6 is analyzed. The relevant period is from around 35 minutes from the start, where the heat flux was reduced, showing the difference in mass loss rate for Test 6-1 and Test 6-2 that extinguished, and Test 6-2 that sustained burning. Test 6-1 had a severe fall in the mass loss rate when the heat flux was reduced and went down to a mass loss rate at  $2\text{-}3 \text{ g/m}^2\text{s}$ . Test 6-2 had a minor mass loss and lay at  $3 \text{ g/m}^2\text{s}$  before it increased. Finally, Test 6-3 decreased slowly to the approximately same level as Test 6-1. The mass loss rate at the time of extinction had a dip at  $1\text{-}1,5 \text{ g/m}^2\text{s}$ , which is less than Bartlett's findings. All tests had observed small flames in the edges of the sample for a period after the heat flux reduction but managed to grow and sustain flaming in two cases, which can explain the low mass loss rate even though it still burned. Tests by Bartlett et al. (2017) have shown that the critical mass loss rate for extinction was  $3,48 \text{ g/m}^2\text{s}$ . This is slightly higher than values found from Test group 6, even though these values cannot be stated precisely based on the cone calorimeter tests.

A higher mass loss rate will also indicate a higher charring rate as the mass loss in a burning sample comes from pyrolysis, turning the wood into char and releasing gases and particles. This will strengthen the belief that the heat flux affects the charring rate after all, even though it is not observable with heat fluxes between  $30$  and  $40 \text{ kW/m}^2$ , as mentioned in section 6.7.

## 6.9 Calculation of Char Depth Based on Mass Loss

From Chapter 5.11, two equations to calculate the char depth from the mass loss were found, one in percentage and one in grams and millimeters. Figure 5.39 and Figure 5.40 in Chapter 5.11 shows some deviations in the graphs indicating that the mass loss decreases at some points, especially around 40-55 minutes. These deviations come from the method used to find the average mass loss. When a sample with a total mass higher than the others has reached 300 °C in TC25 and is removed from the further calculation, the average mass loss for all samples will get a sudden drop as the total mass of all samples suddenly gets lower. This leads to sudden jumps on the graph. Yet, using the data as a basis for the trend lines and the associated equations is considered good enough, on account that the trend line crosses the graph, as it does. Nevertheless, it should still be noticed that these factors affect the equation for calculating the char depth based on mass loss.

Another aspect crucial to specify is that the equation utilized to determine charring based on mass loss in cone calorimeter tests, only is applicable for wood material derived from Norwegian Spruce with the same density and humidity as in these tests. Statements by Frangi and Fontana (2003) saying that a material with thickness less than 50 mm chars faster than others, should be considered as the samples used to prepare for the equations all is 47 mm thick, and may have given a faster charring than a thicker sample would have given. It should also be noted that as the equation is based on a sample at 100 mm x 100 mm, it is most relevant for other samples with the same dimension in a cone calorimeter.

When plotting in the crosses for where the TCs reaches 300 °C, it is chosen only to use the results from TC25. TC30 could not be included as the mass loss after extinction in Phase 2 after TC25 reaches 300 °C would be different than for the others as the heat flux is reduced, and the calculation of the mass loss only yields for the first 25 mm in. TC15 and TC20 is not included to avoid that some of the tests will impact the equation more than others. However, these are plotted in Figure 6.13 and Figure 6.14 as a basis for a comparing trend line for the samples with four TCs.

The red crosses in Figure 5.39 and Figure 5.40 illustrate the charring rate for each sample and show significant deviations between the first two and the last TC25 to reach 300 °C. Especially the cross to the left will affect the trend line. On the other side, this cross also has a related mass loss affecting the blue trend line, which possibly evens out deviations in the equation after all.

Trend lines could be expressed linear, polynomial, exponential, or as a power regression. The linear regression was chosen to simplify the equation and assume a linear mass loss rate over the first 25 mm in charring depth. The ISO standard and findings from the literature review also give a linear charring rate. Choosing a trend line that intersects at zero is also possible, giving an equation expressed in one term without the constant term. However, based on earlier equations expressed by Martinka et al. (2018), it is tried to make it as similar as possible, making comparisons possible. These equations are expressed in Chapter 3.4.6, where one yields for Norwegian Spruce and one for Scots Pine, showing the relationship between char depth and mass loss for each in percentage. These two equations are plotted in Figure 6.13 with the equation found in this thesis, for spruce in yellow and pine in green, with the equations in boxes in the same color.

The dots plotted in Figure 6.13 and Figure 6.14 shows the char depth and mass loss in percentage for the samples with TCs at 15, 20, and 25 mm, with a corresponding trend

line, to compare the equation with the actual values. Equations from Martinka et al. (2018) shows a more rapid charring per mass loss for both Norwegian Spruce and Scots Pine than for the equations calculated from the cone results. Furthermore, compared to the actual char depth and mass loss taken from the TCs, the calculated equation is slightly steeper and with a higher constant value. This yields for both cases; in percentage, and grams and millimeters. As described in Chapter 3.4.6, the equations from Martinka et al. (2018) was based on materials with humidity at 0 %, while the cone calorimeter tests had humidity between 8 and 9 %, and previous literature have assumed that humidity will slow down the burning of wood. If this affects the relationship between char depth and mass loss cannot be stated but could be a possibility. Another factor that could have impacted the relationship between char depth and mass loss is the orientation and the consequence of it. Because the test is orientated horizontally as a floor, the mass loss will not fall off, but sustain on the sample and on the weight, leading to a higher mass than it would have been with a wall- or ceiling-orientated sample. Though, it should be mentioned that tests by Martinka et al. (2018) also was floor-orientated.

Trend line (TC15, TC20, TC25) compared to both Equation 1 and Equation 2 is slightly slacker than the equations itself, indicating that the charring takes a little longer for these samples than the equations suggest. This is also seen in the tables from Chapter Results, showing that tests with multiple thermocouples tends to have a slower charring rate. Though, it is not seen any explanations for this, and it is most likely a result of a natural variation as no other parameters logical could explain this. The regression number for Trend line (TC15, TC20, TC25) compared to Equation 1 is relatively high, indicating that it gives a good representation of the points on the graph. Trend line (TC15, TC20, TC25) compared to Equation 1 is lower, but still between 0,5 and 1 which is the area that suggests that the trend line represents the points well.

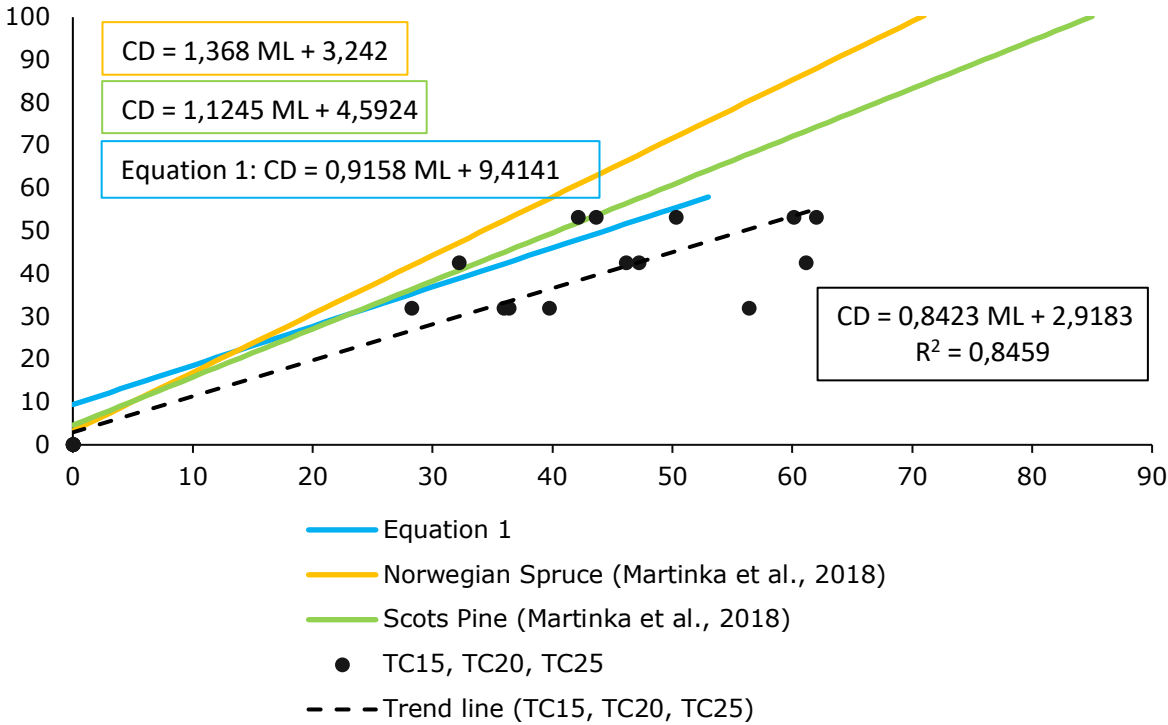


**Figure 6.13 Equation 1. Char depth and mass loss in percent of the total depth and mass.**

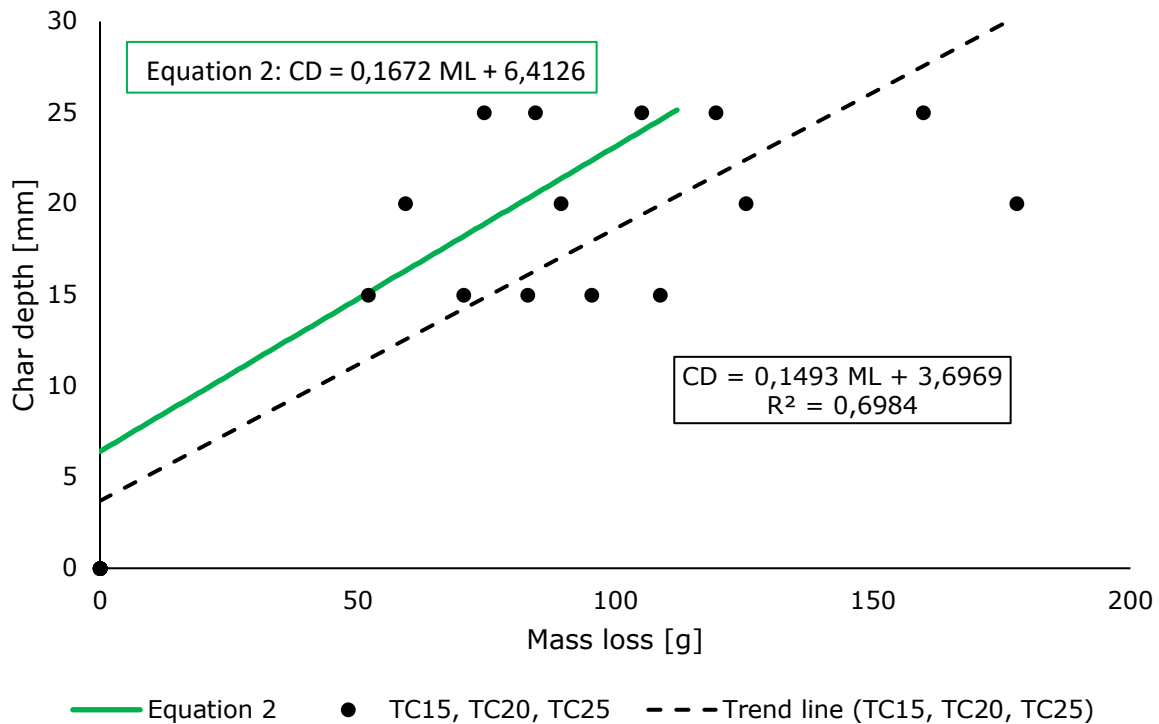


**Figure 6.14 Equation 2. Char depth and mass loss in percent of the total depth and mass.**

Trend line (TC15, TC20, TC25) compared to both Equation 1 and Equation 2 is slightly slacker than the equations itself, indicating that the charring takes a little longer for these samples than the equations suggest. This is also seen in the tables from Chapter Results, showing that tests with multiple thermocouples tends to have a slower charring rate. Though, it is not seen any explanations for this, and it is most likely a result of a natural variation as no other parameters logical could explain this. The regression number for Trend line (TC15, TC20, TC25) compared to Equation 1 is relatively high, indicating that it gives a good representation of the points on the graph. Trend line (TC15, TC20, TC25) compared to Equation 1 is lower, but still between 0,5 and 1 which is the area that suggests that the trend line represents the points well.

Statements by Frangi and Fontana (2003) saying that a material with thickness less than 50 mm chars faster than others, should be considered as the samples used to prepare for the equations all is 47 mm. It should also be noted that as the expression in grams is based on a sample at 100 mm x 100 mm, it is most relevant for other samples with the same dimension in a cone calorimeter.

## 6.10 Char Development in the Cone Calorimeter Compared to Compartment Test

As seen from the diagrams in Chapter 4, none of the TCs at 40 mm inside the elements reached 300 °C, and it was only at 4,7 m from the ignition side that TC30 reached 300 °C. The time for getting a char layer with a thickness of 25 mm increased as it went further away from the starting position of the fuel. The location of the starting fire can explain this, and the compartment is long and narrow and works as a traveling fire, moving from one side to the other. Conversely, the temperature curve at 14,3 meters is more even than at 4,7 meters, leading to more stable charring conditions at 14,3 meters. An explanation can

be that the fire had reached a steady state and did not burn transiently, as it did when the fire was at 4,7 meters, causing on and off from heat and flames.

Another thing observed from the figures in Chapter 4, is that the temperature in the TC at 10 mm, in all locations, increased rapidly until it reached about 600 °C and stabilized here, although the fire continued to burn. This can be explained by the theory mentioned in Chapter 3.4.3, where the fire, after reaching 500 °C, moves into the layers and continues the pyrolysis process instead of continuing to burn at the same point. This is because there are not enough burnable materials that have not been charred, and the charred layer will eventually smolder and move further in instead, leading to no higher temperatures at the given point.

The average char depths measured directly from the elements used in the compartment test at the same location as the thermocouples are 28 mm at 4,8 m, 29 mm at 9,6 m, and 34 mm at 14,3 m from the ignition side. Calculated charring depths based on the temperature inside the elements give 30 mm, 28 mm, and 26 mm char depths, respectively. Both methods for calculating the char depth of the elements result in similar results, indicating that the method of placing thermocouples inside the elements during testing can be used. However, if the charring depth should be calculated based on the charring rate found from the cone calorimeter tests over the exact durations of 122 and 91 minutes, it would have given charring depths of 70 mm and 52 mm, respectively. Charring rates from NS-EN 1995-1-2 at 0,65 mm/min, would give char depths as high as 80 mm and 60 mm for a 122- and 91-minute fire duration. If these values occurred, the cross-section would be drastically reduced, leading to severe reductions in the load-bearing properties of mass timber.

These findings indicate that large elements inside a fire would burn slower than smaller elements inside the test. This could be the case, considering the statement by Frangi and Fontana (2003) that the burning of samples with a thickness smaller than 50 mm burns faster. However, Figure 4.2, presenting the heat flux in the compartment, shows that the heat flux varies over time, leading to no continuity in the charring, in contrast to the cone calorimeter test with constant radiating towards the sample. It could therefore be assumed that a fire with more coherent high heat fluxes would give deeper char depths than what is found from the Compartment Test.

## 7 Conclusion

The thesis addresses the issues concerning how cross-laminated timber behaves under various heat exposures. The research question for the thesis is: "How does cross-laminated timber behave under various heat exposures, with particular emphasis on the ignition, reignition, charring, and self-extinction?". Four secondary research questions are formulated to help answer the research question.

### **1. What is the critical heat flux for unpiloted ignition of fresh and charred timber?**

Critical heat flux for unpiloted ignition is found through testing of small CLT samples in a cone calorimeter according to ISO 5660-1. Results have shown that the critical heat flux unpiloted ignition for fresh wood is 31,5 kW/m<sup>2</sup>, and 35,5 kW/m<sup>2</sup> for charred wood. The critical heat flux for fresh timber is also found by Janssens method, giving a slightly lower heat flux than the cone tests directly gave, at 29,87 kW/m<sup>2</sup>. Both results regarding fresh timber correlate with existing literature, while no literature is found on the critical heat flux for charred timber.

### **2. Does a flaming sample extinguish when the external heat flux is reduced, and when will it happen?**

Critical heat flux for extinction is tested in cone calorimeter tests. In the situation with no heat flux exposure radiating towards the sample, all flaming samples besides one self-extinguished. It shows that the CLT is dependent on an external heat source to sustain burning. However, no critical heat flux for self-extinction has been found during the testing. For testing with reduced heat flux, the lowest heat flux tested for self-extinction was 25 kW/m<sup>2</sup>. At this exposure, two out of four tests self-extinguished.

### **3. How do factors like density, heat flux exposure and irregularities in the surface impact the burning of CLT?**

Test results from the cone calorimeter testing have shown that lower densities lead to an increased charring rate. However, no correlation is found between the density and the time to ignition of samples, or the maximum peak heat release rate. Higher heat fluxes lead to faster ignition and higher peak heat release rates, but there is not found a significant dependency between heat flux and charring rate. Still, there are indications that heat fluxes with more severe differences than tested for in this thesis could impact the charring rate of timber. Results from the compartment test show that the charring is highest in the area where the heat flux was highest. Charring rates from the cone calorimeter testing is found to be higher than charring rates from the Compartment Test, possibly explained by a constant heat flux exposure in the cone, in contrast to the variations in the Compartment Test. Furthermore, there is no correlation between irregularities in the surface, such as holes, twigs, or splines, and the ignition or charring of the CLT samples from the cone calorimeter tests.

### **4. Is it possible to find a relationship between the mass loss and the charring rate of the fire?**

The thesis finds two equations calculating the charring depth based on the mass loss. It yields for the first 25 mm of a burning sample and can be expressed both in the percentage of the total mass and material depth, and in grams and millimeters:

$$\text{Equation 1: Char depth} = 0,1672 * ML + 6,4126 [\%]$$

$$\text{Equation 2: Char depth} = 0,9158 * ML + 9,4141 [mm]$$

Equations found in the literature study relates to these findings, but does not fully agree, potentially due to variations in the specie and humidity of the samples tested.

### **How does cross-laminated timber behave under various heat exposures, with particular emphasis on ignition, reignition, charring and self-extinction?**

Several factors impact the burning of CLT, and predicting how it behaves during the fire is found hard as the results are not always unambiguous. The density of the material is found to affect the charring rate of timber but not the ignition time and PHRR. The heat flux is the most crucial factor regarding time to ignition and PHRR, while no clear findings are found concerning charring. A charred sample requires more heat and time to ignite than fresh samples, indicating that a charred layer will insulate the inner layer and, to some extent, prevent further flare-ups, supporting existing literature. Regarding self-extinguishment, it is found that the CLT will self-extinguish when no heat is radiating toward it. However, it is still necessary with further research to investigate the interfaces for self-extinction or sustained burning. Finally, it is important to notice that findings regarding charring have indicated that the CLT chars independent of if it flames or smolders, as long as there is heat exposure radiating towards the surface, and would, in that case, impact the load-bearing qualities of CLT.

## **7.1 Further Work**

This thesis has investigated how CLT behaves under fire exposures in a large-scale compartment test and a small-scale cone calorimeter test centered around the latter. The fire testing is only valid for Norwegian Spruce with the same humidity and density used in the tests. Even though the testing has given relevant results to the ongoing research of CLT in buildings, it is still necessary with further research on some topics:

- Investigate how CLT behaves in a large-scale test under a longer heat exposure regarding delamination and second flashovers, as this has not been the focus of this thesis.
- As the critical heat flux for self-extinction is an essential parameter for predicting fire development, finding a value for this to occur would be helpful for further research of mass timber.
- Even though critical heat flux for unpiloted ignition is found on charred wood in this thesis, it is still necessary to investigate how this varies with different species, densities, or surrounding conditions. Investigating the critical heat flux for piloted ignition could also be interesting, as flames could contribute to reignition in a real fire.
- The compartment test only had exposed CLT in the ceiling. Exposed CLT in walls and ceilings could also be relevant to investigate since CLT is used as a structural system horizontally and vertically in buildings.

## References

- Aseeva, R., Serkov, B., & Sivenkov, A. (2014). The Ignition of Timber. In *Fire Behavior and Fire Protection in Timber Buildings* (pp. 89–117). Springer Netherlands.  
[https://doi.org/10.1007/978-94-007-7460-5\\_4](https://doi.org/10.1007/978-94-007-7460-5_4)
- Atreya, A., & Abu-Zaid, M. (1991). Effect Of Environmental Variables On Piloted Ignition. *Fire Safety Science, 3*, 177–186. <https://doi.org/10.3801/IAFSS.FSS.3-177>
- Babrauskas, V. (2002). Ignition of Wood: A Review of the State of the Art. *Journal of Fire Protection Engineering - J FIRE PROT ENG, 12*, 163–189.  
<https://doi.org/10.1177/10423910260620482>
- Babrauskas, V. (2005). Charring rate of wood as a tool for fire investigations. *Fire Safety Journal, 40*(6), 528–554. <https://doi.org/10.1016/j.firesaf.2005.05.006>
- Barber, D., Abu, A., Buchanan, A., Dagenais, C., & Klippel, M. (2022). Timber connections. In *Fire Safe Use of Wood in Buildings—Global Design Guide* (pp. 278–312). CRC Press.
- Bartlett, A., Hadden, R., Bisby, L., & Lane, B. (2016). *Auto-extinction of engineered timber: The application of firepoint theory*.
- Bartlett, A. I., Hadden, R. M., & Bisby, L. A. (2019). A Review of Factors Affecting the Burning Behaviour of Wood for Application to Tall Timber Construction. *Fire Technology, 55*(1), 1–49. <https://doi.org/10.1007/s10694-018-0787-y>
- Bartlett, A. I., Hadden, R. M., Hidalgo, J. P., Santamaria, S., Wiesner, F., Bisby, L. A., Deeny, S., & Lane, B. (2017). Auto-extinction of engineered timber: Application to compartment fires with exposed timber surfaces. *Fire Safety Science: Proceedings of the 12th International Symposium, 91*, 407–413.  
<https://doi.org/10.1016/j.firesaf.2017.03.050>
- BioMed Central. (2023). *Peer review process*. BioMedCentral.Com.  
<https://www.biomedcentral.com/getpublished/peer-review-process>
- Bøe, A. S., Friquin, K. L., Brandon, D., Steen-Hansen, A., & Ertesvåg, I. S. (2023). Fire spread in a large compartment with exposed cross-laminated timber and open ventilation conditions. In *Fire Safety Journal*.
- Brandner, R., Flatscher, G., Ringhofer, A., Schickhofer, G., & Thiel, A. (2016). *Cross laminated timber (CLT): Overview and development*.
- Browne, F. L. (1958). *Theories of the Combustion of Wood and its Control. A Survey of the Literature*. Forest Products Laboratory, Forest Service, U.S. Department of Agriculture, 1958.
- Buchanan, A., Dunn, A., Just, A., Klippel, M., Maluk, C., Östman, B., & Wade, C. (2022a). Fire safety in timber buildings. In *Fire Safe Use of Wood in Buildings—Global Design Guide* (pp. 32–66). CRC Press.



- Buchanan, A., Dunn, A., Just, A., Klippel, M., Maluk, C., Östman, B., & Wade, C. (2022b). Fire safety in timber buildings. In *Fire Safe Use of Wood in Buildings* (pp. 33–62).
- Buchanan, A., & Östman, B. (2022). *Fire Safe Use of Wood in Buildings: Global Design Guide* (1st ed.). CRC Press.
- Butler, C. P. (1971). *Notes on charring rates in wood*. Department of Scientific and Industrial Research and Fire Offices' Committee: Joint Fire Research Organisation.
- CEN. (2008). *NS-EN 1991-1-2:2002+NA:2008. Eurocode 1: Actions on structures—Part 1-2: General actions—Actions on structures exposed to fire*. European Committee for Standardization (CEN).
- CEN. (2010). *NS-EN 1995-1-2:2004+NA:2010. Eurocode 5: Design of timber structures—Part 1-2: General—Structural fire design*. European Committee for Standardization (CEN).
- Di Blasi, C., Hernandez, E. G., & Santoro, A. (2000). Radiative Pyrolysis of Single Moist Wood Particles. *Industrial & Engineering Chemistry Research*, 39(4), 873–882. <https://doi.org/10.1021/ie990720i>
- DiDomizio, M. J., Mulherin, P., & Weckman, E. J. (2016). Ignition of wood under time-varying radiant exposures. *Fire Safety Journal*, 82, 131–144. <https://doi.org/10.1016/j.firesaf.2016.02.002>
- Drysdale, D. (2011). *An Introduction to Fire Dynamics* (3rd ed.). John Wiley & Sons Inc.
- Dupal, O., Hasalová, L., Šálek, V., Hejtmánek, P., & Jahoda, M. (2022). Use of photogrammetry to determine spruce and OSB char bulk density. *Fire and Materials*, n/a(n/a). <https://doi.org/10.1002/fam.3113>
- El Gazi, M., Sonnier, R., Giraud, S., Batistella, M., Basak, S., Dumazert, L., Hajj, R., & El Hage, R. (2021). Fire Behavior of Thermally Thin Materials in Cone Calorimeter. *Polymers*, 13(8). <https://doi.org/10.3390/polym13081297>
- Emberley, R., Do, T., Yim, J., & Torero, J. L. (2017). Critical heat flux and mass loss rate for extinction of flaming combustion of timber. *Fire Safety Science: Proceedings of the 12th International Symposium*, 91, 252–258. <https://doi.org/10.1016/j.firesaf.2017.03.008>
- Emberley, R., Putynska, C. G., Bolanos, A., Lucherini, A., Solarte, A., Soriguer, D., Gonzalez, M. G., Humphreys, K., Hidalgo, J. P., Maluk, C., Law, A., & Torero, J. L. (2017). Description of small and large-scale cross laminated timber fire tests. *Fire Safety Science: Proceedings of the 12th International Symposium*, 91, 327–335. <https://doi.org/10.1016/j.firesaf.2017.03.024>
- Frangi, A., & Fontana, M. (2003). Charring rates and temperature profiles of wood sections. *Fire and Materials*, 27, 91–102. <https://doi.org/10.1002/fam.819>
- Frangi, A., Fontana, M., Knobloch, M., & Boichichio, G. (2008). Fire behaviour of cross-laminated solid timber panels. *Fire Safety Science*, 9, 1279–1290. <https://doi.org/10.3801/IAFSS.FSS.9-1279>
- FRIC. (2019). *Om FRIC*. Fire Research and Innovation Centre (FRIC). <https://fric.no/om-fric>

- Friquin, K. (2011). Material properties and external factors influencing the charring rate of solid wood and glue-laminated timber. *Fire and Materials*, 35, 303–327. <https://doi.org/10.1002/fam.1055>
- Frost, J. (2018). *How To Interpret R-squared in Regression Analysis*. Statistics by Jim. <https://statisticsbyjim.com/regression/interpret-r-squared-regression/>
- Harada, T. (2001). Time to ignition, heat release rate and fire endurance time of wood in cone calorimeter test. *Fire and Materials*, 25, 161–167. <https://doi.org/10.1002/fam.766>
- Hasburgh, L., Bourne, K., Peralta, P., Mitchell, P., Schiff, S., & Pang, W. (2016, August). *Effect of Adhesives and Ply Configuration on the Fire Performance of Southern Pine Cross-Laminated Timber*.
- ISO. (1976). *ISO 554:1976. Standard atmospheres for conditioning and/or testing—Specifications*. International Organization for Standardization (ISO).
- ISO. (1999). *ISO 834-1:1991 Fire-resistance tests—Elements of building construction—Part 1: General requirements*. International Organization for Standardization (ISO).
- ISO. (2015). *ISO 5660-1:2015. Reaction-to-fire tests—Heat release, smoke production and mass loss rate—Part 1: Heat release rate (cone calorimeter method) and smoke production rate (dynamic measurement)* (Version 3). the International Organization for Standardization (ISO).
- Janssens, M. L. (1991). Piloted ignition of wood: A review. *Fire and Materials*, 15, 151–167.
- Karbhari, V. M. (2007). *Durability of Composites for Civil Structural Applications*. Woodhead Publishing.
- Kleinhenz, M., Just, A., & Frangi, A. (2021). *Temperature-dependent thermal properties for cross-laminated timber exposed to standard fire*. <https://doi.org/10.3929/ethz-b-000515188>
- Knapic, S., Pirralho, M., Louzada, J. L., & Pereira, H. (2014). Early assessment of density features for 19 Eucalyptus species using X-ray microdensitometry in a perspective of potential biomass production. *Wood Science and Technology*, 48(1), 37–49. <https://doi.org/10.1007/s00226-013-0579-y>
- Kotsovinos, P., Christensen, E., Rackauskaite, E., Glew, A., O’Loughlin, E., Mitchell, H., Amin, R., Robert, F., Heidari, M., Barber, D., Rein, G., & Schulz, J. (2022). Impact of ventilation on the fire dynamics of an open-plan compartment with exposed timber ceiling and columns: CodeRed #02. *Fire and Materials*. <https://doi.org/10.1002/fam.3082>
- Liodakis, S., Vorisis, D., & Agiovlasis, I. P. (2006). Testing the retardancy effect of various inorganic chemicals on smoldering combustion of Pinus halepensis needles. *Thermochimica Acta*, 444(2), 157–165. <https://doi.org/10.1016/j.tca.2006.03.010>
- Lizhong, Y., Zaifu, G., Jingyan, Z., Xiaojun, C., & Zhihua, D. (2002). Experimental Study on Scale Effect on Mass Loss Rate of Some Woods. *Journal of Fire Sciences*, 20(1), 23–35. <https://doi.org/10.1177/0734904102020001608>
- Lolli, N. (2020). *ZEB Laboratory*. <https://zeblab.no/photos>

- Lucherini, A., Jovanović, B., Van Coile, R., & Merci, B. (2021). Background and limitations of the Eurocode parametric fire curves, including the fire decay phase. In *ASFE'21, Proceedings* (pp. 330–335). University of Ljubljana.  
[https://www.asfe21conference.com/static/Proceeding\\_asfe\\_2021.pdf](https://www.asfe21conference.com/static/Proceeding_asfe_2021.pdf)
- Martinka, J., Rantuch, P., & Liner, M. (2018). Calculation of charring rate and char depth of spruce and pine wood from mass loss. *Journal of Thermal Analysis and Calorimetry*, 132. <https://doi.org/10.1007/s10973-018-7039-8>
- NTNU. (n.d.). *Choosing sources*. NTNU. Retrieved May 10, 2023, from <https://i.ntnu.no/academic-writing/choosing-sources>
- Promat. (2020). *International fire curves – useful tool for designing fire safety*. Promat. <https://www.promat.com/en/construction/news/33637/international-fire-curves-fire-safety/>
- Reitan, N. K., Friquin, K. L., & Mikalsen, R. F. (2019). *Brannsikkerhet ved bruk av krysslaminert massivtre i bygninger – en litteraturstudie* (RISE Rapport 2019:09). RISE Research Institutes of Sweden.  
<https://risefr.no/media/publikasjoner/upload/2019/20385brannsikkerhet-ved-bruk-av-kl-rapport-9-2019.pdf>
- Reszka, P., & Torero, J. L. (2006). In-Depth Temperature Measurements of Timber in Fires. *Proceedings of the 4th International Workshop, Structure in Fires;SIF'06*, 2.
- RISE Research Institute of Sweden. (n.d.). *Fire testing according to ISO 5660-1*. RISE Research Institute of Sweden. Retrieved May 7, 2023, from <https://www.ri.se/en/what-we-do/services/fire-testing-according-to-iso-5660-1>
- Santoni, P.-A., Romagnoli, E., Chiaramonti, N., & Barboni, T. (2015). Scale effects on the heat release rate, smoke production rate, and species yields for a vegetation bed. *Journal of Fire Sciences*, 33, 290–319. <https://doi.org/10.1177/0734904115591176>
- Schmid, J., Werther, N., Klippel, M., & Frangi, A. (2019). *Structural Fire Design-Statement on the Design of Cross-Laminated Timber (CLT)*.  
<https://doi.org/10.19080/CERJ.2019.07.555721>
- Shi, L., & Chew, M. Y. L. (2012). Influence of moisture on autoignition of woods in cone calorimeter. *Journal of Fire Sciences*, 30(2), 158–169.  
<https://doi.org/10.1177/0734904111431675>
- Shields, T. J., Silcock, G. W., & Murray, J. J. (1993). The effects of geometry and ignition mode on ignition times obtained using a cone calorimeter and ISO ignitability apparatus. *Fire and Materials*, 17(1), 25–32. <https://doi.org/10.1002/fam.810170105>
- Simms, D. L., & Hird, D. (1958). On the pilot ignition of materials by radiation. In *Fire Research Note No. 365*. Department of Scientific and Industrial Research and Fire Offices' Committee: Joint Fire Research Organisation.
- Terrei, L., Acem, Z., Marchetti, V., Lardet, P., Boulet, P., & Parent, G. (2021). In-depth wood temperature measurement using embedded thin wire thermocouples in cone calorimeter tests. *International Journal of Thermal Sciences*, 162, 106686.  
<https://doi.org/10.1016/j.ijthermalsci.2020.106686>

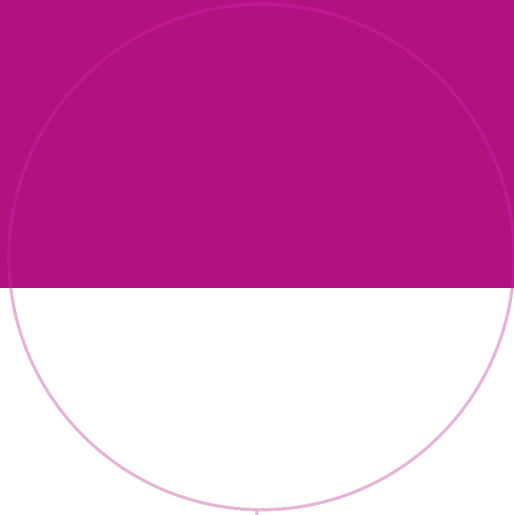
Terrei, L., Acem, Z., Marchetti-Georges, V., Lardet, P., & Boulet, P. (2019, April). *Study of ignition and extinction of spruce glulam exposed to a radiative flux*. 9th International Seminar on Fire and Explosion Hazards, St. Petersburg, Russia.  
<https://doi.org/10.18720/spbpu/2/k19-63>

Tsantaridis, L. (2003). *Reaction to fire performance of wood and other building products*.

Wickström, U. (2016). *Temperature Calculation in Fire Safety Engineering*.  
<https://doi.org/10.1007/978-3-319-30172-3>

Xu, Q., Chen, L., Harries, K. A., Zhang, F., Liu, Q., & Feng, J. (2015). Combustion and charring properties of five common constructional wood species from cone calorimeter tests. *Construction and Building Materials*, 96, 416–427.  
<https://doi.org/10.1016/j.conbuildmat.2015.08.062>

Zhou, B., Yoshioka, H., Noguchi, T., Wang, K., & Huang, X. (2023). Fire Performance of EPS ETICS Facade: Effect of Test Scale and Masonry Cover. *Fire Technology*, 59(1), 95–116. <https://doi.org/10.1007/s10694-021-01195-x>



Norwegian University of  
Science and Technology